Protein Mimics by Molecular Scaffolding of Peptides

Paul Werkhoven

Printed by: Proefschritmaken.nl | | Uitgeverij BoxPress
Published by: Uitgeverij Boxpress, 's-Hertogensbosch

ISBN: 978-94-6295-471-7

The research in this thesis was (partly) financed by Chemical Sciences of The Netherlands Organisation for Scientific Research (NWO)

Printing of this thesis was financially supported by:
Utrecht Institute of Pharmaceutical Sciences (UIPS), Shimadzu Benelux B.V., Screening Devices B.V., and Actu-All Chemicals.

Protein Mimics by Molecular Scaffolding of Peptides

Peptiden op Steiger Moleculen voor het Nabootsen van Eiwitten

(Met een samenvatting in het Nederlands)

PROEFSCHRIFT

ter verkrijging van de graad van doctor aan de Universiteit Utrecht op gezag van de rector magnificus, prof.dr. G.J. van der Zwaan, ingevolge het besluit van het college voor promoties in het openbaar te verdedigen op maandag 18 april des middags te 2.30

door

Paul Ruben Werkhoven

geboren op 3 december 1987 te Nijmegen

Promotor: Prof.dr. R.M.J. Liskamp

Copromotor: dr.ir. J.A.W. Kruijtzer

Table of Contents

List of abbreviations

Ac	acetyl
Alloc	allyloxycarbonyl
Boc	*tert*-butyloxycarbonyl
BOP	(benzotriazol-1-yloxy)tris(dimethylamino)phosphonium hexafluorophosphate
Bu	butyl
CDR	complementarity determining region
CLIPS	chemical linkage of peptides onto scaffolds
CTV	cyclotriveratrylene
CuAAC	Copper(I)-catalyzed azide-alkyne cycloaddtion
d	doublet
DBU	1,8-diazabicyclo[5.4.0]undec-7-ene
DCC	dicyclohexyl carbodiimide
DCM	dichloromethane
DiPEA	*N,N*-diisopropylethylamine
DMA	dimethylacetamide
DMAP	4-dimethylaminopyridine
Dmb	2,4-dimethoxybenzyl
DMF	*N,N*-dimethylformamide
DMSO	dimethyl sulfoxide
EDCI	1-ethyl-3-(3-dimethylaminopropyl)carbodiimide
EDT	1,2-ethanedithiol
ELISA	enzyme-linked immunosorbent assay
ESI	electrospray ionization
Et	ethyl
Fmoc	fluorenylmethyloxycarbonyl
GC	gas chromatography
HBTU	2-(1H-benzotriazol-1-yl)-1,1,3,3-tetramethyluronium hexafluorophosphate
HFIP	hexafluoro-2-propanol
HIV	human immunodeficiency virus
HOBt	1-hydroxybenzotriazole
HPLC	high performance liquid chromatography
HRP	horse radish peroxidase
IC50	concentration at which 50% of the target is inhibited
ITC	isothermal titration calorimetry
KLH	keyhole limpet hemocyanin
m	multiplet

MALDI	matrix-assisted laser desorption ionization
Me	methyl
μW	microwave
MS	mass spectrometry
MTBE	methyl-*tert*-butyl ether
NaAsc	sodium ascorbate
NMM	*N*-methylmorpholine
NMP	*N*-methyl-2-pyrrolidone
NMR	nuclear magnetic resonance
oNBS	ortho-nitrobenzenesulfonyl
p	pentet
Pbf	2,2,4,6,7-pentamethyldihydrobenzofuran-5-sulfonyl
PBS	phosphate-buffered saline
Ph	phenyl
ppm	parts per million
q	quartet
RAFT	regioselectively addressable functionalized template
RAM	rink amide
Rf	retardation factor
rgp120	recombinant gp120
s	singlet
sCD4	soluble CD4
SPAAC	strain-promoted azide-alkyne cycloaddition
SPPS	solid phase peptide synthesis
t	triplet
TAC	triazacyclophane
TASP	template assembled synthetic protein
TBAF	tetra *n*-butylammonium fluoride
TBTA	*tris*[(1-benzyl-1H-1,2,3-triazol-4-yl)methyl]amine
tBu	*tert*-butyl
TCEP	*tris*(2-carboxyethyl)phosphine
TEA	triethylamine
TES	triethylsilyl
TFA	trifluoroacetic acid
Tfa	trifluoroacetyl
THF	tetrahydrofuran
TIC	total ion current
TIPS	triisopropylsilyl
TIS	triisopropylsilane
TMB	tetramethylbenzidine

TMS	tetramethylsilane
TOF	time of flight
Trt	trityl
UV	ultraviolet
δ	chemical shift

Amino Acids

Ala	A	Alanine
Arg	R	Arginine
Asn	N	Asparagine
Asp	D	Aspartic acid
Cys	C	Cysteine
Gln	Q	Glutamine
Glu	E	Glutamic acid
Gly	G	Glycine
His	H	Histidine
Ile	I	Isoleucine
Leu	L	Leucine
Lys	K	Lysine
Met	M	Methionine
Phe	F	Phenylalanine
Pro	P	Proline
Ser	S	Serine
Thr	T	Threonine
Trp	W	Tryptophan
Tyr	Y	Tyrosine
Val	V	Valine

1

Chapter 1

General Introduction

Parts of this chapter have been published in:

P.R. Werkhoven and R.M.J. Liskamp in Biotherapeutics: Recent Developments using Chemical and Molecular Biology (Eds: L.H. Jones and A.J. McKnight) RSC books, 2013 pp. 263-284

1.1 Epitopes: Introduction, definitions and different types

The term "epitope" originates from the field of immunology, where it is mainly used as a synonym for an antigenic determinant, which is the part of an antigen that is recognized by molecules of the immune system. Different types of epitopes can be distinguished, for example B- and T-cell epitopes, immuno-dominant epitopes, and neutralizing epitopes.[1,2] These names refer to the occurrence and/or role of the epitope. For example, immuno-dominant epitopes indicate epitopes that can diminish the role of other epitopes present in the antigen. B-cell epitopes are the part of an antigen that binds an antibody, either in its free state or membrane-bound to a B-cell, while T-cell epitopes are peptides that are the product of proteolytic cleavage of the antigen which are presented by T-cells.

More specifically, the epitope of an (protein) antigen molecule is a defined region of its structure to which an antibody binds.[4,5] Nowadays, the term "epitope" is increasingly used outside immunology. Since an antigen-antibody interaction is essentially a protein-protein interaction, all protein-protein interactions can be considered interactions between two epitopes. In the antigen-antibody interaction example, this involves interaction between the epitope on the antigen and the epitope of the antibody, which is in immunology referred to as "paratope". It is hard to overestimate the importance of protein-protein interactions, as it is estimated that there are about 650,000 protein-protein interactions in the human interactome.[6] This makes protein-protein interactions very interesting as a therapeutic target area. One approach to utilize this space is to mimic the epitope in the form of a synthetic construct. These synthetic mimics may for example be able to interfere with undesired protein-protein interactions. These and other applications of synthetic protein mimics will be discussed below.

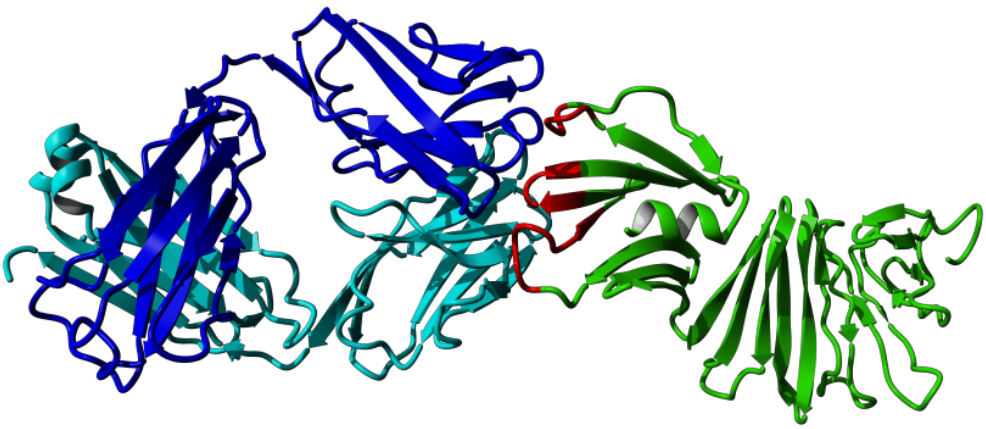

Figure 1. Crystal structure of Lyme disease antigen OSPA (green) in complex with a neutralizing antibody (FAB light and heavy chain, blue). The residues that are recognized by the antibody, the B-cell epitope, are highlighted in red.[3] PDB structure: 1FJ1.

1.2 Epitope mimics and their applications

Synthetic mimics of epitopes may have a wide range of therapeutic applications. They may not only be used as protein-protein interaction inhibitors, they may also serve as small molecular equivalents of a large protein and therefore may be used as synthetic vaccines or even synthetic antibodies. The legitimate questions concerning all these applications are how accurate epitope mimicry should be and which approaches are required for adequate mimicry.

1.2.1 Epitope mimics as synthetic vaccines

In our opinion, the development of synthetic vaccines is a promising and extremely attractive area for the application of epitope mimicry of antigenic proteins. Mimics of epitopes that are present in antigenic proteins of pathogens may be able to induce the production of antibodies, making these mimics interesting candidates for synthetic vaccines. The promise of preparing vaccines synthetically is very attractive, since most vaccines are based on the original pathogen. Some contain a killed or attenuated version of the original pathogen, while others contain an inactivated version of the pathogen's toxin. The production of these types of vaccines is very laborious and potentially hazardous because they all have the live pathogen as a starting point. For this reason considerable research efforts are spent on the development of synthetic vaccines, for example by epitope mimicry (of both T-cell and B-cell epitopes).[7–10]

Vaccination is a prophylactic approach, and as such may represent the ultimate protection strategy against diseases or toxic proteins originating from pathogens, by removing and destroying them through pathways of the immune system. Alternatively, the therapeutic approach involving molecular constructs, which can inhibit undesired protein-protein interactions, may also be an attractive avenue in the fight against diseases like Parkinson's or Alzheimer's.

1.2.2 Epitope mimics as protein-protein interaction modulators

Protein-protein interaction sites are, due to their size and complexity, difficult targets for small-molecule inhibitors, although some promising examples exist of inhibitors and even stabilizing molecules of protein-protein interactions.[11–14] Therefore, there is a growing interest in the development of especially "intermediate size" molecular constructs for interfering with undesired protein-protein interactions.[15–18] Many of these constructs are peptide-based and the importance of the conformation of these constructs is often emphasized.[19] A prominent example of peptides capable of interfering with protein-protein interactions is the cyclic pentapeptides containing an RGD sequence, which are able to inhibit the interaction between the α- and β-subunits of integrins.[20] Other examples are the peptides described by Hunke et al., which inhibit the binding between the bacterial protein ActA and host protein Mena EVH1,[21] and the peptides described by Hancock et al., which inhibited the interaction between Keap1 and transcription factor Nrf2.[22,23] However, these are examples of peptides that mimic a relatively simple continuous interaction site. Development of mimics of more complex interaction sites that are able to inhibit protein-protein interactions is still in its infancy. A few promising examples have already appeared in the literature hinting at the potential of these

molecular constructs.[24–28]

1.2.3 Epitope mimics as synthetic antibodies

As described above, epitope mimics can be used in the development of synthetic vaccines by mimicking the structure of the antigenic determinant. However, the paratope, the part of the antibody that binds the antigen, can also be mimicked. Mimicry of the complementary-determining region is, because of its size and complexity, very challenging, but these paratope-mimics may ultimately approach the specificity and binding affinity of antibodies. Although no mimics with the same affinity as antibodies have been obtained so far, important progress has been made towards the realization of this goal.[29–32]

1.3 Shape and structure of epitopes

1.3.1. Epitope structure

Similar to a protein, the primary structure of a proteinogenic epitope refers to its amino acid sequence, the secondary structure refers to its loop, helix or sheet character and the tertiary structure relates to the relative positioning of the parts of the epitope in space.

The amino acid composition of an epitope is clearly of vital importance. Analysis of multiple protein-protein complexes, including antigen-antibody complexes, and alanine-scan studies have provided important insights into amino acid compositions of the interaction sites. These studies have not only identified some amino acids as being more prevalent in interaction sites than others but have also shown the role of backbone atoms.[33–36] Most epitopes contain amino acids whose side chain can be replaced without significant loss of binding affinity. These residues are present either for spacing between essential binding residues or their backbone atoms play a role in binding.[33] The collection of residues that cannot be replaced without a significant loss in binding affinity is sometimes referred to as the "functional" epitope, or in the case of non-antibody-antigen interactions as the "hot spot".[5,34]

Besides the amino acid composition, the secondary structure of the epitope is also of crucial importance. Epitopes are often encountered as loops,[37–40] although helices[41–46] and β-chains/sheets are not uncommon.[47–50] A β-hairpin conformation is also encountered, of which the turn of the hairpin resembles a loop-like epitope, albeit more constrained and ordered, because of the additional beta-strand structure.[51,52] In the case of discontinuous epitopes, combinations of different secondary structural elements are also encountered.

1.3.2 Continuous and discontinuous epitopes

Based on their tertiary structure, epitopes are divided into two categories: continuous epitopes – sometimes denoted as linear epitopes - and discontinuous epitopes (Figure 2).[5,28] Although the latter category is by far the largest, approaches to express or mimic discontinuous epitopes have been very limited so far and therefore this is a challenging area for further research.

A continuous epitope consists of a single contiguous stretch of amino acids. However, it

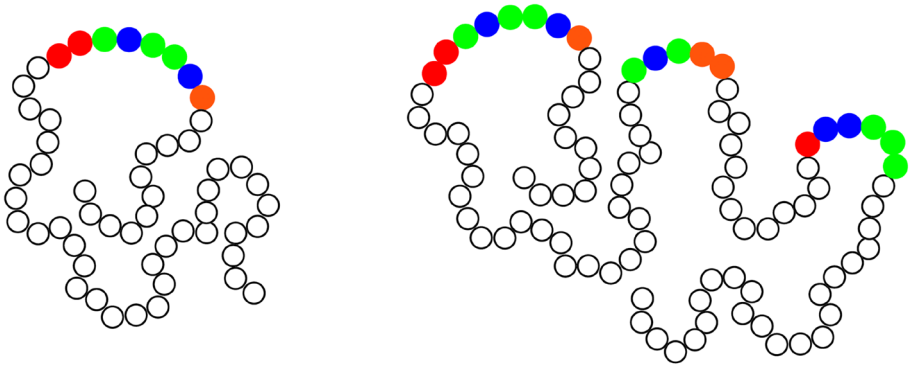

Figure 2. Left: continuous, sequential or linear epitope; right: discontinuous epitope.

must be noted that each residue in this peptide segment does not necessarily play a crucial role in binding to the antibody. In contrast to continuous epitopes, discontinuous epitopes are composed of multiple peptide segments that are remotely located in the protein sequence, but are brought into spatial proximity by folding of the protein to its tertiary structure. So, in addition to possible other functions, the remainder of the protein will act as a scaffold presenting the discontinuous epitope. In the discontinuous epitope the positioning and shape of the peptide segments relative to each other is essential for a high affinity and selectivity with an interacting partner. For example, antibodies that bind to discontinuous epitopes present in the antigen often do not bind to the denatured antigen, in which the spatial characteristics of the epitope have been lost.[2] These features of discontinuous epitopes contribute to the challenging nature of research in this area especially with respect to structural investigations and mimicry.

1.3.3. Influence of other structural properties

Besides the effects of the primary, secondary, and tertiary structure of an epitope, there are other structural properties that have to be taken into account. The exclusion of water molecules from the hydrophobic contact surfaces of the two proteins has been shown to be a beneficial factor for binding. The immune system can use this effect to mature an antibody. After initial creation of the antibody, the binding affinity can be enhanced by increasing the buried surface of the antibody-antigen interaction site, leading to an increase in the number of excluded water molecules and resulting hydrophobic interactions.[53]

Another important factor is the accessibility of the epitope. For an antibody to recognize an epitope in a protein, that particular epitope has to be accessible for binding by relatively large antibody molecules. As a consequence, when an epitope is more accessible, it will be easier to generate antibodies binding to this site. It may even be so that this easily accessible epitope can obscure the presence of other (more hidden) potential epitopes and therefore this accessible epitope may become an immuno-dominant epitope.[54] This is illustrated by the ternary complex of HIV protein gp120, its binding partner CD4 and an anti-gp120 antibody

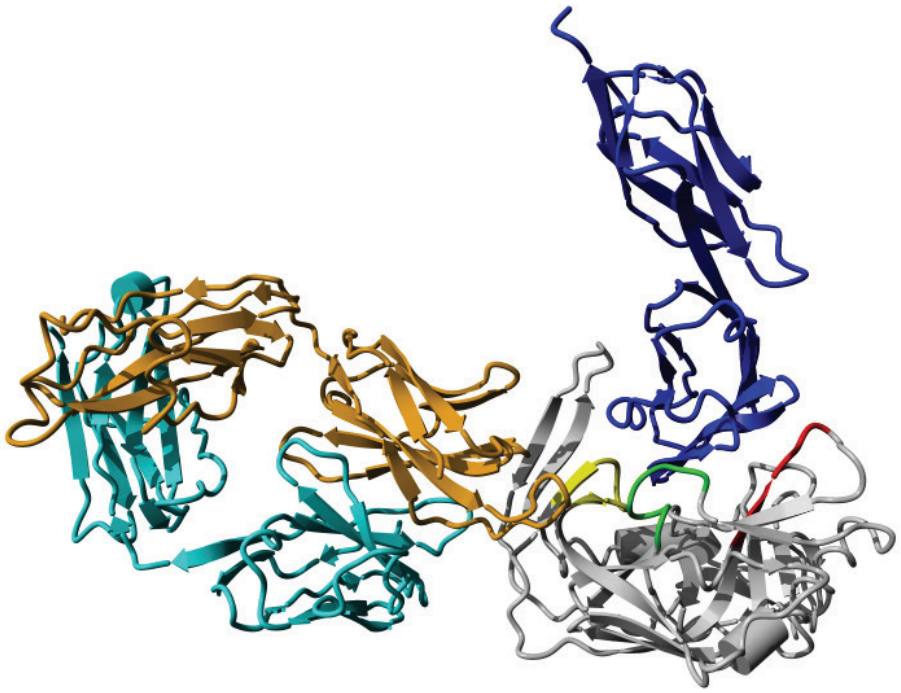

Figure 3. X-ray structure of gp120-CD4-antibody complex. CD4 (blue) binds to gp120 (gray) through interactions with three conserved loops (yellow, green and red). The antibody (cyan & orange) on the other hand binds to the variable, immuno-dominant V3 loop, which due to its relative accessibility is the preferred site for binding of antibodies.[40]

(Figure 3). The antibody (cyan/orange) in this structure binds to a large loop that is easily accessible and through the high variability of this loop, HIV can evade the immune system. The more conserved CD4-binding site (red/green/blue) is less accessible than the variable loop and is therefore not as easily recognized by the immune system. Not only immuno-dominant epitopes can be used for the evasion of the immune system. Another way for viruses to block access to a conserved epitope is the use of glycosylation of the protein. These so-called glycan shields can protect epitopes from being recognized.[54] By shifting these glycans, the virus tries to stay one step ahead of the immune system and renew its resistance.[55]

Furthermore, it must be noted that although close structural resemblance of the epitope can be of great significance, it is not an absolute requirement for a synthetic mimic. Examples are known of compounds capable of binding an antibody without possessing any apparent sequence similarity with the epitope.[56] This suggests that interaction between antibody and antigen is not completely dependent on entire amino acid residues, but more so on the correct spatial positioning of certain atoms in the side chain and/or the backbone.[5]

1.3.4. Determination of the primary, secondary or tertiary structure of epitopes

Classical approaches of determining the primary sequence of an epitope include synthesis of overlapping peptides of an antigenic protein and evaluation of the binding properties

with an antibody.[57,58] The most potent antibody-binding peptides are believed to include the peptide sequences of the epitope(s). A disadvantage of this method is that only short stretches of linear peptides are synthesized, which lack the often-needed secondary structure of the peptide segments present in the context of the antigenic protein. Understandably, this method is therefore best suited for the identification of continuous epitopes and less so for discontinuous epitopes.

The most comprehensive information with respect to the identity of the involved peptide segment(s) and their (spatial) structure is supplied by X-ray and/or NMR structural analysis. This structural biological information is of crucial importance for the identification of epitopes.

Using X-ray crystallography, structures of antibody-antigen complexes have been elucidated. These provide a direct visualization and detailed structural insights into which residues of the antigen are in close proximity to the antibody and can therefore be considered an epitope. Several examples of X-ray crystallography guided epitope localization of antigens have been published, for example in the area of Influenza and HIV.[40,59,60]

NMR spectroscopy can also provide valuable insights into the structure of an antibody-antigen complex. As an integral part of the structure elucidation using NMR, the binding residues of an epitope can be determined. An advantage of NMR over X-ray crystallography is the ability to measure the complex in solution. As a result, it is possible to determine differences between the free antigen and the antigen bound in the antigen-antibody complex. Binding an antibody restricts the mobility of residues present in the antigen, thus changing their relaxation time. Using different NMR techniques, such as dynamic filtering, heteronuclear NOE and HSQC, these changes can be measured and quantified resulting in the identification of the residues important for binding.[61–65]

Another increasingly important technique for identification of epitope sites is mass spectrometry (MS). From deuterium exchange and/or acetylation MS experiments, it is in principle possible to determine the interaction sites of an antigen-antibody complex. From this the epitope site can be derived. In addition, mild proteolytic digestion of the antigen-antibody complex and subsequent analysis using MS can provide insight into the peptides capable of binding to the paratope of the antibody. Although this MS method does provide information on those parts of the antigen that are in close proximity to the antibody, it does not supply information on the individual amino acid residues or atoms important for binding.[66–74]

In general, peptide arrays can be used to explore protein-protein interactions to dissect the interacting epitopes.[75] However, most of the current techniques lead to preparation and screening of arrays of linear peptides, while arrays of cyclic peptides would be far more desirable, since they mimic loop-like structures more closely.

Another - more “brute force” - method for localization of epitopes, is the generation of a phage display peptide library. This usually involves the generation of a large number ($>10^9$) of peptides, followed by establishing which peptides are capable of binding to, for example, antibodies.[76] The method has also been adapted to accommodate the formation of cyclic

peptides, which increases the potential of the epitope.[77,78] The phage display method will produce - besides peptides corresponding to the primary structure of the protein of interest[79] - peptides with an amino acid sequence not (clearly) related to this sequence. However, as long as these peptides are capable of binding the protein partner, they can be used in the production of epitope mimics.[77,80]

Complementary to using the previously discussed crystallographic, mass-spectrometric or NMR-spectroscopic experimental information, bio-informatics approaches, including modeling, also allow the prediction of peptide segments, which may be accessible for binding by a large molecule such as an antibody. From this, epitope sequences can be derived as suitable candidates for mimicry et cetera. The availability of structural data on the epitope bearing protein is of great value and makes modeling a great deal more accurate.[81–83]

1.4. Mimicry of epitopes by peptides

In order to adequately mimic the epitope site(s) of a parent protein, one has to establish first whether the epitope is of continuous or discontinuous nature. A continuous epitope can in principle be mimicked by a single peptide with a corresponding amino acid sequence, while a discontinuous epitope will usually require several peptides for adequate mimicry. However, even for mimicry of a continuous epitope it is important to look at its *secondary* structure and try to mimic this as closely as possible, for example mimicry of loops by cyclization or mimicry of helices by "stapling". For mimicry of discontinuous epitopes, information about its *tertiary* structure has to be included, leading to proper arrangement of the peptides in space as well as relative to each other. The development of such molecular constructs is a great challenge, involving advanced synthetic methodology.

1.4.1. Single linear peptides as continuous epitope mimics

As was stated above, a continuous epitope might be mimicked by a linear or a constrained peptide.

Despite the absence of any significant secondary structure, relatively small linear (15-mer) peptides led to the first peptide vaccine providing protection against parvovirus.[84] Linear (12-mer) peptide epitopes of snake venom displayed on phages were also immunogenic in mice.[85] In another example, a linear peptide was used in vaccination against influenza virus and provided protection in mice. The peptide was probably sufficiently long (>60 residues) to assume a high percentage of its original secondary structure, i.e. a significant α-helix character, thus increasing its structural resemblance to the original epitope.[86]

Linear peptide epitope mimics containing carbohydrate residues have also been prepared to mimic glycosylated epitopes. The presence of these carbohydrate residues increased the complexity of the synthesis of these glycopeptides.[87,88]

Despite the abundance of examples of single peptides that were capable of eliciting an immunogenic response in animals, none have successfully survived clinical trials.[4,89] One explanation for this may be the poor biological stability of linear peptides.

1.4.2. Constraining peptides for optimization of structural mimicry

Most epitope sequences have secondary structure, like loops, helices and beta sheets, to some degree. However, mimicry of these epitopes is still mainly achieved by the preparation of a linear peptide sequence, either through chemical synthesis or through for example phage display.[79,90–92] Although in a number of cases this has led to successful mimicry of epitopes present in antigenic proteins,[90,91,93] it is expected that the success rate can be increased by a closer mimicry of the conformation or secondary structure of the epitope, through for example a better resemblance of the loop-like structure. Various methods have been reported, capable of constraining peptides in order to control their secondary structure.[19]

In several of the above examples illustrating the use of single peptides as epitope mimics, the importance of a secondary structure already became apparent. In the Influenza example, the peptide was of sufficient length to have a considerable percentage of α-helical character. Shorter peptides, which are more reluctant towards forming a helical structure spontaneously, can be induced to do so by linking the side chains of two properly spaced amino acids in order to stabilize this secondary structure. This can be done by various chemical modifications such as ring-closing metathesis (often referred to as peptide stapling (Figure 4)),[94–98] salt bridges, disulfide formation and amide bond formation.[99]

Loops are a common structural motif in epitopes, which is not surprising since they are common secondary structure element at the surface of proteins amenable for post-translational modification, but also for recognition by antibodies and other proteins. Clearly, the most prominent loops are the CDR-loops of the heavy and light chains in an antibody. It is increasingly realized that a cyclic peptide is a better mimic of a loop-like structure. Therefore, the use of cyclic peptides is attractive for obtaining improved epitope mimics.[104,105]

A specific loop type is the β-hairpin, which can be mimicked by cyclization of the peptide with, for example, a D-proline-L-proline template (Figure 4). Examples are the preparation of epitope mimics of a malaria parasite protein and epitope mimics of the V3 loop of HIV gp120 protein.[101–103]

Other examples of the use of cyclic peptides are the phage-displayed cyclic hexapeptide library of which some peptides were able to bind to anti-rabies glycoprotein antibodies[77] and the cyclic peptides designed by Villén et al. mimicking the epitope on the capsid of the foot-and-mouth disease virus.[106]

An additional advantage of cyclic/constrained peptide-containing molecular constructs may be the reduced sensitivity to proteolytic degradation, which facilitates their use in a biological context by prolonging the half-life.[107] However, despite the widespread use of cyclic peptides in every conceivable branch of chemistry and biology, their synthesis and purification, irrespective of their size and amino acid composition, is still often a major hurdle.[24,107] For this reason, linear peptides are still being used in approaches to determine the epitope sequences and ensuing preparation of epitope mimics. Improving access to cyclic peptides by improving their synthetic approaches should broaden the possibilities of obtaining meaningful and adequate epitope mimics. Increased attention for the shape of an epitope should also enable

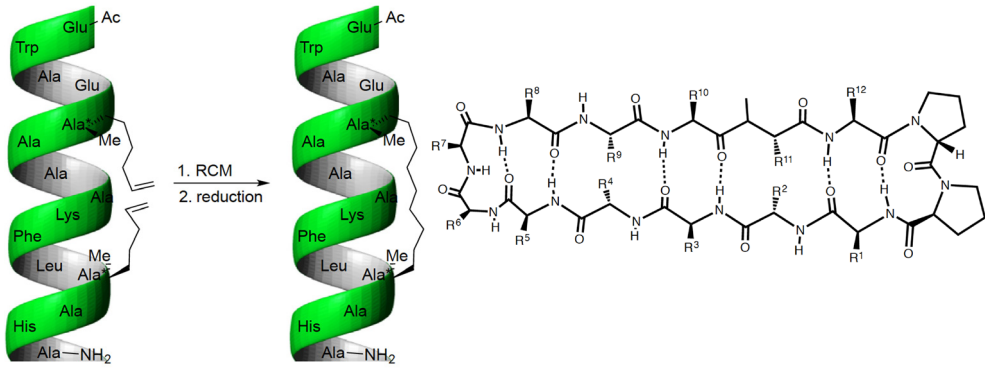

Figure 4. Left: Strategy for stabilizing alpha-helices by an all-hydrocarbon cross linker by Ring Closing Metathesis, nowadays often referred to as "stapling".[104] Right: General structure of β-hairpin mimics developed and applied by Robinson et al.[105–107]

mimicry of helix and beta-chain character containing epitopes.

Secondary structural elements can also be mimicked by non-peptide mimetics. These mimetics often consist of a rigid scaffold backbone that directs their substituents, which mimic the side chains of important residues, in the correct spatial positioning. This approach has been used to prepare mimics of alfa-helices[41,108–111] and beta strands.[112,113] However, this approach is mainly used for the mimicry of a continuous epitope or a single segment of a discontinuous epitope.

1.4.3. Assembly of peptides for mimicry of discontinuous epitopes

In attempts to closely mimic the tertiary structure of a discontinuous epitope, the individual peptides mimicking the corresponding segments of the discontinuous epitope have to be assembled into a single molecular entity. This can be done using a spacer or linker molecule, a molecular scaffold, a surface, or a dendrimer/polymer to provide the confined presentation of the peptide-mimicking epitopes. There are large differences between all these approaches and a priori it is hard to predict what will be the most successful approach.

1.4.3.1 Assembly of peptides by the preparation of dimers or multimers

In principle the simplest approach for mimicking a discontinuous epitope - especially one consisting of random coil peptide segments - is to judiciously combine the different peptide segments into a single construct by using spacers of appropriate length and rigidity. This approach has been followed in a number of cases. Some examples of linked peptides as epitope mimics are the immunogenic construct for foot-and-mouth disease virus by Villen et al.[37] and the HIV gp120 mimics by Franke et al.[93] Other, more complex, examples are the hFSH and hGC mimics by Smeenk et al., in which two cyclic peptides are linked together by an oxime linkage and a disulfide bond.[114] Connecting several identical peptide segments may lead to a multivalency effect, thereby increasing the affinity of the mimicked epitope.[115]

1.4.3.2. Assembly of Peptides by Scaffolding

Because of its more pre-organized character, a scaffold may represent the best approach to mimic the tertiary structure of the discontinuous epitope of a protein. In a way, the scaffold will act as a replacement of most of the framework of the native protein and the molecular construct of scaffold and peptides is in fact a pars-pro-toto of the entire protein.[25,27] The concept of discontinuous epitope mimics by scaffolding peptides is illustrated in Figure 5. The character and size of the cyclic peptides, the choice of the linkers as well as the scaffold determine the flexibility and therefore pre-organization of the entire molecular construct.

Assembly of cyclic peptides onto a scaffold clearly has advantages over assembly of linear peptides, such as a better mimicry of loops and increased proteolytic stabilization. Nevertheless, the number of examples of combinations of cyclic peptides and scaffold molecules is restricted, which points to the limited synthetic accessibility of cyclic peptides and/or synthetic methods for the assembly of peptides on scaffolds.[24,116]

1.4.3.3. Scaffolds

A large variety of scaffolds are available, each with its advantages and disadvantages. The most seminal contribution in this area was probably the cyclic peptide template TASP (Template Assembled Synthetic Protein), originally developed by Mutter and Vuilleumier,[117] and further developed by, among others, Dumy et al. to the so-called RAFT (Regioselectively Addresssable Functionalized Template) (Figure 6).[118,119] Although it is, in principle, possible to attach four different groups to this cyclic decapeptide system, this template is a relatively large flexible system lacking sufficient pre-organization. On the other hand, the highly pre-organized calixarene (Figure 6) system used by Hamilton et al. to which four albeit identical cyclic peptides can be introduced is also available.[120] Another example of the assembly of peptide loops onto a scaffold is the CLIPS method (Chemical Linkage of Peptide onto Scaffolds) by Timmerman et al. In this method a single peptide is anchored on a benzylic bis-, tri-, or tetra-bromide scaffold using multiple cysteine residues to create loops.[30,121,122]

We have developed a relatively small molecular scaffold with sufficient pre-organization, which could be conveniently synthesized on a large scale for solid phase synthesis and library preparation purposes, but moreover would allow the introduction of at least *three different peptide segments*. This triazacylcophane-scaffold (TAC-scaffold, Figure 6) has been applied successfully to incorporate both linear and cyclic peptides.[24,25,123]

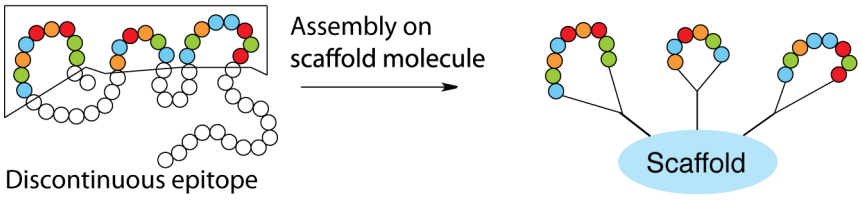

Figure 5. Discontinuous epitope mimicry by scaffolding of the corresponding cyclic peptides. Peptide fragments corresponding to the discontinuous epitope are synthesized as cyclic peptides. These peptides are then incorporated onto a scaffold molecule. The scaffold replaces the bulk of the protein.

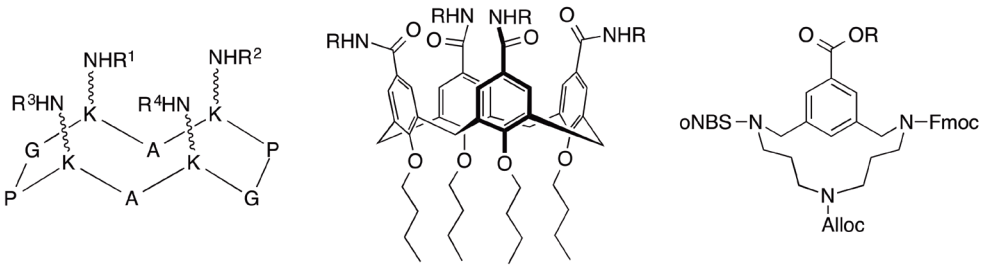

Figure 6. TASP/RAFT scaffold (left), calixarene scaffold (middle) and TAC-scaffold (right). The positions now occupied by the protecting groups in the TAC-scaffold allow introduction of *different* molecular moieties. The fourth position (R-group) is in principle also available.

Although the number of molecular scaffolds for multiple orthogonal conjugations is gradually increasing, it still is a challenge to incorporate *different* molecular entities onto a molecular scaffold in an efficient and robust manner. Approaches for the sequential introduction of multiple different peptides will be further discussed in chapter 3.

The choice of scaffold seems an important aspect in the design of epitope mimics since each scaffold presents the (cyclic) peptides in a different way. It is hard to predict the required amount of rigidity and pre-organization for creation of the best mimic of the epitope, as was recently shown by Mulder et al. in a study comparing different scaffolds.[124] Adequate spacing and positioning of cyclic peptide on the scaffold present challenges, which have hardly been touched, but will be extremely important for proper structural mimicry of discontinuous epitopes.

In addition to the synthetic organic scaffolds, there is an increasing use of various biomolecules as scaffolds. One example is the family of cyclotides, a family of polycyclic peptides containing a cystine knot. Via either chemical synthesis or recombinant expression the desired peptide sequences can be incorporated into the cyclotide.[125,126] Other examples are nucleotides (G-quadruplex),[127] engineered virus particles,[102] and (parts of) proteins.[128,129]

1.4.4. Requirements for discontinuous epitope containing protein mimics

The size and complexity of proteins show that, if one wishes to develop adequate protein mimics, the following requirements are essential. Firstly, a scaffold must provide a good platform with respect to flexibility, rigidity, positioning, and relative involvement of the different discontinuous epitope-representing peptides. Secondly, it must be possible to introduce peptides of any size or character at desired positions on the scaffold. Thirdly, it has to be possible to construct these epitope mimics, which comprise cyclic peptides of any desired size and character. Fourthly, innovative screening approaches have to be developed to find the best protein mimic. Finally, the resulting protein mimics should be amenable to further development as for example synthetic vaccine, other biologics or even synthetic antibodies, thus demanding reliable and reproducible state-of-the-art chemo- and biosynthesis.

1.5. Aim and outline of this thesis.

The research described in this thesis aims to develop a robust method for the synthesis of discontinuous epitope mimics, through the sequential introduction of cyclic peptides on a molecular scaffold.

Cyclic peptides are crucial for the construction of potent and stable discontinuous epitope mimics. Peptide cyclization should improve both mimicry of the loop-like structure common in epitopes and their proteolytic stability. Two approaches for the cyclization of unprotected peptides containing two cysteine residues are described in **Chapter 2**. In the first approach, a bisbromobenzyl derivative is used as alkylating agent for the thiol moieties. The second approach uses a bromomaleimide derivative. The additional presence of an azide functionality in these cyclization agents allowed the resulting cyclic peptides to be introduced onto scaffolds using copper-catalyzed azide-alkyne cycloaddition (CuAAC).

A common strategy to correctly mimic the spatial structure of a complex discontinuous epitope is to incorporate (cyclic) peptides corresponding to an epitope loop onto a molecular scaffold. However, the number of methods to introduce peptides onto a scaffold in a highly controlled and convergent manner is still limited. **Chapter 3** describes a new approach to achieve this. The described method uses a silyl protection group strategy for the protection of alkynes, which allows for the sequential CuAAC ligation of azide-bearing peptides onto the TAC-scaffold. The use of a single ligation-method and the convergent synthesis demonstrate the robustness and convenience of this approach.

Chapter 4 describes a complete and improved synthesis of a new TAC-scaffold suitable for the sequential introduction of cyclic peptides. Based on the literature procedure for the synthesis of the original TAC-scaffold, we describe an optimized synthesis of the new TAC-scaffold, which contains three alkynes protected by a silyl protecting group strategy. Furthermore, compared to the scaffold described in Chapter 3, the linker length between the scaffold and the alkyne is shortened to a pentynoic acid moiety, which allows for easier comparison with previous work. Finally, cyclic peptides are sequentially introduced on the scaffold, resulting in a mimic of the CD4-binding site of the HIV protein gp120. The procedure for the sequential introduction of the cyclic peptides is improved by omitting the use of microwave irradiation for the ligation reaction. This resulted in an increased overall yield and a reduction of the number of purification steps, compared to the procedure described in Chapter 3.

Chapter 5 describes investigations into the biological activity of mimics of the CD4-binding site of the HIV gp120 protein. The mimics were synthesized using the method for synthesis of discontinuous epitope mimics described in Chapters 3 and 4. We describe the ability of our binding site mimics to interfere with the binding of natural gp120 to CD4 in an ELISA assay. We describe the influence that the relative positioning of the cyclic peptides on the scaffold has on the activity of the mimic. Furthermore, we show the importance of using cyclic peptides for the mimicry of epitopes consisting of loops to improve both the activity and the stability of the mimic. Finally, we describe a promising first attempt to assess the CD4-

binding site mimics using Isothermal Titration Calorimetry (ITC).

One of the most appealing applications of epitope mimics is the development of synthetic vaccines. In order to obtain the optimal immune response to synthetic compounds, they are often conjugated to a carrier protein. This conjugation is often achieved via a maleimide-thiol reaction. **Chapter 6** describes a first attempt at the synthesis of an epitope mimic with a thiol-containing arm for the ligation to a carrier protein.

References

1 T. J. Kindt, R. A. Goldsby and B. A. Osborne, in *Kuby Immunology*, W.H. Freeman & Company, New York, 6th Ed., 2007, p. 84.

2 I. Roitt, J. Brostoff and D. Male, in *Immunology*, Mosby, Edinburgh, 6th Ed., 2001, p. 73.

3 W. Ding, X. Huang, X. Yang, J. J. Dunn, B. J. Luft, S. Koide and C. L. Lawson, *J. Mol. Biol.*, 2000, **302**, 1153–1164.

4 M. Van Regenmortel, *Open Vaccine J.*, 2009, **2**, 33–44.

5 M. Van Regenmortel, in *Epitope Mapping Protocols*, eds. M. Schutkowski and U. Reineke, Humana Press, Totowa, NJ, 2nd Ed., 2009, vol. 524, pp. 3–20.

6 M. Stumpf, T. Thorne, E. de Silva, R. Stewart, H. J. An, M. Lappe and C. Wiuf, *Proc. Natl. Acad. Sci. U. S. A.*, 2008, **105**, 6959–6964.

7 P. R. Dormitzer, G. Grandi and R. Rappuoli, *Nat. Rev. Microbiol.*, 2012, **10**, 807–813.

8 P. Moyle and I. Toth, *ChemMedChem*, 2013, **8**, 360–376.

9 J. Neefjes and H. Ovaa, *Nat. Chem. Biol.*, 2013, **9**, 769–75.

10 D. R. Flower, *Nat. Chem. Biol.*, 2013, **9**, 749–53.

11 P. Thiel, M. Kaiser and C. Ottmann, *Angew. Chem. Int. Ed.*, 2012, **51**, 2012–2018.

12 L. Milroy, T. N. Grossmann, S. Hennig, L. Brunsveld and C. Ottmann, *Chem. Rev.*, 2014, **114**, 4695–4748.

13 D. Rognan, *Med. Chem. Commun.*, 2015, **6**, 51–60.

14 C. Sheng, G. Dong, Z. Miao, W. Zhang and W. Wang, *Chem. Soc. Rev.*, 2015, **44**, 8238–8259.

15 D. J. Craik, D. P. Fairlie, S. Liras and D. Price, *Chem. Biol. Drug Des.*, 2013, **81**, 136–147.

16 L. Nevola and E. Giralt, *Chem. Commun.*, 2015, **51**, 3302–3315.

17 E. Giralt, *J. Pept. Sci.*, 2015, **21**, 447–453.

18 N. London, B. Raveh and O. Schueler-Furman, *Curr. Opin. Chem. Biol.*, 2013, **17**, 952–959.

19 M. Pelay-Gimeno, A. Glas, O. Koch and T. N. Grossmann, *Angew. Chem. Int. Ed.*, 2015, **54**, 8896–8927.

20 R. Haubner, D. Finsinger and H. Kessler, *Angew. Chem. Int. Ed.*, 1997, **36**, 1375–1389.

21 C. Hunke, T. Hirsch and J. Eichler, *ChemBioChem*, 2006, **7**, 1258–1264.

22 R. Hancock, H. C. Bertrand, T. Tsujita, S. Naz, A. El-Bakry, J. Laoruchupong, J. D. Hayes and G. Wells, *Free Radic. Biol. Med.*, 2012, **52**, 444–51.

23 R. Hancock, M. Schaap, H. Pfister and G. Wells, *Org. Biomol. Chem.*, 2013, **11**, 3553–3557.

24 G. E. Mulder, J. A. W. Kruijtzer and R. M. J. Liskamp, *Chem. Commun.*, 2012, **48**, 10007–10009.

25 M. Hijnen, D. J. Van Zoelen, C. Chamorro, P. Van Gageldonk, F. R. Mooi, G. Berbers and R. M. J. Liskamp, *Vaccine*, 2007, **25**, 6807–6817.

26 D.-J. Van Zoelen, M. R. Egmond, R. J. Pieters and R. M. J. Liskamp, *ChemBioChem*, 2007, **8**, 1950–1956.

27 R. Franke, T. Hirsch and J. Eichler, *J. Recept. Signal Tr. R.*, 2006, **26**, 453–460.

28 J. Eichler, *Curr. Opin. Chem. Biol.*, 2008, **12**, 707–713.

29 P. Timmerman, S. G. Shochat, J. Desmet, R. Barderas, J. I. Casal, R. H. Meloen and D. Altschuh, *J. Mol. Recognit.*, 2010, **23**, 559–568.

30 P. Timmerman, R. Barderas, J. Desmet, D. Altschuh, S. Shochat, M. J. Hollestelle, J. W. M. Höppener, A.

Monasterio, J. I. Casal and R. H. Meloen, *J. Biol. Chem.*, 2009, **284**, 34126–34134.

31 J. J. Adams and S. S. Sidhu, *Curr. Opin. Struct. Biol.*, 2014, **24**, 1–9.

32 P. J. Mcenaney, K. J. Fitzgerald, A. X. Zhang, E. F. Douglass, W. Shan, A. Balog, M. D. Kolesnikova and D. A. Spiegel, *J. Am. Chem. Soc.*, 2014, **136**, 18034–18043.

33 L. Lo Conte, C. Chothia and J. Janin, *J. Mol. Biol.*, 1999, **285**, 2177–2198.

34 W. L. Delano, *Curr. Opin. Struct. Biol.*, 2002, **12**, 14–20.

35 A. Bogan and K. Thorn, *J. Mol. Biol.*, 1998, **280**, 1–9.

36 B. Ma, T. Elkayam, H. Wolfson and R. Nussinov, *Proc. Natl. Acad. Sci. U. S. A.*, 2003, **100**, 5772–5777.

37 J. Villén, E. Borràs, W. M. M. Schaaper, R. H. Meloen, M. Dávila, E. Domingo, E. Giralt and D. Andreu, *ChemBioChem*, 2002, **3**, 175–182.

38 T. G. Johns, T. E. Adams, J. R. Cochran, N. E. Hall, P. A. Hoyne, M. J. Olsen, Y.-S. Kim, J. Rothacker, E. C. Nice, F. Walker, G. Ritter, A. a Jungbluth, L. J. Old, C. W. Ward, A. W. Burgess, K. D. Wittrup and A. M. Scott, *J. Biol. Chem.*, 2004, **279**, 30375–30384.

39 V. Chitarra, P. M. Alzari, G. A. Bentley, T. N. Bhat, J.-L. Eiselé, A. Houdusse, J. Lescar, H. Souchon and R. J. Poljak, *Proc. Natl. Acad. Sci. U. S. A.*, 1993, **90**, 7711–7715.

40 P. D. Kwong, R. Wyatt, J. Robinson, R. W. Sweet, J. Sodroski and W. A. Hendrickson, *Nature*, 1998, **393**, 648–659.

41 J. Becerril and A. D. Hamilton, *Angew. Chem. Int. Ed.*, 2007, **46**, 4471–4473.

42 J. D. Sadowsky, W. D. Fairlie, E. B. Hadley, H.-S. Lee, N. Umezawa, Z. Nikolovska-Coleska, S. Wang, D. C. S. Huang, Y. Tomita and S. H. Gellman, *J. Am. Chem. Soc.*, 2007, **129**, 139–154.

43 H. Hori, D. R. Keene, L. Y. Sakai, M. K. Wirtz, H. P. Bächinger, M. Godfrey and D. W. Hollister, *Mol. Immunol.*, 1992, **29**, 759–770.

44 F. A. Robey, T. Kelson-Harris, P. P. Roller and M. Robert-Guroff, *J. Biol. Chem.*, 1995, **270**, 23918–23921.

45 C. Dreyfus, N. S. Laursen, T. Kwaks, D. Zuijdgeest, R. Khayat, D. C. Ekiert, J. H. Lee, Z. Metlagel, M. V Bujny, M. Jongeneelen, R. van der Vlugt, M. Lamrani, H. J. W. M. Korse, E. Geelen, Ö. Sahin, M. Sieuwerts, J. P. J. Brakenhoff, R. Vogels, O. T. W. Li, L. L. M. Poon, M. Peiris, W. Koudstaal, A. B. Ward, I. A. Wilson, J. Goudsmit and R. H. E. Friesen, *Science*, 2012, **337**, 1343–1348.

46 D. Corti, J. Voss, S. J. Gamblin, G. Codoni, A. Macagno, D. Jarrossay, S. G. Vachieri, D. Pinna, A. Minola, F. Vanzetta, C. Silacci, B. M. Fernandez-Rodriguez, G. Agatic, S. Bianchi, I. Giacchetto-Sasselli, L. Calder, F. Sallusto, P. Collins, L. F. Haire, N. Temperton, J. P. M. Langedijk, J. J. Skehel and A. Lanzavecchia, *Science*, 2011, **333**, 850–856.

47 S. Padavattan, S. Flicker, T. Schirmer, C. Madritsch, S. Randow, G. Reese, S. Vieths, C. Lupinek, C. Ebner, R. Valenta and Z. Markovic-Housley, *J. Immunol.*, 2009, **182**, 2141–2151.

48 V. Novitskaya, N. Makarava, A. Bellon, O. V Bocharova, I. B. Bronstein, R. A. Williamson and I. V Baskakov, *J. Biol. Chem.*, 2006, **281**, 15536–15545.

49 R. Kayed, E. Head, F. Sarsoza, T. Saing, C. W. Cotman, M. Necula, L. Margol, J. Wu, L. Breydo, J. L. Thompson, S. Rasool, T. Gurlo, P. Butler and C. G. Glabe, *Mol.Neurodegener.*, 2007, **2**, 18.

50 J. A. Robinson, *J. Pept. Sci.*, 2013, **19**, 127–140.

51 V. Tugarinov, A. Zvi, R. Levy and J. Anglister, *Nat. Struc. Biol*, 1999, **6**, 331–335.

52 A. Jackson, T. Klonisch, A. Lapthorn, P. Berger, N. Isaacs, P. Delves, T. Lund and I. Roitt, *J. Reprod. Immunol.*, 1996, **31**, 21–36.

53 Y. Li, H. Li, F. Yang, S. J. Smith-Gill and R. A. Mariuzza, *Nat. Struc. Biol*, 2003, **10**, 482–488.

54 R. Pejchal, K. J. Doores, L. M. Walker, R. Khayat, P.-S. Huang, S.-K. Wang, R. L. Stanfield, J.-P. Julien, A. Ramos, M. Crispin, R. Depetris, U. Katpally, A. Marozsan, A. Cupo, S. Maloveste, Y. Liu, R. McBride, Y. Ito, R. W. Sanders, C. Ogohara, J. C. Paulson, T. Feizi, C. N. Scanlan, C.-H. Wong, J. P. Moore, W. C. Olson, A. B. Ward, P. Poignard, W. R. Schief, D. R. Burton and I. A. Wilson, *Science*, 2011, **334**, 1097–1103.

55 H. Pantua, J. Diao, M. Ultsch, M. Hazen, M. Mathieu, K. McCutcheon, K. Takeda, S. Date, T. K. Cheung,

Q. Phung, P. Hass, D. Arnott, J.-A. Hongo, D. J. Matthews, A. Brown, A. H. Patel, R. F. Kelley, C. Eigenbrot and S. B. Kapadia, *J. Mol. Biol.*, 2013, **425**, 1899–914.
56 P. Delmastro, a Meola, P. Monaci, R. Cortese and G. Galfrè, *Vaccine*, 1997, **15**, 1276–1285.
57 R. H. Maier, C. J. Maier, R. Rid, H. Hintner, J. W. Bauer and K. Önder, *J. Biomol. Screen.*, 2010, **15**, 418–426.
58 R. Volkmer, *ChemBioChem*, 2009, **10**, 1431–1442.
59 Y. Li, H. Li, S. Smith-Gill and R. Mariuzza, *Biochemistry*, 2000, **39**, 6296–6309.
60 D. Ekiert, R. Friesen and G. Bhabha, *Science*, 2011, **333**, 843–850.
61 O. Rosen and J. Anglister, in *Epitope Mapping Protocols*, eds. M. Schutkowski and U. Reineke, Humana Press, Totowa, NJ, 2nd Ed., 2009, vol. 524, pp. 37–57.
62 O. Rosen, M. Sharon, S. R. Quadt-Akabayov and J. Anglister, *Proc. Natl. Acad. Sci. U. S. A.*, 2006, **103**, 13950–13955.
63 B. Zilber, T. Scherf, M. Levitt and J. Anglister, *Biochemistry*, 1990, **29**, 10032–10041.
64 A. Zvi, I. Kustanovich, D. Feigelson, R. Levy, M. Eisenstein, S. Matsushita, P. Richalet-Sécordel, M. H. van Regenmortel and J. Anglister, *Eur. J. Biochem.*, 1995, **229**, 178–187.
65 A. Zvi, V. Tugarinov, G. A. Faiman, A. Horovitz and J. Anglister, *Eur. J. Biochem.*, 2000, **267**, 767–779.
66 E. O. Hochleitner, C. Borchers, C. Parker, R. J. Bienstock and K. B. Tomer, *Protein Sci.*, 2000, **9**, 487–496.
67 E. O. Hochleitner, M. K. Gorny, S. Zolla-Pazner and K. B. Tomer, *J. Immunol.*, 2000, **164**, 4156–4161.
68 C. E. Parker, D. Papac, S. K. Trojak and K. B. Tomer, *J. Immunol.*, 1996, **157**, 198–206.
69 C. Hager-Braun and K. B. Tomer, *Expert Rev. Proteomics*, 2005, **2**, 745–756.
70 M. J. Chalmers, S. A. Busby, B. D. Pascal, G. M. West and P. R. Griffin, *Expert Rev. Proteomics*, 2011, **8**, 43–59.
71 K. M. Downard, B. Morrissey and A. B. Schwahn, *Mass Spectrom. Rev.*, 2009, **28**, 35–49.
72 M. Dragusanu, B.-A. Petre, S. Slamnoiu, C. Vlad, T. Tu and M. Przybylski, *J. Am. Soc. Mass Spectrom.*, 2010, **21**, 1643–1648.
73 X. Lu, M. R. DeFelippis and L. Huang, *Anal. Biochem.*, 2009, **395**, 100–107.
74 N. Olsson, S. Wallin, P. James, C. A. K. Borrebaeck and C. Wingren, *Protein Sci.*, 2012, **21**, 1897–1910.
75 C. Katz, L. Levy-Beladev, S. Rotem-Bamberger, T. Rito, S. G. D. Rüdiger and A. Friedler, *Chem. Soc. Rev.*, 2011, **40**, 2131–2145.
76 M. Paschke, *Appl. Microbiol. Biotechnol.*, 2006, **70**, 2–11.
77 M. Houimel and K. Dellagi, *Vaccine*, 2009, **27**, 4648–4655.
78 C. Heinis, T. Rutherford, S. Freund and G. Winter, *Nat. Chem. Biol.*, 2009, **5**, 502–507.
79 M. Xue, X. Shi, J. Zhang, Y. Zhao, H. Cui, S. Hu, H. Gao, X. Cui and Y.-F. Wang, *PLoS One*, 2012, **7**, e49842.
80 K. Dorgham, I. Dogan, N. Bitton, C. Parizot, V. Cardona, P. Debré, O. Hartley and G. Gorochov, *Aids Res. Hum. Retrov.*, 2005, **21**, 82–92.
81 R. Liu and J. Hu, *J. Proteomics Bioinform.*, 2011, **04**, 10–15.
82 I. Mayrose, O. Penn, E. Erez, N. D. Rubinstein, T. Shlomi, N. T. Freund, E. M. Bublil, E. Ruppin, R. Sharan, J. M. Gershoni, E. Martz and T. Pupko, *Bioinformatics*, 2007, **23**, 3244–3246.
83 V. Moreau, C. Granier, S. Villard, D. Laune and F. Molina, *Bioinformatics*, 2006, **22**, 1088–1095.
84 J. P. Langeveld, J. I. Casal, A. D. M. E. Osterhaus, E. Cortés, R. de Swart, C. Vela, K. Dalsgaard, W. C. Puijk, W. M. M. Schaaper and R. H. Meloen, *J. Virol.*, 1994, **68**, 4506–4513.
85 R. Cardoso, M. I. Homsi-Brandeburgo, V. M. Rodrigues, W. B. Santos, G. L. R. Souza, C. R. Prudencio, A. C. S. Siquieroli and L. R. Goulart, *Toxicon*, 2009, **53**, 254–261.
86 T. T. Wang, G. S. Tan, R. Hai, N. Pica, L. Ngai, D. C. Ekiert, I. A. Wilson, A. García-Sastre, T. M. Moran and P. Palese, *Proc. Natl. Acad. Sci. U. S. A.*, 2010, **107**, 18979–18984.
87 N. Gaidzik, U. Westerlind and H. Kunz, *Chem. Soc. Rev.*, 2013, **42**, 4421–4442.
88 A.-B. M. Abdel-Aal, D. El-Naggar, M. Zaman, M. Batzloff and I. Toth, *J. Med. Chem*, 2012, **55**, 6968–6974.

89 D. Hans, P. Young and D. Fairlie, *Med. Chem.*, 2006, **2**, 627–646.

90 C. Peri, P. Gagni, F. Combi, A. Gori, M. Chiari, R. Longhi, M. Cretich and G. Colombo, *ACS Chem. Biol.*, 2013, **8**, 397–404.

91 M. B. Irving, L. Craig, A. Menendez, B. P. Gangadhar, M. Montero, N. E. Van Houten and J. K. Scott, *Mol. Immunol.*, 2010, **47**, 1137–1148.

92 Y. Cao, Z. Lu, P. Li, P. Sun, Y. Fu, X. Bai, H. Bao, Y. Chen, D. Li and Z. Liu, *J. Virol. Methods*, 2012, **185**, 124–128.

93 R. Franke, T. Hirsch, H. Overwin and J. Eichler, *Angew. Chem. Int. Ed.*, 2007, **46**, 1253–1255.

94 C. J. Brown, S. T. Quah, J. Jong, A. M. Goh, P. C. Chiam, K. H. Khoo, M. L. Choong, M. a Lee, L. Yurlova, K. Zolghadr, T. L. Joseph, C. S. Verma and D. P. Lane, *ACS Chem. Biol.*, 2012, 2–8.

95 L. D. Walensky, A. L. Kung, I. Escher, T. J. Malia, S. Barbuto, R. D. Wright, G. Wagner, G. L. Verdine and S. J. Korsmeyer, *Science*, 2004, **305**, 1466–1470.

96 H. Jo, N. Meinhardt, Y. Wu, S. Kulkarni, X. Hu, K. E. Low, P. L. Davies, W. F. Degrado and D. C. Greenbaum, *J. Am. Chem. Soc.*, 2012, **134**, 17704–17713.

97 C. E. Schafmeister, J. Po and G. L. Verdine, *J. Am. Chem. Soc.*, 2000, **122**, 5891–5892.

98 P. S. Kutchukian, J. S. Yang, G. L. Verdine and E. I. Shakhnovich, *J. Am. Chem. Soc.*, 2009, **131**, 4622–4627.

99 V. Haridas, *Eur. J. Org. Chem.*, 2009, **2009**, 5112–5128.

100 R. M. J. Liskamp, D. T. S. Rijkers, J. A. W. Kruijtzer and J. Kemmink, *ChemBioChem*, 2011, **12**, 1626–1653.

101 J. A. Robinson, S. Demarco, F. Gombert, K. Moehle and D. Obrecht, *Drug Discov. Today*, 2008, **13**, 944–951.

102 A. Ghasparian, T. Riedel, J. Koomullil, K. Moehle, C. Gorba, D. I. Svergun, A. W. Perriman, S. Mann, M. Tamborrini, G. Pluschke and J. A. Robinson, *ChemBioChem*, 2011, **12**, 100–109.

103 J. Robinson, *J. Pept. Sci.*, 2013, **19**, 127–140.

104 N. Sewald and H.-D. Jakubke, in *Peptides, Chemistry and Biology*, Wiley-VCH, Weinheim, 2002, p. 311.

105 R. Liskamp, D. T. S. Rijkers and S. E. Bakker, in *Modern Supramolecular Chemistry: Strategies for Macrocycle Synthesis*, eds. F. Diederich, P. J. Stang and R. R. Tykwinski, Wiley-VCH, Weinheim, 2008, pp. 1–27.

106 J. Villén, R. a Rodríguez-Mias, J. I. Núñez, E. Giralt, F. Sobrino and D. Andreu, *Chem. Biol*, 2006, **13**, 815–823.

107 C. J. White and A. K. Yudin, *Nat. Chem.*, 2011, **3**, 509–524.

108 L. R. Whitby, K. E. Boyle, L. Cai, X. Yu, M. Gochin and D. L. Boger, *Bioorg. Med. Chem. Lett.*, 2012, **22**, 2861–2865.

109 F. Campbell, J. P. Plante, T. A. Edwards, S. L. Warriner and A. J. Wilson, *Org. Biomol. Chem.*, 2010, **8**, 2344–2351.

110 K. Long, T. A. Edwards and A. J. Wilson, *Bioorg. Med. Chem.*, 2012.

111 A. Barnard, K. Long, H. L. Martin, J. A. Miles, T. A. Edwards, D. C. Tomlinson, A. Macdonald and A. J. Wilson, *Angew. Chem. Int. Ed.*, 2015, **54**, 2960–2965.

112 C. W. Robinson, C. S. Rye, N. E. A. Chessum and K. Jones, *Org. Biomol. Chem.*, 2015, **13**, 7402–7407.

113 W. A. Loughlin, J. D. A. Tyndall, M. P. Glenn and D. P. Fairlie, *Chem. Rev.*, 2004, **104**, 6085–6118.

114 L. E. J. Smeenk, D. Timmers-Parohi, J. J. Benschop, W. C. Puijk, H. Hiemstra, J. H. van Maarseveen and P. Timmerman, *ChemBioChem*, 2015, **16**, 91–99.

115 P. Van de Vijver, M. Schmitt, D. Suylen, L. Scheer, M. C. L. G. D. Thomassen, L. J. Schurgers, J. H. Griffin, R. R. Koenen and T. M. Hackeng, *J. Am. Chem. Soc.*, 2012, **134**, 19318–19321.

116 R. Franke, C. Doll, V. Wray and J. Eichler, *Org. Biomol. Chem*, 2004, **2**, 2847–2851.

117 M. Mutter and S. Vuilleumier, *Angew. Chem. Int. Ed.*, 1989, **28**, 535–554.

118 D. Boturyn, J.-L. Coll, E. Garanger, M.-C. Favrot and P. Dumy, *J. Am. Chem. Soc.*, 2004, **126**, 5730–5739.

119 Y. Singh, G. T. Dolphin, J. Razkin and P. Dumy, *ChemBioChem*, 2006, **7**, 1298–1314.

120 H. S. Park, Q. Lin and A. D. Hamilton, *J. Am. Chem. Soc.*, 1999, **121**, 8–13.
121 P. Timmerman, W. C. Puijk, R. S. Boshuizen, P. Van Dijken, J. W. Slootstra, F. J. Beurskens, P. W. H. I. Parren, A. Huber, M. F. Bachmann and R. H. Meloen, *Open Vaccine J.*, 2009, **2**, 56–67.
122 P. Timmerman, J. Beld, W. C. Puijk and R. H. Meloen, *ChemBioChem*, 2005, **6**, 821–824.
123 C. Chamorro, J. A. W. Kruijtzer, M. Farsaraki, J. Balzarini and R. M. J. Liskamp, *Chem. Commun.*, 2009, 821–823.
124 G. E. Mulder, H. C. Quarles van Ufford, J. van Ameijde, A. J. Brouwer, J. A. W. Kruijtzer and R. M. J. Liskamp, *Org. Biomol. Chem.*, 2013, **11**, 2676–2684.
125 V. Baeriswyl and C. Heinis, *ChemMedChem*, 2013, **8**, 377–384.
126 T. L. Aboye, H. Ha, S. Majumder, F. Christ, Z. Debyser, A. Shekhtman, N. Neamati and J. A. Camarero, *J. Med. Chem*, 2012, **55**, 10729–10734.
127 P. Ghosh and A. Hamilton, *J. Am. Chem. Soc.*, 2012, **134**, 13208–13211.
128 A. Angelini, P. Diderich, J. Morales-Sanfrutos, S. Thurnheer, D. Hacker, L. Menin and C. Heinis, *Bioconjug. Chem.*, 2012, **23**, 1856–1863.
129 A. Nuccitelli, R. Cozzi, L. J. Gourlay, D. Donnarumma, F. Necchi, N. Norais, J. L. Telford, R. Rappuoli, M. Bolognesi, D. Maione, G. Grandi and C. D. Rinaudo, *Proc. Natl. Acad. Sci. U. S. A.*, 2011, **108**, 10278–10283.

2

Chapter 2

Synthesis of azide-functionalized cyclic peptides by chemo-selective modification of cystein residues

Parts of this chapter have been published in:

P.R. Werkhoven, H. van de Langemheen, S. van der Wal, J.A.W. Kruijtzer, R.M.J. Liskamp
J. Pept. Sci. 2014, 20, 235-239
and
P.R. Werkhoven, M. Elwakiel, T.J. Meuleman, H.C. Quarles van Ufford, J.A.W. Kruijtzer,
R.M.J. Liskamp Org. Biomol. Chem. 2016, 14, 701-710

2.1 Introduction

Interest in using peptides as therapeutics has grown significantly over the past decade. These molecules of so-called "intermediate size" fill the gap between the small molecules which obey Lipinski's rule of five and large biomolecules like antibodies.[1]

Especially cyclic peptides are of great interest when it comes to biological applications. Cyclization of a peptide can have great influence on the biological activity, availability, and stability of the peptide.[2] Cyclization may for example improve the permeability through intestinal membranes[3] or the penetration of the blood-brain barrier,[4] or it may increase the proteolytic stability or the bioactivity of the peptide.[5–7]

Although cyclic peptides are widely used in many areas, their synthesis and purification remains challenging. The accessibility of a cyclic peptide is largely determined by its amino acid sequence, desired ring size, and cyclization strategy. Strategies for peptide cyclization can be divided into four categories, based on which connection is made: head-to-tail, head-to-side chain, side chain-to-tail, and side chain-to-side chain (Figure 1).[8] A large number of macrocyclization procedures is available to make the desired connection and this number is still growing.[8,9] Commonly used reactions for peptide cyclization are macrolactamization, macrolactonization, and disulfide formation, but also orthogonal ligation strategies, like copper-catalyzed azide-alkyne cycloaddition (CuAAC), native chemical ligation, oxime ligation, ring-closing metathesis, and Staudinger ligation, have been employed to form macrocycles.[8–13]

The amino acid sequence is a major factor in the choice of cyclization strategy, because it determines what reactive groups are available. The reactive moieties can be used for cyclization directly or can be modified to accommodate other reactive groups. The side chain moieties might also interfere with the desired cyclization reaction, in which case an appropriate protection strategy will have to be employed.

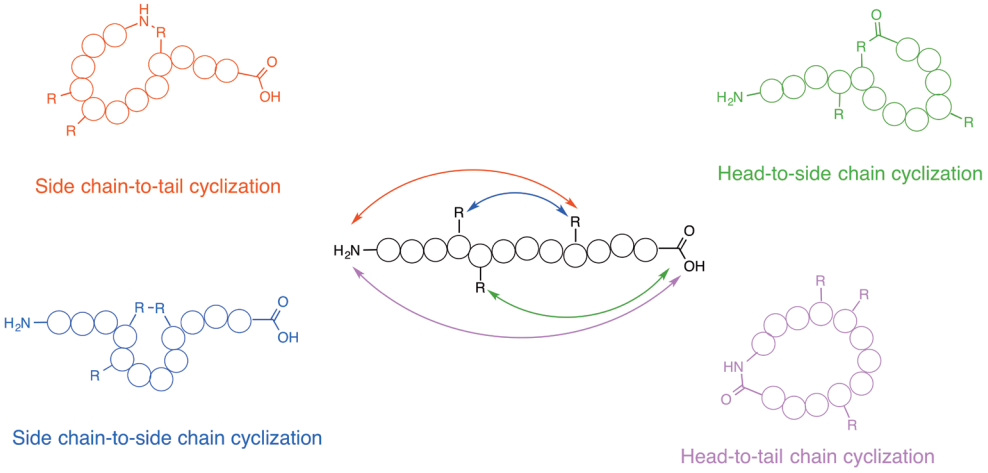

Figure 1. Four types of peptide cyclization.

In the field of protein or epitope mimicry, cyclic peptides may offer an added benefit: they may better represent the natural configuration of the protein/epitope that is mimicked. This increases the similarity to the epitope and thus the mimicry. Depending on the cyclization strategies the peptide may approach the desired secondary structure in order to fit the structure of the epitope.[14] Naturally occurring motifs like loops,[15,16] beta-strands/hairpins,[17] and helices[18,19] can be induced by cyclization of the peptide (see also Chapter 1).

As described in Chapter 1, a common approach for the synthesis of discontinuous epitope mimics is to attach multiple cyclic peptides on a molecular scaffold. For this the peptides have to be equipped with a ligation handle. In this work, we chose CuAAC as ligation method because this reaction between an azide and an alkyne is fast, efficient, and orthogonal to the side chain functionalities present in the peptide. Furthermore, CuAAC has been used successfully in combination with the TAC-scaffold.[16,20] For the ligation either the peptide has to be equipped with an azide and the scaffold with an alkyne or vice versa. In this work, we chose to equip the peptide with an azide because alkynes can be protected with silyl-based protecting groups. This will allow for orthogonal ligation on a scaffold containing multiple (protected) alkynes (Chapter 3).

This chapter describes the development of methods for the side chain-to-side chain macrocyclization of peptides containing two cysteine residues and the simultaneous introduction of an azide moiety for the attachment to an alkyne-containing scaffold.

2.2 Results and discussion

2.2.1 Benzylic dibromide cyclization

An elegant method of peptide cyclization, developed by Timmerman et al., is the "Chemical Linkage of Peptides onto Scaffolds" or CLIPS-method.[21] This method uses the thiol moieties of cysteine residues combined with benzylic bromides to cyclize a peptide in a side chain-to-side chain fashion (Scheme 1). The reaction between the thiol and the benzylic bromide has several clear advantages. The reaction is very quick (5-10 minutes), works in an aqueous environment but also tolerates large quantities of organic solvents like MeCN, DMF and DMSO, can be carried out at room temperature and mild pH (7.5-8.0), and can be performed on fully unprotected peptides.[22] The scaffold has been further adapted to incorporate ligation handles and to improve the solubility in water.[23] Because of these advantages, this method has

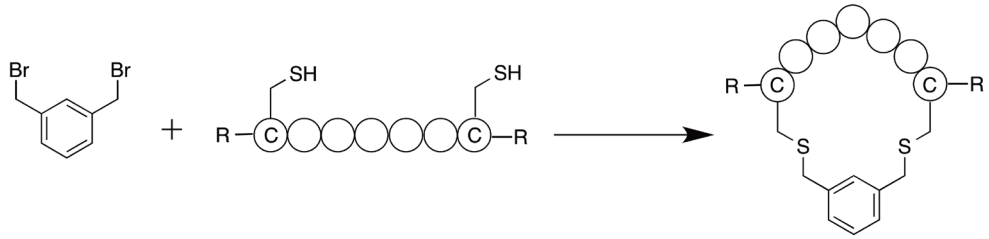

Scheme 1. Peptide cyclization by the CLIPS method. The peptide is cyclized side chain to side chain by reaction between an benzylic bisbromide and the thiol moieties of two cysteine residues.

been successfully applied in many fields, like epitope mimics[24] and α-helix stabilization.[19] The reaction can even be performed on peptides expressed on proteins[25,26] or on the outside of bacterial phage for the purpose of modifying phage displayed peptides/proteins.[27–29]

Inspired by this versatile reaction, we wanted to expand on this by attaching an azide on the benzylic bisbromide. This allows for the simultaneous cyclization and incorporation of the azide functionality. However, other ligation handles may also be attached to the benzylic bisbromide. To obtain the azide-functionalized benzylic bisbromide ,we started from commercially available 1,3,5-tris(bromomethyl)benzene (**1**). The azide was introduced by a nucleophilic substitution on tribromide **1** with sodium azide (Scheme 2). Purification was done by column chromatography using a slow flow because of similar Rf values of the product, starting material, and side-product, which yielded bisbromide **2** in a 42% yield.

Bisbromide **2** could then be applied for the cyclization of peptides (Scheme 3). The desired peptide sequences were flanked by a cysteine residue on each side. The peptides were synthesized using standard Fmoc/tBu chemistry on a Rink amide resin and the N-terminus was acetylated using Ac_2O. The peptide was then cleaved and deprotected using a mixture of TFA, EDT, TIS and water. During first attempts with this method, the crude linear peptide was purified using preparative HPLC before the cyclization reaction. Later it was found that for most peptides this was not necessary and the yield did not drop when the crude linear peptide mixture was used instead of the purified linear peptide.

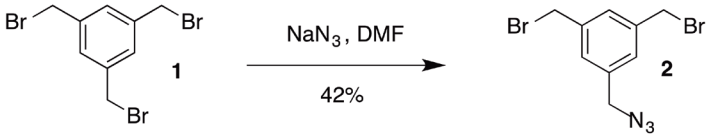

Scheme 2. Synthesis of azide-functionalized bisbromide.

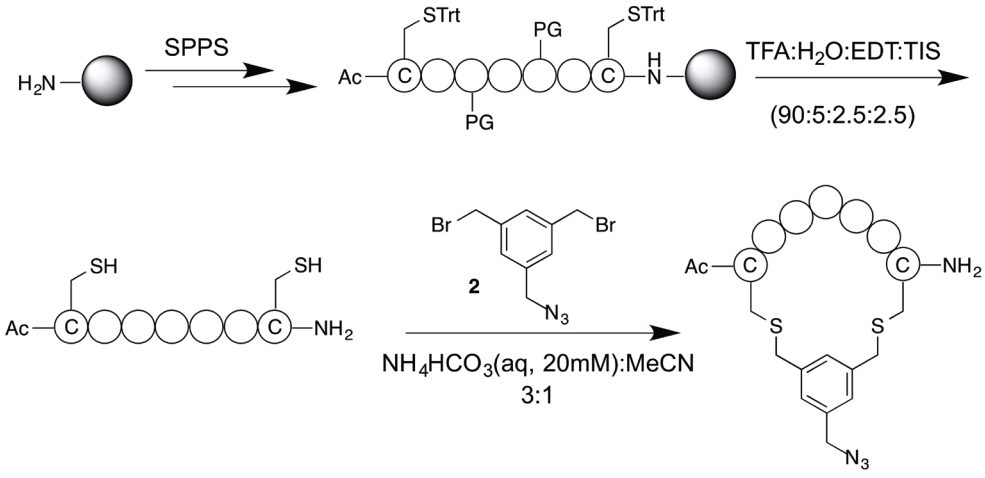

Scheme 3. Synthesis of azide-functionalized cyclic peptides.

Table 1. The six synthesized cyclic peptides were based on the epitope sequences of the pertactin protein and the HIV gp120 protein. General structure of the azide-bearing cyclic peptides (right).

Linear sequence	Sequence origin	Yield
Ac-CGGFGPC-NH_2 (**3**)	Pertussis Pertactin	17%
Ac-CGERQHC-NH_2 (**4**)	Pertussis Pertactin	14%
Ac-CGDTWDDDC-NH_2 (**5**)	Pertussis Pertactin	26%
Ac-CLTRDGGKC-NH_2 (**6**)	HIV gp120	34%
H-CINMWQEVGKAC-NH_2 (**7**)	HIV gp120	17%
Ac-CSGGDPEIVTC-NH_2 (**8**)	HIV gp120	29%

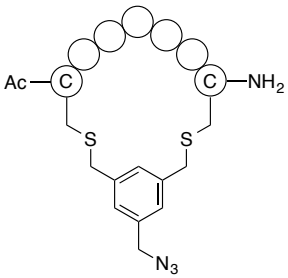

The peptide was cyclized using conditions similar to those of the original CLIPS-method.[21] The linear peptide was dissolved in a mixture of aqueous ammonium bicarbonate (20mM) and acetonitrile to obtain a peptide concentration of 1 mM. A solution of bisbromide **2** was then added to the mixture to cyclize the peptide. Next, the peptide was purified using preparative HPLC.

Using this method, six peptides were synthesized (Table 1), each corresponding to a part of either the Pertusiss Pertactin (Chapter 3) or the HIV gp120 protein (Chapters 4 and 5) epitope. The peptides consisted of the amino acids as they occur in the peptide segments of the epitope, flanked by cysteine residues, and had ring sizes varying between 7 and 12 amino acids (including the two flanking cysteines). Yields of purified cyclic peptides varied, depending on the sequence, between 14 and 34%, which is excellent considering the number of steps required starting from the bare resin. This corresponded to 90-95% average yield per step. In conclusion, this method for the synthesis of azide-functionalized cyclic peptides works on crude unprotected peptides, provides excellent yields, and has a high sequence tolerance.

2.2.2 Bromomaleimide cyclization

The chemoselective reaction between a thiol and a maleimide moietie is well known and highly versatile and the maleimide motif is widely used in, for example, the chemical modification of cysteine residues of proteins in complex systems.[30–32] In recent years, the possibilities of the maleimide moiety have been expanded by the development of bromomaleimides (Figure 2).[33,34]

The different possibilities for the modification of a thiol with (bromo)maleimides are shown in Scheme 4. A standard maleimide moiety (**9**) reacts with a thiol in an irreversible manner, giving rise to Michael adduct **12**. A mono-bromomaleimide moiety **10** can first react with one thiol to form a thiomaleimide (**13**). The thiol can be regained by the treatment of the thiomaleimide with TCEP or an excess of a different thiol (e.g. mercaptoethanol or glutathione). The thiomaleimide (**13**) can also react with a second thiol to form a bisthioether **15**.[34] Bisbromomaleimide derivatives (**11**) can also react with two equivalent thiols, first forming a thiobromomaleimide **14** and then dithiomaleimide **15**. However, the thiols can be

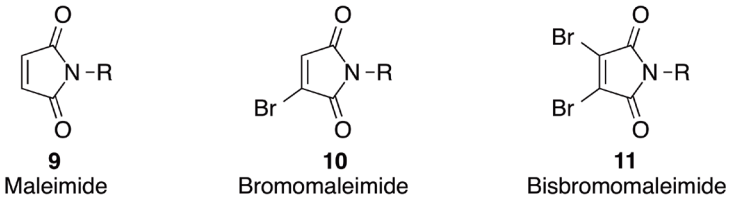

Figure 2. Structures of (bromo)maleimides.

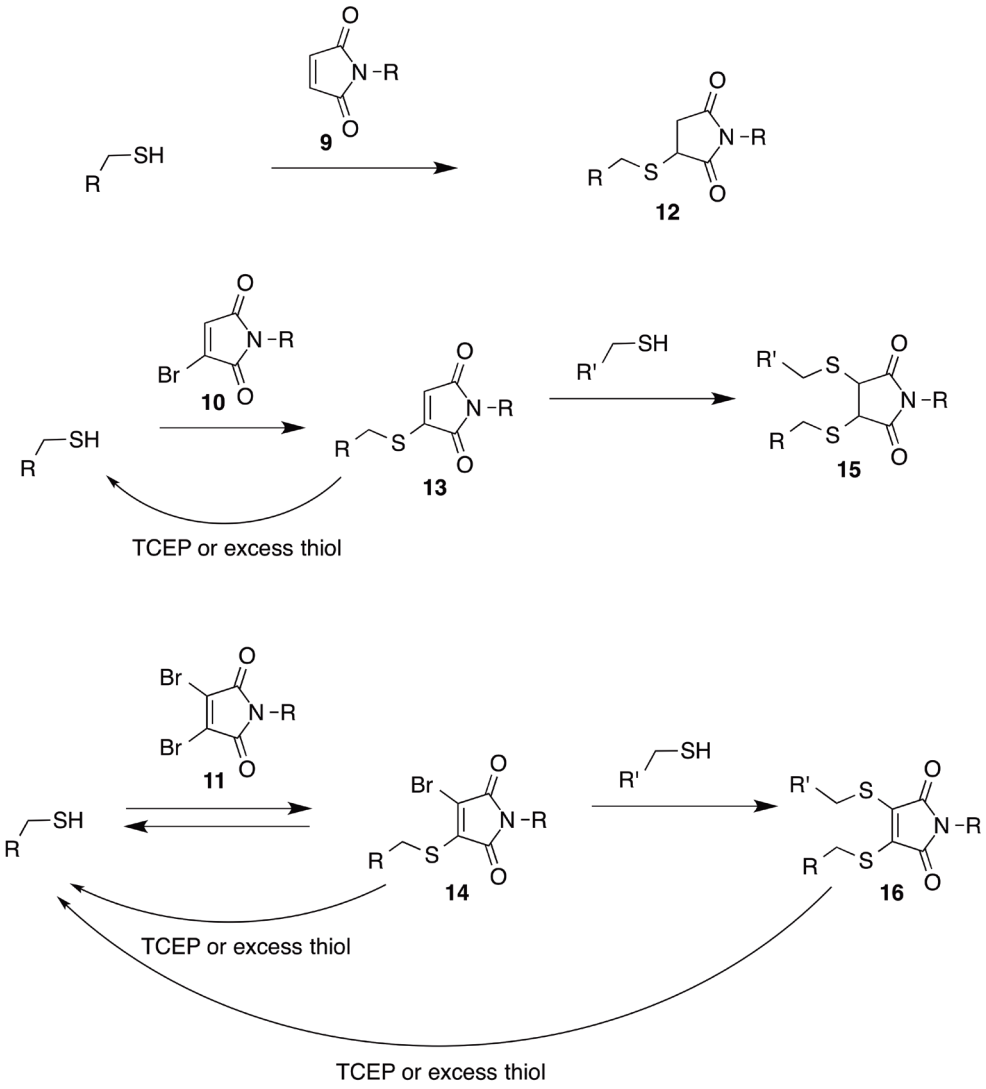

Scheme 4. Possibilities for the modification of thiol moieties by (bromo)maleimide derivatives. Bromomaleimides offer the possibility for reaction with multiple thiols and reversible reaction.

released again by treatment with TCEP or an excess of thiol.

The two thiol-attachment points in bromomaleimides **10** and **11** are suited for use in the cyclization of peptides bearing two cysteine residues. Furthermore, in the R-group on the nitrogen of the maleimide, an azide functionality may be incorporated in order to synthesize azide-containing cyclic peptides. In comparison with the previously described benzylic bromide reagent **2**, the maleimide moiety is more polar, which should improve the water solubility of the resulting cyclic peptides. Bisbromomaleimide derivatives (**11**) have been successfully used for the cyclization of peptides, but the reversible nature of the product made this approach less suitable for the synthesis of stable cyclic peptides.[35,36] Therefore, a monobromomaleimide derivative (**10**) is better suited for this purpose.[37] An azide-bearing monobromomaleimide derivative (**17**, Scheme 5) was designed that could be used for the cyclization of peptides that contain two cysteine residues.

The synthesis of the azide bromomaleimide derivative **17** (Scheme 6) started from bromopropylamine hydrobromide (**18**). First, the amine was protected with a Boc-group to afford Boc-protected propylamine **19**, after which the bromide was substituted for an azide to afford Boc-azidopropylamine (**20**). Finally, the Boc-group was removed through treatment with TFA to obtain 3-azidopropaneamine as the TFA salt (**21**).

Azidopropylamine **21** was then used to prepare bromomaleimide **12** (Scheme 7). To achieve this, amine **21** was reacted with bromomaleic anhydride (**22**) in acetic acid in order to form the maleimide moiety.[38,39] However, this reaction failed to yield the desired product **17** and attempts to render the reaction successful by changing the reaction conditions (solvent, temperature, and addition of base) also did not result in the desired product (**17**).

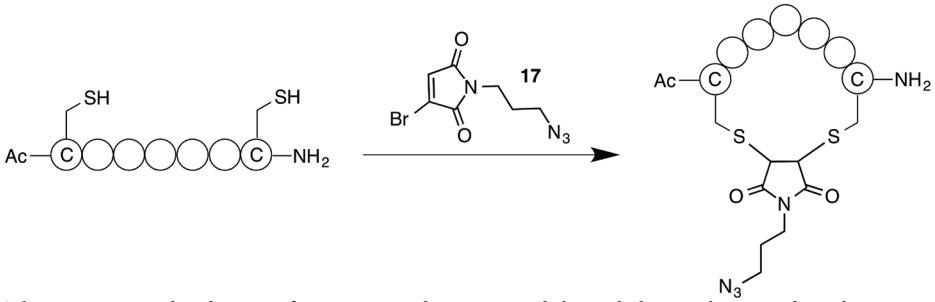

Scheme 5. Proposed cyclization of a two cysteine bearing peptide by azide-bearing bromomaleimide **17**.

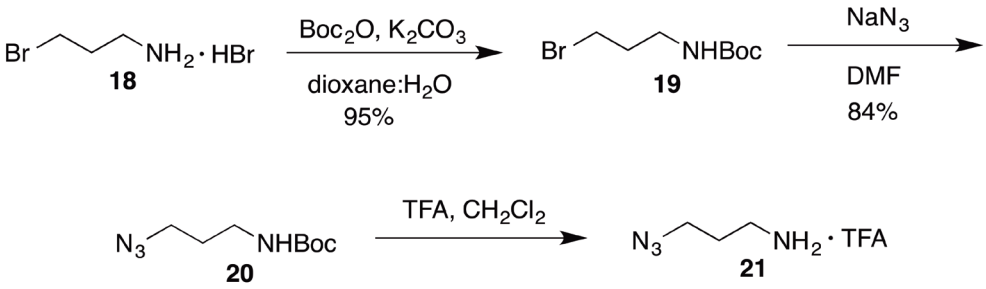

Scheme 6. Synthesis of 3-azidopropylamine (**21**).

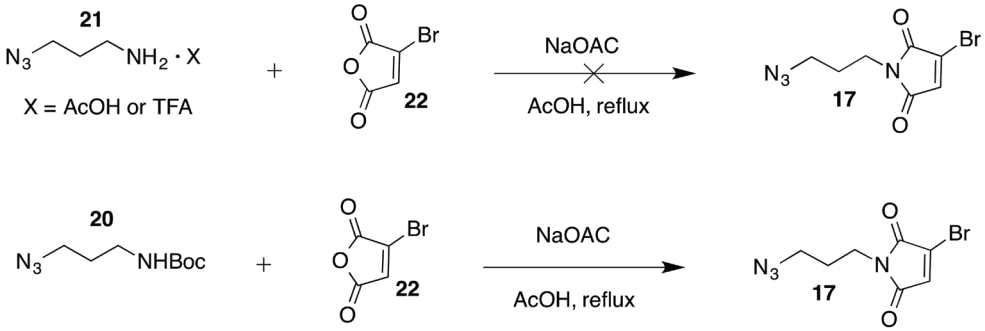

Scheme 7. Reactions of azidopropylamine (**21**) and Boc-azidopropylamine (**20**) with bromomaleic anhydride (**22**).

Also, attempts to remove the TFA salt or replace it with the acetate salt and react this with bromomaleic anhydride were also unsuccessful.

However, when Boc-protected compound **20** was reacted with bromomaleic anhydride (**22**) under the same conditions, substituted bromomaleimide **17** was obtained in good yield (61%).

The azide-functionalized monobromomaleimide derivative (**17**) was attempted to used for an attempt at the cyclization of a peptide. Peptide **23** (linear sequence Ac-CSGGDPEIVTC-NH_2, based on a HIV gp120 epitope) was treated with bromomaleimide **17** in an aqueous solution.[34] This reaction was performed a number of times, under slightly varying conditions, namely the pH of the solvent (ammonium bicarbonate, neutral water, and sodium acetate) and the reaction time (three hours and overnight). Nevertheless, the reaction never reached completion. The desired cyclic peptide **24** (Scheme 8) was usually observed as a minor peak. The major product was the single substitution product, i.e. linear peptide **25** (Scheme 8, note the maleimide can also be attached to the N-terminal cysteine). Another side-product that could occasionally be identified was peptide **26**, in which the maleimide moiety had hydrolyzed.

Interestingly, when the cyclization reaction was performed in a more basic solvent (aqueous 0.1 M Na_2HPO_4 and 1.5 M NaCl), cyclic product **24** was observed after 3 hours but was no longer observed when the reaction was left to stir overnight. This observation, together with the occasional observation of hydrolyzed product **26**, indicated the instability of the desired cyclic peptide. Therefore it was decided to not pursue this line of research further and return to our original cyclization using functionalized bisbromide **2**. Moreover, the instability of the dithioether product was later reported in the work of Nathani et al., who described the hydrolysis of mono-adduct **29** to ring-opened product **30**, depending on the substituent on the nitrogen of the maleimide (Scheme 9).[39] Furthermore, they rationalized the instability of the dithiosuccinimides (**31**) by the pK_a of the succinimide proton, resulting in the elimination of one of the thiols (Scheme 9).[40]

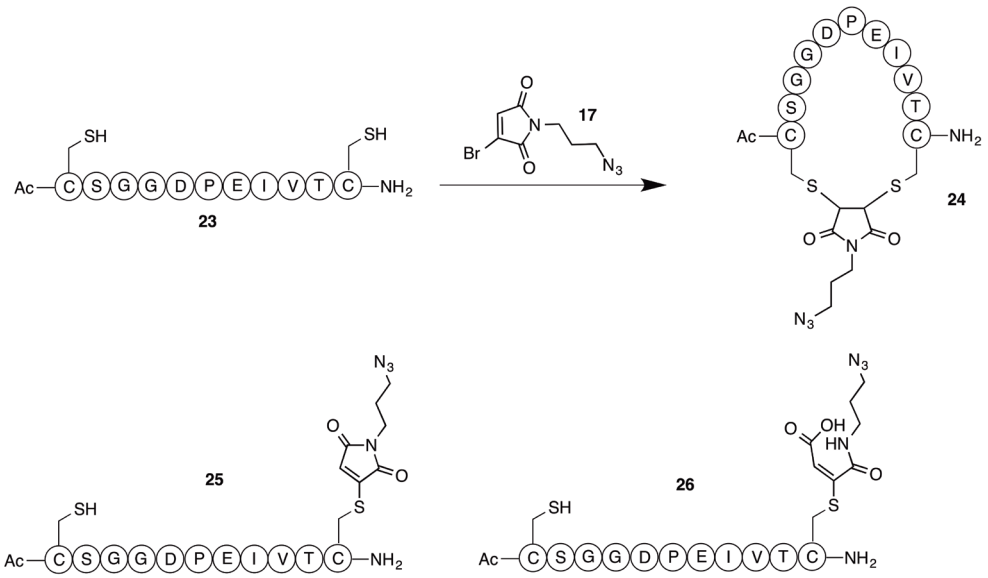

Scheme 8. Attempted peptide cyclization using bromomaleimide derivative **17**. Peptide **23** was treated with maleimide **17** to form cyclic peptide **24**. However, the major product of the reaction was linear peptide **25**. Hydrolyzed peptide **26** was also observed occasionally.

2.3 Conclusions

Despite being widely used in many fields of chemistry and biology and their potential therapeutic applications, the synthesis of cyclic peptides, irrespective of size and amino acid composition, remains challenging. This chapter describes two approaches to the synthesis of azide-bearing cyclic peptides, through chemoselective reactions on the thiols of cysteine side-chains. The first method was inspired by the CLIPS method and uses a benzylic dibromide as a thiol-alkylating agent. This method enabled a fast and efficient synthesis of azide-containing cyclic peptides from crude and unprotected linear peptides. The second method was based on the selectivity of the reaction between bromomaleimides and thiols. An azide-bearing bromomaleimide derivative was synthesized and it was attempted to cyclize a peptide by employing this reagent. Unfortunately, this maleimide reagent did not afford a cyclic peptide in a reliable manner.

These results show once more that the synthesis of cyclic peptides remains challenging. However, the method, using thiols and benzylic bromides, enables the synthesis of cyclic peptides reliably from crude and unprotected linear peptides. Using this method azide-bearing cyclic peptides have been synthesized and these peptides have been used successfully in the synthesis of protein mimics.

2.4 Experimental

2.4.1 General information

Chemicals were obtained from commercial sources and used without further purification, unless stated otherwise. Peptide grade D*i*PEA, CH_2Cl_2, TFA and HPLC grade solvents were purchased from Biosolve B.V. (Valkenswaard, the Netherlands) and peptide grade NMP and DMF were purchased from Actu-All Chemicals (Oss, the Netherlands). Fmoc-protected amino acids, BOP, and HBTU were purchased from GL Biochem Ltd. (Shanghai, China). Amino acid side chain protecting groups were as follows: Arg(Pbf), Asp(OtBu), Cys(Trt), Gln(Trt), Glu(OtBu), His(Trt), Thr(tBu) and Trp(Boc). TentaGel S RAM resin (particle size 90 μm, capacity 0.25 mmol/g) was purchased from Rapp Polymere GmbH (Tübingen, Germany). Unless stated otherwise, reactions were performed at room temperature.

Solid phase peptide synthesis was performed on an Applied Biosystems 433A peptide synthesizer or a C.S. Bio Co. peptide synthesizer (model CS336X). TLC analysis was performed on Merck precoated silica gel 60 F-254 plates. Spots were visualized with UV-light, ninhydrin stain (1.5 g ninhydrin and 3.0 mL acetic acid in 100 mL *n*-butanol), and/or molybdenum staining agent (12 g ammonium molybdate and 0.5 g ammonium cerium(IV) sulfate in 250 mL 10% H_2SO_4). Column chromatography was performed using Silica-P Flash silica gel (60 Å, particle size 40-63 μm) from Silicycle. Lyophilizations were performed on a Christ Alpha 1–2 apparatus. ^{1}H NMR (300 MHz) and ^{13}C NMR (75 MHz) experiments were conducted on a 300 MHz Varian G-300 spectrometer. Chemical shifts are given in ppm (δ) relative to TMS (0.00 ppm) (^{1}H NMR) or relative to $CDCl_3$ (77 ppm) (^{13}C NMR).

Analytical HPLC was performed on a Shimadzu-10Avp (Class VP) system using a Phenomenex Gemini C18 column (110 Å, 5 μm, 250×4.60 mm) at a flow rate of 1 mL min^{-1}. Buffers used were 0.1% trifluoroacetic acid in MeCN/H_2O 5:95 (buffer A) and 0.1% trifluoroacetic acid in MeCN/H_2O 95:5 (buffer B). Runs were performed using a standard protocol: 100% buffer A for 2 min, then a linear gradient of buffer B (0-100% in 48 min) and UV-absorption was measured at 214 and 254 nm. Peptide-containing compounds were purified on a Prep LCMS QP8000α HPLC system (Shimadzu) using a Phenomenex Gemini C18 column (10 μm, 110 Å, 250×21.2 mm) at a flow rate of 12.5 mL min^{-1}. Runs were performed using a standard protocol: 100% buffer A for 5 min followed by a linear gradient of buffer B (0-100% in 75 min) with the same buffers as were described for analytical HPLC.

ESI-TOF MS spectra were recorded on a microTOF mass spectrometer (Bruker). Samples were diluted with tuning mix (1:1, v/v) and infused at a speed of 300 μl/h using a nebulizer pressure of 5.8 psi, a dry gas flow of 3.0 L/min, a drying temperature of 180°C and a capillary voltage of 5.5 kV. Analytical LC-MS (electrospray ionization) was preformed on Thermo-Finnigan LCQ Deca XP Max using the same buffers and protocol as described for analytical HPLC. MALDI-TOF MS spectra were recorded on a Kratos Analytical (Shimadzu) AXIMA CFR mass spectrometer using α-cyano-4-hydroxycinnamic acid (CHCA) as a matrix and human ACTH (18-39), $P_{14}R$ synthetic peptide or bovine insulin oxidized B chain as references.

GC-MS experiments were performed on a Perkin Elmer Clarus 680 coupled to a Perkin Elmer Clarus SQ8T mass spectrometer, using a PE Elite 5 MS column (15 m x 0.25 mm ID x 0.25 µm) using a standard protocol: started at 150°C rising to 280°C with 10°C per minute and held at 280°C for 40 minutes. All reported mass values are monoisotopic.

2.4.2 Synthetic procedures and analytical data

1-(azidomethyl)-3,5-bis(bromomethyl)benzene (2)

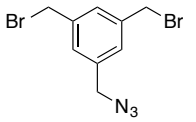

1,3,5-tris(bromomethyl)benzene (**1**, 2.0 g; 5.6 mmol) was dissolved in DMF (100 mL). Sodium azide (0.33 g; 5.04 mmol) was added and the resulting mixture was stirred at room temperature for 3 hours. The solvent was evaporated *in vacuo* and CH_2Cl_2 (100 mL) was added. The salts were filtered off and the filtrate was concentrated. The crude product was purified using silica gel column chromatography (1.5% EtOAc in hexanes) to obtain the pure product as a yellow clear oil (670 mg; 2.1 mmol; 42%).

^{1}H NMR (300 MHz, $CDCl_3$): δ= 4.37 (s, 2H, CH_2N_3), 4.47 (s, 4H, CH_2Br), 7.28 (m, 2H, ArH), 7.39 (m, 1H, ArH)

^{13}C NMR (75 MHz, $CDCl_3$): δ= 32.3 (CH_2Br), 54.1 (CH_2N_3), 128.5, 129.4 (Ar-CH), 137.0, 139.1 (Ar-C)

Monoisotopic mass calculated $[M]^+$: 316.9163; GC-MS measured: 316.9220

R_f: 0.52 (10% EtOAc/hexanes)

Solid phase peptide synthesis

Linear peptides were synthesized on a peptide synthesizer using Tentagel S RAM resin (rink amide linker) on a 0.25-mmol scale. Removal of the Fmoc-group was performed using 20% piperidine in NMP. Amino acids were coupled using 4 equiv. of amino acid and HBTU as an activating agent with D*i*PEA as a base and NMP as solvent. Capping was performed using acetic anhydride (12 mL), HOBt (0.5 g) and D*i*PEA (5.5 mL) in NMP (250 mL). Note: In the synthesis of the peptide containing a Asp-Gly, the glycine residue was coupled as Fmoc-(Dmb)-Gly-OH to prevent aspartimide formation.

General procedure for the cleavage and deprotection of the linear peptide from the solid support

The side chain-protected linear peptide was cleaved from the resin and deprotected using a mixture of TFA/H_2O/EDT/TIS (90:5:2.5:2.5) (v/v/v/v), 10 mL per gram resin. The reaction mixture was stirred for 3 hours after which the mixture was filtered and concentrated to a volume of 2 mL, followed by precipitation of the peptides by MTBE/hexane (1:1 v/v). After centrifugation (3500 rpm, 5 min), the supernatant was decanted and the pellet was resuspended in MTBE/hexane (1:1 v/v) and centrifuged again. Then, the pellet was dissolved in *t*-BuOH/H_2O (1:1 v/v) and lyophilized. The purity of the peptides was analyzed with analytical HPLC and the peptides were characterized with mass spectrometry.

General procedure for peptide cyclization by azido-bisbromide 2[21]

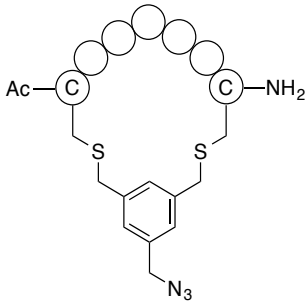

To a 1 mM solution of the crude linear peptide in a (1:3 v/v) mixture of MeCN/ NH_4HCO_3 (aq, 20 mM, pH 7.8) a solution of 1-(azidomethyl)-3,5-bis(bromomethyl)benzene **2** (1.25 equiv.) in MeCN (2 mL) was added dropwise. The resulting mixture was stirred at room temperature for 3 hours before being concentrated and lyophilized. The crude cyclic peptide was purified using preparative HPLC. The product-containing fractions were pooled and lyophilized to yield the purified cyclic peptides as white fluffy powder.

Cyclic Ac-CGGFGPC-NH_2 (Pertussis Pertactin) (**3**): 35 mg (42 μmol), 17% (18 steps, 91% per step). Mass calculated $[M + H]^+$: 838.31; MALDI-TOF MS found: 838.41. Rt = 27.00 min.

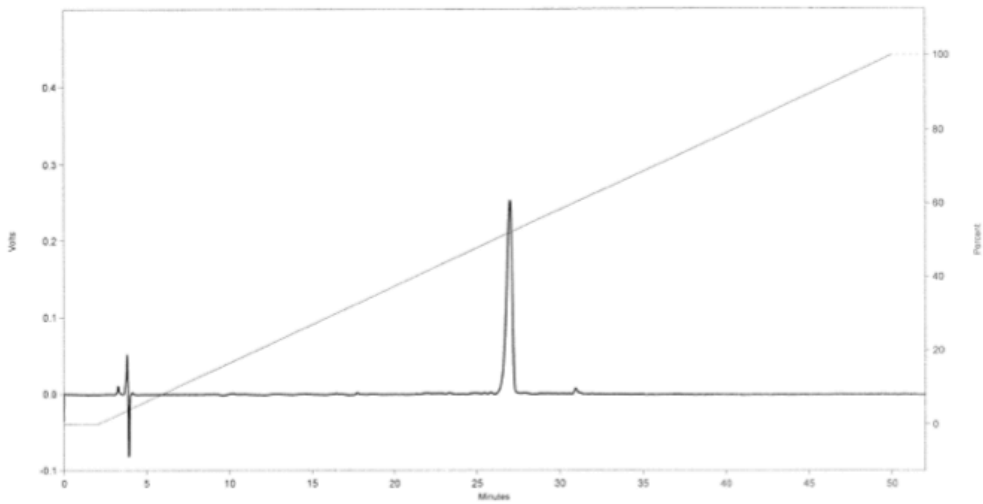

Cyclic Ac-CGERQHC-NH_2 (Pertussis Pertactin) (**4**): 35.8 mg (35 μmol), 14% (18 steps, 90% per step). Mass calculated $[M + H]^+$: 1030.40; MALDI-TOF MS found: 1030.40. Rt = 17.87 min. Note: Preperative HPLC was performed with 0.1% trifluoroacetic acid in H_2O (buffer A) and 0.1% trifluoroacetic acid in MeCN/H_2O 95:5 (buffer B) using the same protocol as described above.

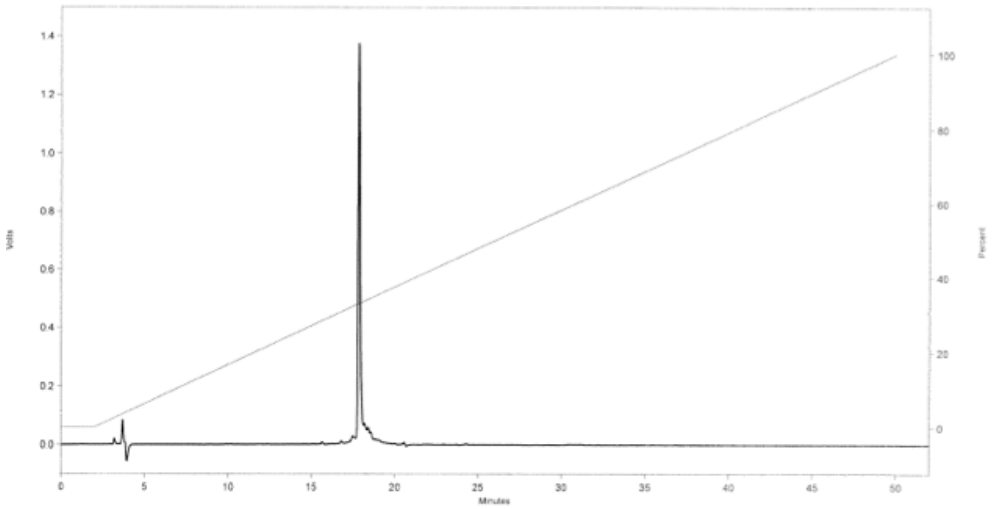

Cyclic Ac-CGDTWDDDC-NH_2 (Pertussis Pertactin) (**5**): 78 mg (64 μmol), 26% (22 steps, 94% per step). Mass calculated $[M + H]^+$: 1227.24; MALDI-TOF MS found: 1227.24. Rt = 22.98 min.

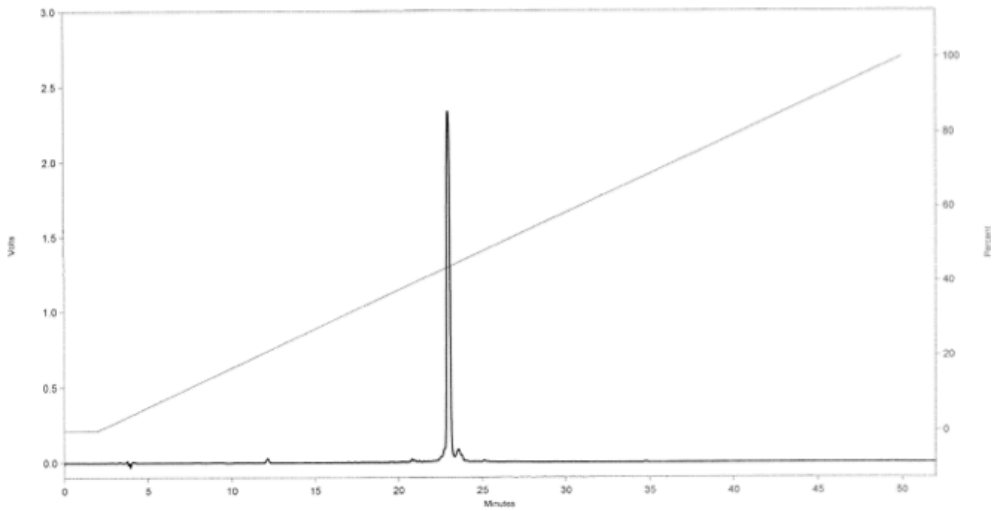

Cyclic Ac-CLTRDGGKC-NH_2 (HIV gp120) (**6**): 69 mg (60 μmol), 34%, (21 steps, average 95% per step) Mass calculated $[M + H]^+$: 1150.5250; ESI-TOF MS found: 1150.5263. Rt = 19.90 min.

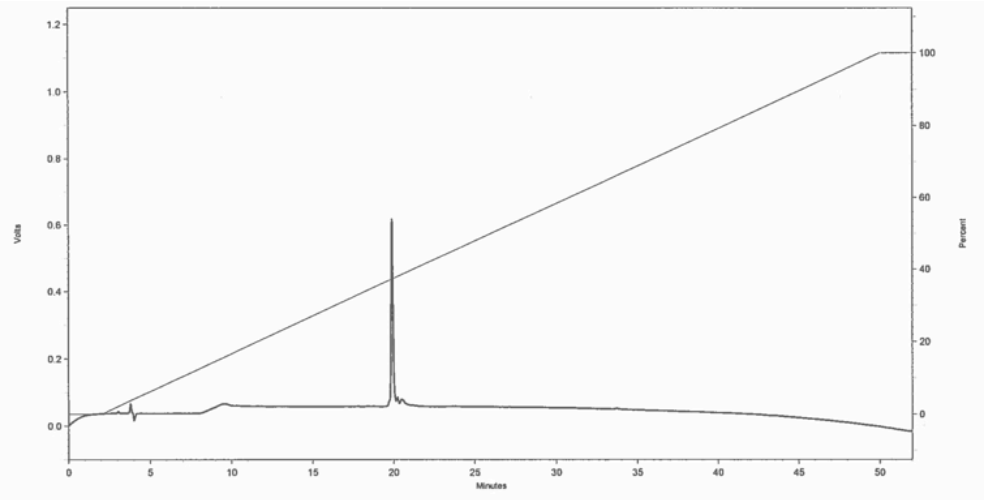

Cyclic H-CINMWQEVGKAC-NH_2 (HIV gp120) (**7**): 65 mg (42 μmol), 17%, (26 steps, average 93% per step). Mass calculated $[M + 2H]^{2+}$: 769.3472; ESI-TOF MS found: 769,3464. Rt = 22.05 min.

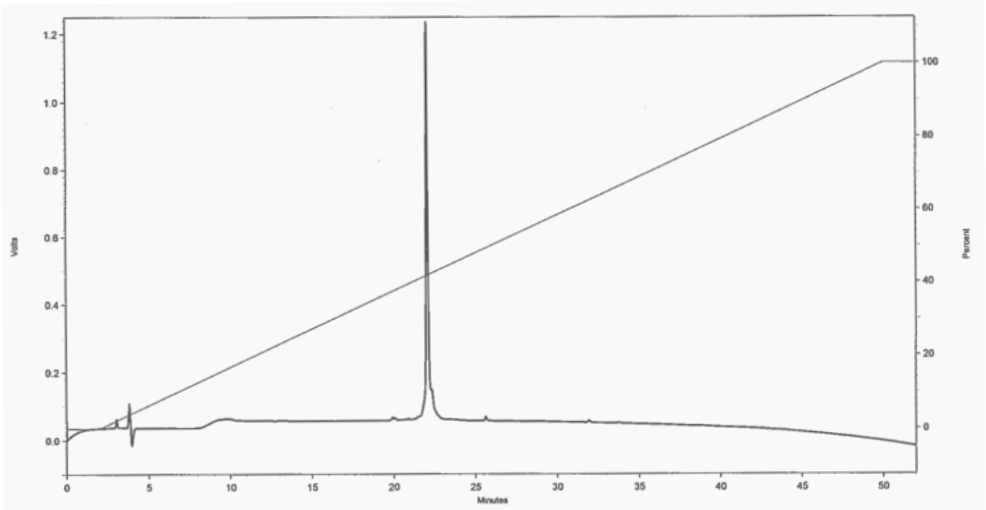

Cyclic Ac-CSGGDPEIVTC-NH_2 (HIV gp120) (**8**): 92 mg (72 μmol), 29%, (25 steps, average 95% per step). Mass calculated $[M + H]^+$: 1278.5247; ESI-TOF MS found: 1278.5269. Rt = 22.58 min.

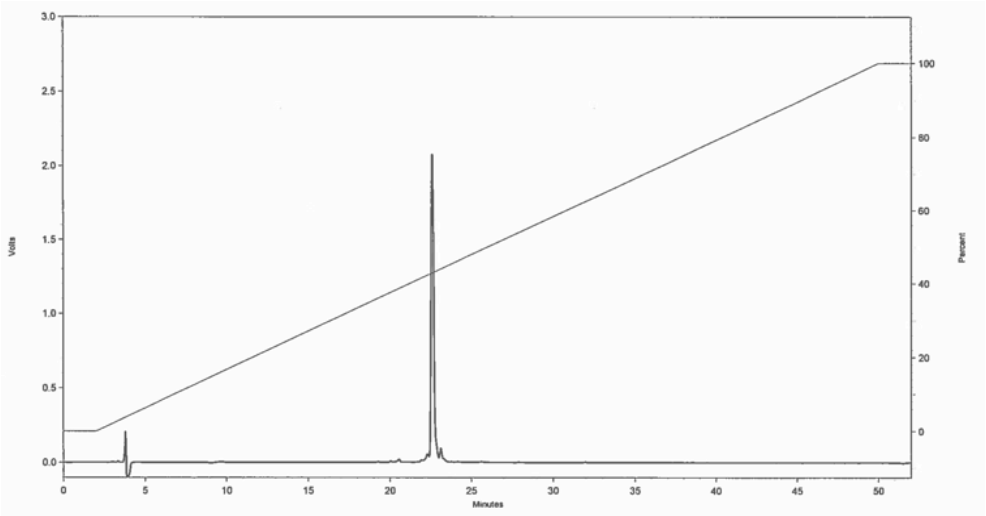

***tert*-Butyl (3-bromopropyl)carbamate (19)**

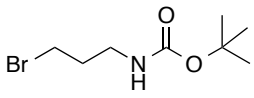

Boc_2O (2.18 g, 10 mmol) was added to a solution of 3-bromopropan-1-amine.HBr (**18**) (2.18 g, 10 mmol) in dioxane/H_2O (1:1, v/v, 80 mL) and K_2CO_3 was added until the reaction mixture reached a pH of 8. The reaction mixture was stirred at room temperature for 75 minutes, after which it was diluted with EtOAc (150 mL) and washed with H_2O (150 mL), 1N $KHSO_4$ (150 mL) and brine (150 mL). The organic layer was dried over Na_2SO_4, filtered, and the solvent was removed *in vacuo* to yield Boc-protected bromopropylamine **19** as a light-yellow liquid (2.27 g, 9.5 mmol, 95%).

^{1}H NMR (300 MHz, $CDCl_3$) δ = 1.45 (s, 9H, $C(CH_3)_3$), 2.07 (q, J = 6.6 Hz, 2H, $CH_2C\underline{H}_2CH_2$), 3.26 (q, J = 6.4 Hz, 2H, CH_2N), 3.44 (t, J = 6.5 Hz, 2H, CH_2Br), 4.66 (s, 1H, NH).

***tert*-Butyl (3-azidopropyl)carbamate (20)**

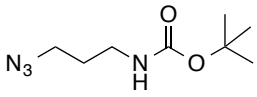

tert-Butyl (3-bromopropyl)carbamate **19** (2.27 g, 9.5 mmol) was dissolved in DMF (70 mL) and a suspension of NaN_3 (0.75 g, 11.5 mmol) in DMF (50 mL) was added and the resulting mixture was stirred at room temperature overnight. The solvent was evaporated and the residue was suspended in EtOAc (100 mL). The suspension was filtered and the solvent to obtain the product (**20**) as a light-yellow liquid (1.42 g, 7.1 mmol, 84%).

^{1}H NMR (300 MHz, $CDCl_3$) δ =1.45 (s, 9H, $C(CH_3)_3$), 1.77 (q, J = 6.7 Hz, 2H, $CH_2C\underline{H}_2CH_2$), 3.22 (q, J = 6.4 Hz, 2H, CH_2N), 3.36 (t, J = 6.7 Hz, 2H, CH_2N_3), 4.64 (s, 1H, NH).

1-(3-Azidopropyl)-3-bromo-1H-pyrrole-2,5-dione (17)

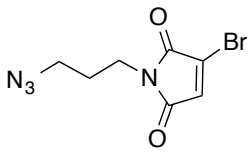

To a solution of tert-butyl (3-azidopropyl)carbamate **19** (0.20 g, 1 mmol) in AcOH (50 mL) bromomaleic anhydride **22** (177 mg, 1 mmol) and sodium acetate (41 mg, 0.5 mmol) were added. The resulting reaction mixture was refluxed overnight. The AcOH was removed by evaporation and co-evaporation with toluene. The residue was dissolved in EtOAc (70 mL) and washed with H_2O (3x 70 mL), $NaHCO_3$ (aq, 1M, 70 mL) and brine (70 mL). The organic layer was dried over Na_2SO_4, filtered and concentrated to give the crude product. Purification by silica gel column chromatography (CH_2Cl_2) afforded the product (**17**) as a clear oil (157 mg, 0.61 mmol, 61%).

^{1}H NMR (300 MHz, $CDCl_3$) δ = 1.88 (q, J = 6.7 Hz, 2H, $CH_2C\underline{H}_2CH_2$), 3.35 (t, J = 6.5 Hz, 2H, CH_2NCO), 3.67 (t, J = 6.8 Hz, 2H, CH_2N_3), 6.90 (s, 1H, CHCO).

^{13}C NMR (75 MHz, $CDCl_3$) δ = 27.8 ($CH_2\underline{C}H_2CH_2$), 36.3 ($\underline{C}H_2NC(O)$), 48.9 (CH_2N_3), 131.5(CHBr), 131.9($\underline{C}HC=O$), 165.2, 168.4 (C=O)

General procedure for cyclization of peptide 23 by monobromomaleimide derivative 17

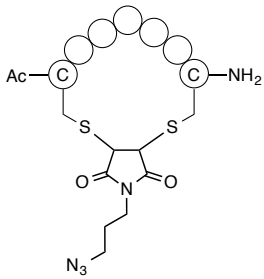

Linear peptide **23** was synthesized as described above. The crude linear peptide was purified by preparative HPLC, after which it (10 mg, 8.9 μmol) was dissolved in buffer/MeCN (8.9 mL, 3/1, v/v) to a final concentration of 1 mM. Then, a solution of bromomaleimide **17** (2.3 mg, 8.9 μmol) in MeCN was added. The resulting reaction mixture was stirred at room temperature and was analyzed using LCMS. Results are shown in Table 2.

Note: Because cyclic and linear products **24** and **25** have the same mass they cannot be distinguished from each other on LC-MS. They do have different retention times, so one reaction mixture containing both products was purified using preparative HPLC and the pure fractions were tested for free thiols using Ellman's reagent (5,5'-dithiobis-(2-nitrobenzoic acid)). A little of the pure fraction was dissolved in aqueous NH_4HCO_3 (20 mM, 1 mL) and Ellman's reagent (0.5 mg) was added. The solution turned yellow in the presence of free thiol moieties, thus the solution cyclic product **24** remained colorless and the solution of linear product **25** turned bright yellow. This identified the peak at Rt=13.5 min to be linear product **25** and the peak at Rt=14.7 min to be cyclic product **24**, based on LC-MS data with the following protocol: 100% buffer A for 2 min, then a linear gradient of buffer B (0-100% in 28 min).

Table 2. Results from the reaction of bromomaleimide **17** and linear peptide **23**

Buffer	pH	Reaction time	Outcome
H_2O	7	Overnight	Peptides **24** and **25**
20 mM NH_4HCO_3	7.8	3h	Linear peptide **25**
20 mM NH_4HCO_3	7.8	Overnight	Mostly linear peptide **25** (90%) Some product **24** (10%)
20 mM NH_4OAc	6.5	Overnight	Cyclic and linear products **24**(70%) & **25** (20%) observed. Also hydrolysis to product **26** (10%)
0.1 M acetic acid, 0.1 M sodium acetate	4.8	5h	Linear peptide **25**
0.1 M Na_2HPO_4, 1.5 M NaCl	8.1	3h	Mostly linear peptide **25** (65%), some cyclic product **24** (30 %)
0.1 M Na_2HPO_4, 1.5 M NaCl	8.1	Overnight	Linear peptide **25**

References

1 D. J. Craik, D. P. Fairlie, S. Liras and D. Price, *Chem. Biol. Drug Des.*, 2013, **81**, 136–147.

2 J. E. Bock, J. Gavenonis and J. A. Kritzer, *ACS Chem. Biol.*, 2012, **8**, 488–499.

3 J. G. Beck, J. Chatterjee, B. Laufer, M. U. Kiran, A. O. Frank, S. Neubauer, O. Ovadia, S. Greenberg, C. Gilon, A. Hoffman and H. Kessler, *J. Am. Chem. Soc.*, 2012, **134**, 12125–12133.

4 M. Malakoutikhah, B. Guixer, P. Arranz-Gibert, M. Teixidō and E. Giralt, *ChemMedChem*, 2014, **9**, 1594–1601.

5 L. Nevola, A. Martín-Quirōs, K. Eckelt, N. Camarero, S. Tosi, A. Llobet, E. Giralt and P. Gorostiza, *Angew. Chem. Int. Ed.*, 2013, **52**, 7704–7708.

6 L. Y. Chan, V. M. Zhang, Y. H. Huang, N. C. Waters, P. S. Bansal, D. J. Craik and N. L. Daly, *ChemBioChem*, 2013, **14**, 617–624.

7 S. Xu, H. Li, X. Shao, C. Fan, B. Ericksen, J. Liu, C. Chi and C. Wang, *J. Med. Chem.*, 2012, **55**, 6881–6887.

8 C. J. White and A. K. Yudin, *Nat. Chem.*, 2011, **3**, 509–524.

9 J. M. Smith, J. R. Frost and R. Fasan, *J. Org. Chem.*, 2013, **78**, 3525–3531.

10 C. A. G. N. Montalbetti and V. Falque, *Tetrahedron*, 2005, **61**, 10827–10852.

11 S. Punna, J. Kuzelka, Q. Wang and M. G. Finn, *Angew. Chem. Int. Ed.*, 2005, **44**, 2215–2220.

12 A. Parenty, X. Moreau, G. Niel and J.-M. Campagne, *Chem. Rev.*, 2013, **113**, PR1–PR40.

13 R. M. J. Liskamp, D. T. S. Rijkers, J. A. W. Kruijtzer and J. Kemmink, *ChemBioChem*, 2011, **12**, 1626–1653.

14 T. A. Hill, N. E. Shepherd, F. Diness and D. P. Fairlie, *Angew. Chem. Int. Ed.*, 2014, **53**, 13020–13041.

15 R. Franke, C. Doll, V. Wray and J. Eichler, *Org. Biomol. Chem*, 2004, **2**, 2847–2851.

16 G. E. Mulder, J. A. W. Kruijtzer and R. M. J. Liskamp, *Chem. Commun.*, 2012, **48**, 10007–10009.

17 J. A. Robinson, S. DeMarco, F. Gombert, K. Moehle and D. Obrecht, *Drug Discov. Today*, 2008, **13**, 944–951.

18 S. Y. Shim, Y. W. Kim and G. L. Verdine, *Chem. Biol. Drug Des.*, 2013, **82**, 635–642.

19 H. Jo, N. Meinhardt, Y. Wu, S. Kulkarni, X. Hu, K. E. Low, P. L. Davies, W. F. Degrado and D. C. Greenbaum, *J. Am. Chem. Soc.*, 2012, **134**, 17704–17713.

20 G. E. Mulder, H. C. Quarles van Ufford, J. van Ameijde, A. J. Brouwer, J. A. W. Kruijtzer and R. M. J. Liskamp, *Org. Biomol. Chem.*, 2013, **11**, 2676–2684.

21 P. Timmerman, J. Beld, W. C. Puijk and R. H. Meloen, *ChemBioChem*, 2005, **6**, 821–824.

22 P. Timmerman, W. C. Puijk, R. S. Boshuizen, P. Van Dijken, J. W. Slootstra, F. J. Beurskens, P. W. H. I. Parren, A. Huber, M. F. Bachmann and R. H. Meloen, *Open Vaccine J.*, 2009, **2**, 56–67.

23 L. E. J. Smeenk, N. Dailly, H. Hiemstra, J. H. van Maarseveen and P. Timmerman, *Org. Lett.*, 2012, **14**, 1194–7.

24 L. E. J. Smeenk, D. Timmers-Parohi, J. J. Benschop, W. C. Puijk, H. Hiemstra, J. H. van Maarseveen and P. Timmerman, *ChemBioChem*, 2015, **16**, 91–99.

25 A. Angelini, J. Morales-Sanfrutos, P. Diderich, S. Chen and C. Heinis, *J. Med. Chem.*, 2012, **55**, 10187–10197.

26 A. Angelini, P. Diderich, J. Morales-Sanfrutos, S. Thurnheer, D. Hacker, L. Menin and C. Heinis, *Bioconjugate Chem.*, 2012, **23**, 1856–1863.

27 I. R. Rebollo, A. Angelini and C. Heinis, *Med. Chem. Commun.*, 2013, **4**, 145–150.

28 C. Heinis, T. Rutherford, S. Freund and G. Winter, *Nat. Chem. Biol.*, 2009, **5**, 502–507.

29 V. Baeriswyl, H. Rapley, L. Pollaro, C. Stace, D. Teufel, E. Walker, S. Chen, G. Winter, J. Tite and C. Heinis, *ChemMedChem*, 2012, **7**, 1173–1176.

30 J. D. Gregory, *J. Am. Chem. Soc.*, 1955, **77**, 3922–3923.

31 R. A. Bednar, *Biochemistry*, 1990, **29**, 3684–3690.

32 J. M. Chalker, G. J. L. Bernardes, Y. A. Lin and B. G. Davis, *Chem. - An Asian J.*, 2009, **4**, 630–640.

33 L. M. Tedaldi, M. E. B. Smith, R. I. Nathani and J. R. Baker, *Chem. Commun.*, 2009, **67**, 6583–6585.

34 M. E. B. Smith, F. F. Schumacher, C. P. Ryan, L. M. Tedaldi, D. Papaioannou, G. Waksman, S. Caddick and J. R. Baker, *J. Am. Chem. Soc.*, 2010, **132**, 1960–1965.

35 F. F. Schumacher, M. Nobles, C. P. Ryan, M. E. B. Smith, A. Tinker, S. Caddick and J. R. Baker, *Bioconjugate Chem.*, 2011, **22**, 132–136.

36 M. W. Jones, R. a Strickland, F. F. Schumacher, S. Caddick, J. R. Baker, M. I. Gibson and D. M. Haddleton, *J. Am. Chem. Soc.*, 2012, **134**, 1847–52.

37 S. Ramesh, P. Cherkupally, T. Govender, H. G. Kruger, F. Albericio and B. G. D. La Torre, *Org. Lett.*, 2015, **17**, 464–467.

38 S. G. Stewart, M. E. Polomska and R. W. Lim, *Tetrahedron Lett.*, 2007, **48**, 2241–2244.

39 A. S. Kalgutkar, B. C. Crews and L. J. Marnett, *J. Med. Chem.*, 1996, **39**, 1692–1703.

40 R. I. Nathani, V. Chudasama, C. P. Ryan, P. R. Moody, R. E. Morgan, R. J. Fitzmaurice, M. E. B. Smith, J. R. Baker and S. Caddick, *Org. Biomol. Chem.*, 2013, **11**, 2408.

3

Chapter 3

Protein mimics of the *Bordetella pertussis* Pertactin epitope by sequential ligation of a trialkyne scaffold

Parts of this chapter have been published in:

P.R. Werkhoven, H. van de Langemheen, S. van der Wal, J.A.W. Kruijtzer, R.M.J. Liskamp
J. Pept. Sci. 2014, 20, 235-239

3.1 Introduction

As described in Chapter 1, discontinuous epitopes are composed of multiple peptide segments separated in the protein sequence, but brought into spatial proximity by folding of the protein to its tertiary structure. To mimic such a complex ensemble peptides, corresponding to these segments have to be brought together on a molecular scaffold. However, the synthesis of these large and complex molecular constructs consisting of multiple peptides is very challenging.

Our group has developed a method for the synthesis of discontinuous epitope mimics using a non-stop solid-phase procedure where the scaffold is mounted on a solid-support and the peptides are assembled on the scaffold using solid phase peptide synthesis.[1,2] However, this approach has two inherent disadvantages: 1) the approach requires even with high yields extensive purification to yield a relatively small amount of the desired mimic and 2) collections or libraries of mimics, for example to optimize the biological activity, have to be synthesized one after the other, which is very time-consuming. These disadvantages can be remedied by using a convergent synthesis strategy in which the peptides are synthesized separately and then attached to a scaffold using ligation chemistry.

An outstanding example of convergent introduction is the attachment of –albeit identical- peptides onto a calix[4]arene scaffold by Hamilton et al. (Figure 1).[3] Examples of other scaffolds that have been used for the convergent attachment of multiple identical peptides are the Triazacyclophane (TAC) and the Cyclotriveratrylene (CTV) scaffolds (Figure 1).[4,5] Mulder et al. adapted these scaffolds for the use of copper-catalysed azide-alkyne cycloaddition (CuAAC) and showed the efficient synthesis of a small library of mimics in a single reaction step via the simultaneous reaction between different trialkyne scaffolds and three different azide-functionalized peptides.[6,7]

The availability of convergent methods for the introduction of both different and several peptide loops onto suitable scaffolds is limited.[8] The most seminal contribution in this area was probably the Template-Assembled Synthetic Protein (TASP), originally developed by Mutter and Vuilleumier,[9] which was further developed by, among others, Dumy et al. to the Regioselectively Addressable Functionalized Template (RAFT) (Figure 2).[10–12] However, the RAFT scaffold relies on orthogonally protected amine functionalities for the sequential introduction and is therefore incompatible with peptides containing unprotected amines like lysine residues or a free N-terminus. Therefore, the peptides have to be protected when they

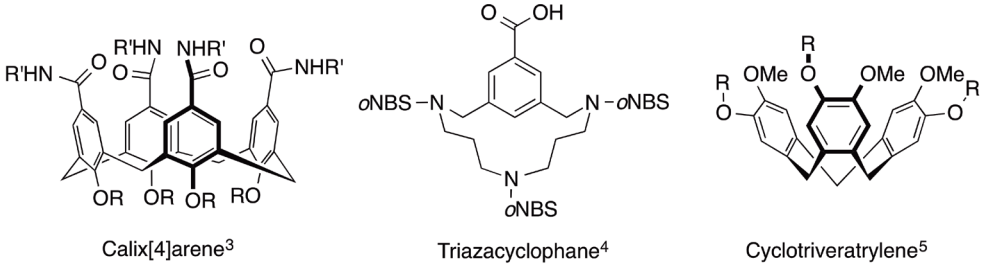

Figure 1. Molecular scaffolds on which multiple identical peptides can be ligated.

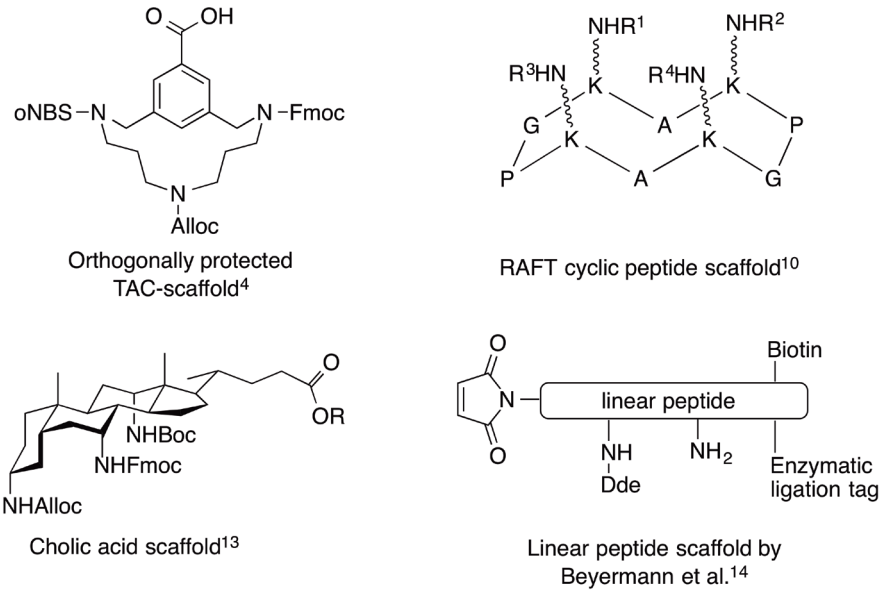

Figure 2. Scaffolds suitable for the sequential introduction of different peptides using orthogonally protected amines.

are coupled onto the scaffold, which often results in limitations like poor solubility.[12] Other examples of scaffolds using orthogonally protected amines for sequential introduction are the TAC-scaffold,[1,2,4] the cholic acid scaffold[13] and the linear peptide scaffold described by Beyermann et al.[14] (Figure 2)

Other approaches to sequential introduction often use different (bioorthogonal) ligation methods on a scaffold.[8] Examples of this are the CuAAC-SPAAC-thiol scaffold,[15] the oxime-thiol-CuAAC scaffold,[16] and the oxime-maleimide-4xCuAAC functionalized RAFT scaffold (Figure 3).[17] However, these methods require each peptide to be equipped with a different ligation handle. In order to investigate the influence of the relative positioning of the peptides on the scaffold, each peptide will have to be synthesized separately for each ligation handle.

The aim was to develop a versatile convergent synthesis of protein mimics containing three peptide loops through successive introduction of peptides on a scaffold. It was also desired that the introduction of the three peptides would proceed via the same ligation method so that each peptide could be equipped with the same ligation handle. This will allow for the easy variation of the position of the peptides. The CuAAC chemistry was particularly attractive, because this proved to be highly successful in the preparation of 'smart libraries' by the ligation of a mixture of peptides.[6,7] However, the scaffold used for these smart libraries (**1**) was not suited for the successive introduction of peptides. Therefore, an adapted scaffold was designed (**2**), in which the alkynes were protected using a silyl protection group strategy (Figure 4). The different chemical reactivity of the protected alkynes allowed them to be addressed one after the other, making sequential introduction of peptides possible. This protection group strategy was inspired by the elegant orthogonal system of Valverde et al. (**3**), which employed

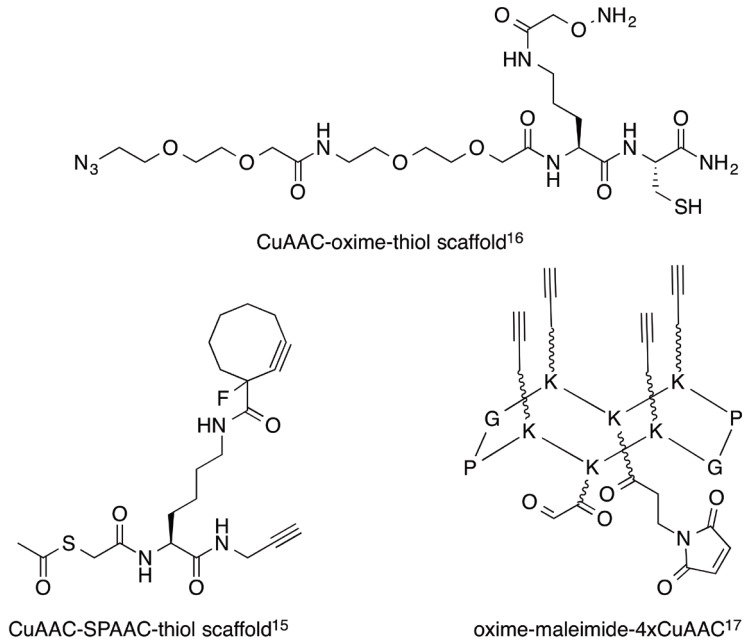

Figure 3. Scaffolds suitable for the sequential introduction of peptides using different ligation methods.

triethylsilyl and triisopropylsilyl groups for the orthogonal protection of alkynes.[18] (Figure 4)

This chapter describes the synthesis of a TAC-scaffold derivative (**2**), which is equipped with orthogonal protected alkyne moieties. The new scaffold is used for the synthesis of a protein mimic of the Pertactin protein of the whooping cough-causative organism *Bordetella pertussis*. Three azide-functionalized cyclic peptides, which correspond to the discontinuous epitope of Pertactin, are successively introduced on the scaffold resulting in the synthesis of a discontinuous epitope mimic (Figure 5). However, it must be noted that the synthesis of the Pertactin protein mimics is a proof-of-principle and the combination of this scaffold and

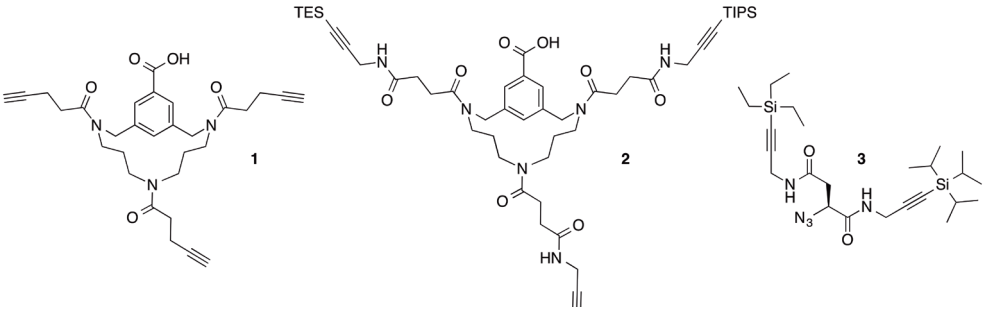

Figure 4. Left: TAC-scaffold used for the synthesis of smart libraries (**1**). Middle: The designed adapted TAC-scaffold (**2**) containing three alkynes with an orthogonal silyl protection group strategy. Right: Scaffold by Valverde et al. (**3**) containing an azide and two protected alkynes. [18]

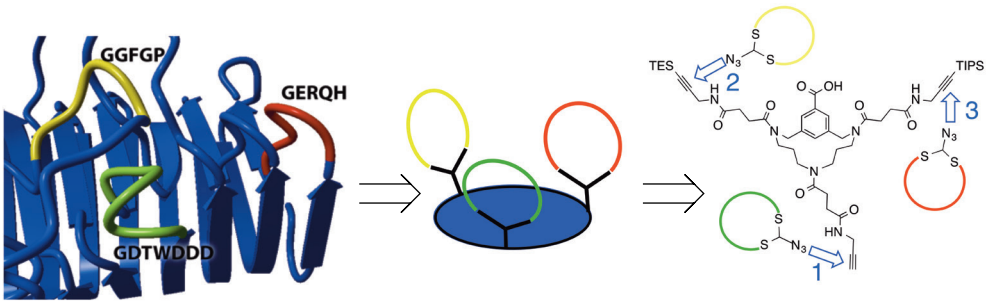

Figure 5. Design of a discontinuous epitope mimic of the Pertactin protein. The epitope consists of three loops (left). Peptides with the same sequences as these loops can be mounted on a scaffold in order to mimic the epitope (middle). This can be achieved by sequentially introducing the peptide by CuAAC using the orthogonally protected trialkyne TAC-scaffold (right).

azide-functionalized peptides should in principle enable the synthesis of any discontinuous epitope mimic composed of three loops in a high yielding and convergent manner.

3.2 Results and discussion

For the introduction of silyl-protected alkyne moieties onto the scaffold, the appropriate silyl-functionalized propargyl amines were needed. The silyl protecting groups were introduced on propargyl amine (**4**) through reaction with the appropriate silyl chloride at low temperatures. After purification, silyl protected propargylamines **5a** and **5b** were obtained in good yields (Scheme 1).

The designed protected trialkyne TAC-scaffold was accessible from our Alloc-, Fmoc-, and o-NBS-protected scaffold, of which the synthesis has been described in literature.[4,19] This TAC-scaffold was loaded on a 2-chlorotrityl chloride resin leading to a resin-bound scaffold **6** (Scheme 2). The Alloc-group was removed by palladium tetrakis(triphenylphosphine), after which succinic anhydride and propargylamine (**4**) were subsequently introduced to the unprotected amine leading to **7**. Removal of the Fmoc-group by piperidine, followed by reaction with succinic anhydride and coupling of TIPS-protected propargylamine, **5b** yielded resin-bound scaffold **8**. Next, the *o*NBS-group was removed by DBU and β-mercaptoethanol and TES-propargylamine **5a** was introduced. Finally, the scaffold was cleaved from the resin using 30% HFIP in CH_2Cl_2 to give, after purification by preparative HPLC, pure scaffold **2** in 58% overall yield (11 steps, average yield of 95% per step, Scheme 2).

The cyclic peptide loops used were based on the epitope of the Pertactin protein of *Bordetella pertussis* (Figure 6).[20] The linear peptide sequences were previously used by Hijnen et al. for the preparation of a synthetic pertussis vaccine and were capable of inducing formation of

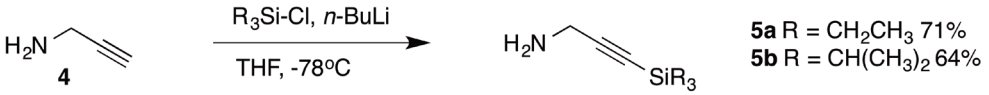

Scheme 1. Synthesis of TIPS- and TES-protected propargylamine.

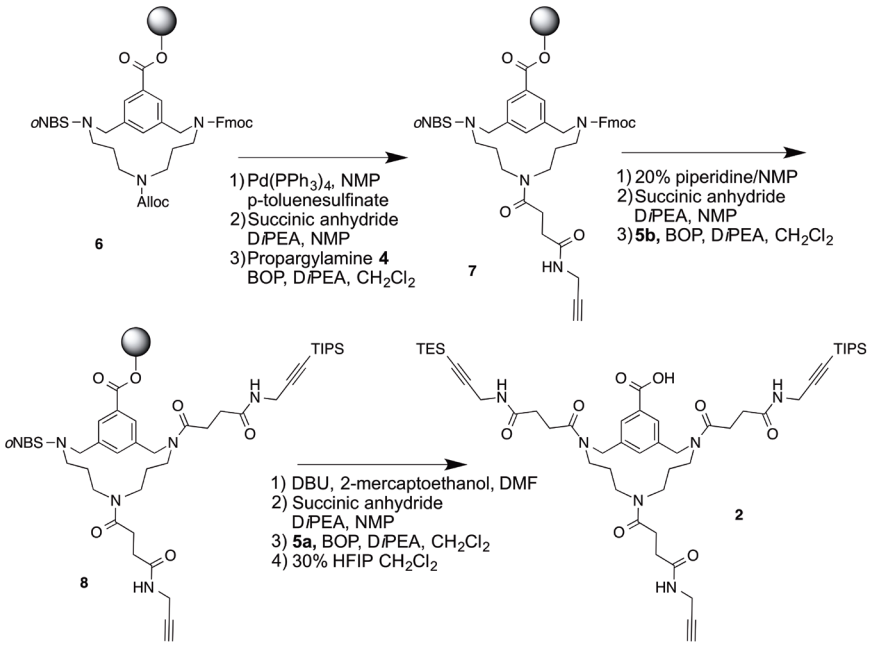

Scheme 2. Synthesis of the protected trialkyne TAC-scaffold (**2**) using solid-phase synthesis protocols.

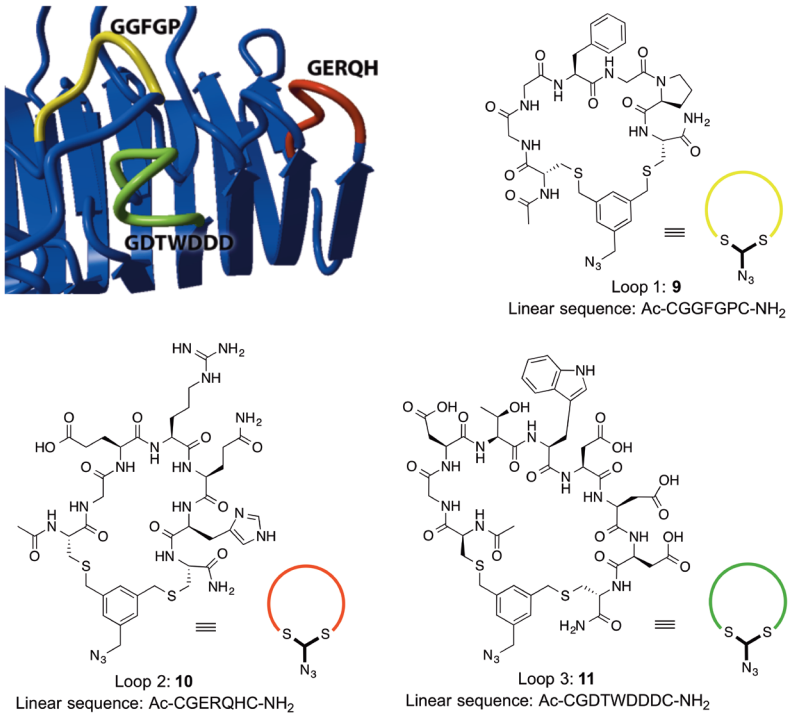

Figure 6. Top left: Part of the crystal structure of the Pertactin protein. The stretches of the protein that form the discontinuous epitope, as determined by Hijnen et al., are highlighted in yellow, red, and green.[20] Bottom and top right: structure of the three cyclic peptides that resemble the structure of the epitope.

protective antibodies.[2] Hijnen et al. also described preliminary modeling studies to determine the optimal arrangement of the peptides on the scaffold. The cyclic peptides were synthesized, as previously described in Chapter 2, by the bisalkylation of terminal cysteine residues by an azide-functionalized bisbenzylbromide.

The stage was now set for the successive introduction of the peptide loops onto scaffold **2** (Scheme 3). To achieve the same relative positioning of the peptides on the scaffold as described by Hijnen et al., the peptides were introduced in the following order: first loop 2, then loop 3, and finally loop 1. First, peptide loop 2 (**10**), containing pertactin peptide

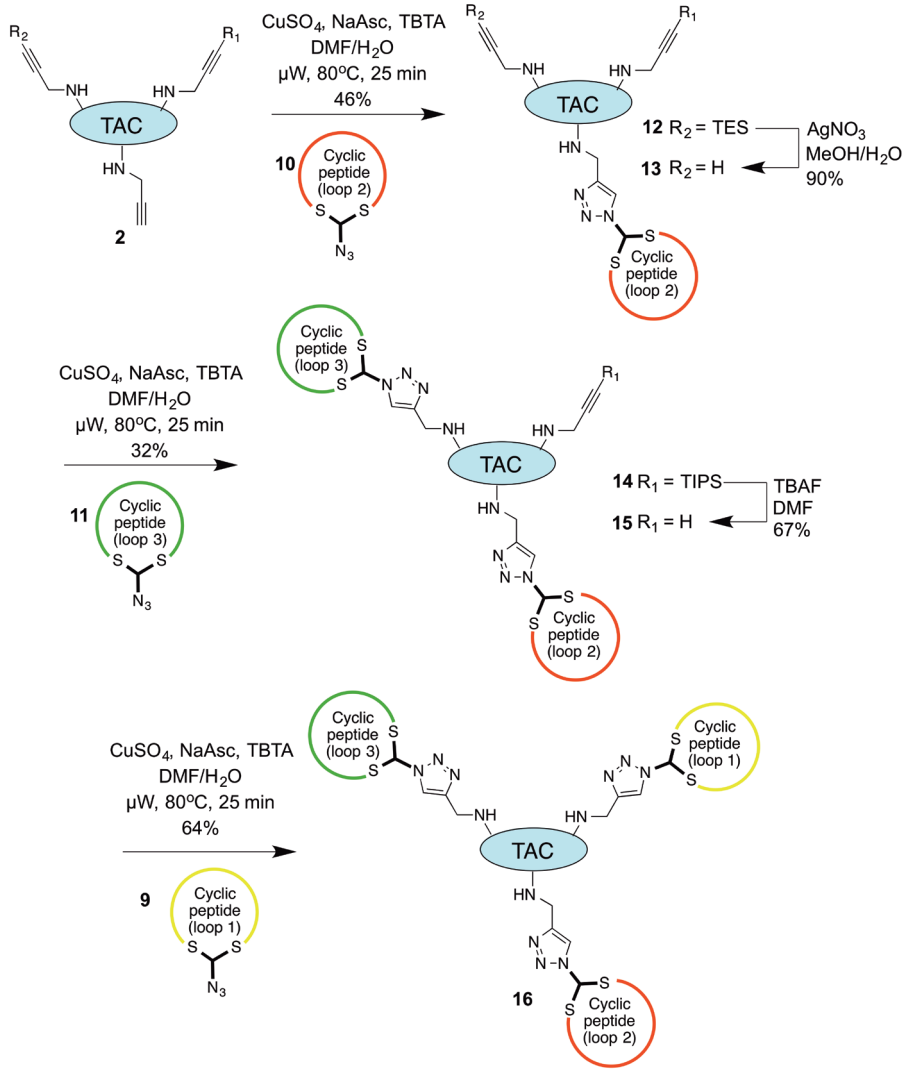

Scheme 3. The synthesis of discontinuous epitope mimic **16** by the sequential introduction of the three cyclic peptides, corresponding to the discontinuous epitope of Pertactin, onto the adapted TAC-scaffold (**2**).

segment GERQH, was introduced on the unprotected alkyne moiety of TAC-scaffold **2** by CuAAC ($CuSO_4$, sodium ascorbate, and tris-(benzyltriazolylmethyl)amine TBTA)) in DMF/H_2O using the microwave leading to **12**. After removal of the TES group by $AgNO_3$, leading to deprotected scaffold **13** in a high yield (90%), peptide loop 3 (**11**) containing the GDTWDDD sequence was introduced by CuAAC affording TAC-scaffold **14**, bearing two cyclic peptides. Finally, peptide loop 1 (**7**), representing sequence GGFGP, was attached for completion of the pertactin protein mimic. This was achieved by removal of the TIPS protecting group by TBAF in DMF to give TAC-scaffold **15** in a good yield (67%), followed by CuAAC of cyclic peptide **9** to furnish the desired molecular construct carrying three different cyclic peptides (**16**) (Figure 2) in a good yield (64%). The overall yield of the five-step introduction of the three cyclic peptides onto protected scaffold **6** was 6% (corresponding to an average yield of 56% per step) including HPLC purification after each reaction.

3.3 Conclusions

In this chapter, we have described a new versatile addition to the relatively scarce approaches for convergent synthesis of discontinuous epitope mimics. This method can provide access to appreciable quantities of biomolecular constructs consisting of three different peptide loops. For assembly of the protein mimics, a protected alkyne functionalized TAC-scaffold, which could be equipped with three (different) peptide loops in a successive manner using CuAAC, proved to be very versatile. The approach was exemplified by the synthesis of a protein mimic of the pertussis pertactin epitope. However, it should be emphasized that this approach is expected to be applicable to a wide range of discontinuous epitopes consisting of three loops.

3.4 Experimental procedures

3.4.1 General information

Chemicals were obtained from commercial sources and used without further purification, unless stated otherwise. Peptide grade D*i*PEA, CH_2Cl_2, TFA and HPLC grade solvents were purchased from Biosolve B.V. (Valkenswaard, the Netherlands) and peptide grade NMP and DMF were purchased from Actu-All Chemicals (Oss, the Netherlands). Fmoc-protected amino acids, BOP, and HBTU were purchased from GL Biochem Ltd. (Shanghai, China). Amino acid sidechain protecting groups were as follows: Arg(Pbf), Asp(OtBu), Cys(Trt), Gln(Trt), Glu(OtBu), His(Trt), Thr(tBu) and Trp(Boc). TentaGel S RAM resin (particle size 90 μm, capacity 0.25 mmol/g) was purchased from Rapp Polymere GmbH (Tübingen, Germany).

Solid phase peptide synthesis was performed on an Applied Biosystems 433A peptide synthesizer. Unless stated otherwise, reactions were performed at room temperature. TLC analysis was performed on Merck precoated silica gel 60 F-254 plates. Spots were visualized with UV-light, ninhydrin stain (1.5 g ninhydrin and 3.0 mL acetic acid in 100 mL *n*-butanol), and/or molybdenum staining agent (12 g ammonium molybdate and 0.5 g ammonium

cerium(IV) sulfate in 250 mL 10% H_2SO_4). Column chromatography was performed using Silica-P Flash silica gel (60 Å, particle size 40-63 μm) from Silicycle. Lyophilizations were performed on a Christ Alpha 1–2 apparatus. ^{1}H NMR (300 MHz) and ^{13}C NMR (75 MHz) experiments were conducted on a 300 MHz Varian G-300 spectrometer. Chemical shifts are given in ppm (δ) relative to TMS (0.00 ppm) (^{1}H NMR) or relative to $CDCl_3$ (77 ppm) (^{13}C NMR).

Analytical HPLC was performed on a Shimadzu-10Avp (Class VP) system using a Phenomenex Gemini C18 column (110 Å, 5 μm, 250×4.60 mm) at a flow rate of 1 mL min^{-1}. Buffers used were 0.1% trifluoroacetic acid in MeCN/H_2O 5:95 (buffer A) and 0.1% trifluoroacetic acid in MeCN/H_2O 95:5 (buffer B). Runs were performed using a standard protocol: 100% buffer A for 2 min, then a linear gradient of buffer B (0-100% in 48 min) and UV-absorption was measured at 214 and 254 nm. Peptide-containing compounds were purified on a Prep LCMS QP8000α HPLC system (Shimadzu) using a Phenomenex Gemini C18 column (10 μm, 110 Å, 250×21.2 mm) at a flow rate of 12.5 mL min^{-1}. Runs were performed using a standard protocol: 100% buffer A for 5 min followed by a linear gradient of buffer B (0-100% in 75 min) with the same buffers as were described for analytical HPLC.

Microwave reactions were performed in a Biotage Initiator (300W) reactor. ESI-TOF MS spectra were recorded on a microTOF mass spectrometer (Bruker). Samples were diluted with tuning mix (1:1, v/v) and infused at a speed of 300 μl/h using a nebulizer pressure of 5.8 psi, a dry gas flow of 3.0 L/min, a drying temperature of 180°C and a capillary voltage of 5.5 kV. Analytical LC-MS (electrospray ionization) was preformed on Thermo-Finnigan LCQ Deca XP Max using same buffers and protocol as described for analytical HPLC. MALDI-TOF MS spectra were recorded on a Kratos Analytical (Shimadzu) AXIMA CFR mass spectrometer using α-cyano-4-hydroxycinnamic acid (CHCA) as a matrix and human ACTH (18-39), $P_{14}R$ synthetic peptide or bovine insulin oxidized B chain as references. All reported mass values are monoisotopic.

3.4.2 Synthetic procedures and analytical data

Triethylsilyl propargylamine 5a

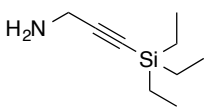

According to a literature procedure,[18] a solution of propargylamine (**4**, 2 g, 2.3 mL, 36 mmol) in anhydrous THF (200 mL) was cooled to -78°C and n-BuLi (14.5 mL, 2.5 M in hexanes, 36 mmol) was added dropwise. The solution was allowed to stir for 15 min at -78°C , after which it was allowed to warm up to 0°C and triethylsilyl chloride (7.3 mL, 43.6 mmol) was added dropwise. The reaction mixture was stirred overnight at r.t. and then quenched with a saturated aqueous $NaHCO_3$ solution (150 mL). The aqueous layer was extracted with EtOAc twice and the combined organic layers were dried over Na_2SO_4, filtered and concentrated *in vacuo*. The crude product was obtained as a yellow oil (4.36 g, 25.7 mmol, 71%). Spectroscopic data were in accordance with literature data.[18]

Triisopropylsilyl propargylamine 5b

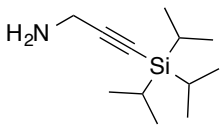

According to a literature procedure,[18] a solution of propargylamine (5.0 g, 91 mmol) in anhydrous THF (200 mL) was cooled to -78°C and n-BuLi (36.4 mL, 2.5 M in hexanes, 91 mmol) was added dropwise. The solution was allowed to stir for 15 min at -78°C, after which it was allowed to warm up to 0°C and triisoproylsilyl chloride (21.39 mL, 100 mmol) was added dropwise. The reaction mixture was stirred overnight at r.t. and then quenched with a saturated aqueous $NaHCO_3$ solution. The aqueous layer was extracted with EtOAc twice and the combined organic layers were dried over Na_2SO_4, filtered and concentrated *in vacuo*. Purification using silica gel column chromatography (EtOAc:Hexanes 1:1) yielded the product as a yellow liquid (12.4 g, 59 mmol, 64%). Spectroscopic data were in accordance with literature data.[18]

Tetrakis(triphenylphosphine)palladium[21]

DMSO (40 mL) was deoxygenated through nitrogen purging for 1 hour in a two-neck roundbottom flask and $PdCl_2$ (0.5 g, 2.8 mmol) and PPh_3 (3.7 mg, 14.1 mmol, 5 equiv.) were subsequently added under an argon atmosphere. The flask was fitted with a reflux condenser, warmed to 150°C and stirred for 1h after which a homogeneous orange solution was obtained. The oil bath was removed and hydrazine monohydrate (0.55 mL, 11.3 mmol) was added dropwise to form a yellow precipitate. The mixture was cooled to 0°C and the precipitated yellow solid was collected by filtration and washed with degassed EtOH (3x 50 mL) and degassed Et_2O (3x 50 mL) to yield the product as a yellow solid in quantative yield (3.2 g, 2.8 mmol).

Anilinium p-toluenesulfinate[1]

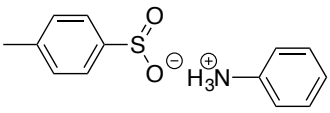

p-Toluenesulfinic acid sodium salt trihydrate (15 g) was dissolved in boiling water (250 mL) and HCl (1N, 85 mL) was added. The reaction was cooled down to room temperature and the p-toluenesulfinic acid crystals were collected by filtration, washed with cold water and dried *in vacuo*. The p-toluenesulfinic acid (4 g) was dissolved in CH_2Cl_2 (25 mL) and aniline (2.33 mL) was added. Slow addition of hexanes to this solution yielded the title compound as white crystals after collection by filtration and drying.

Cyclic peptide synthesis

Solid phase peptide synthesis

Linear peptides were synthesized on a peptide synthesizer using Tentagel S RAM resin (rink amide linker) on a 0.25-mmol scale. Removal of the Fmoc-group was performed using 20% piperidine in NMP. Amino acids were coupled using 4 equiv. of amino acid and HBTU as an activating agent with D*i*PEA as a base and NMP as solvent. Capping was performed using

acetic anhydride (12 mL), HOBt (0.5 g) and D*i*PEA (5.5 mL) in NMP (250 mL).

General procedure for the cleavage and deprotection of the linear peptide from the solid support

The sidechain-protected linear peptide was cleaved from the resin and deprotected using a mixture of TFA/H_2O/EDT/TIS (90:5:2.5:2.5) (v/v/v/v), 10 mL per gram resin. The reaction mixture was stirred for 3 hours after which the mixture was filtered and concentrated to a volume of 2 mL, followed by precipitation of the peptides by MTBE/hexane (1:1 v/v). After centrifugation (3500 rpm, 5 min), the supernatant was decanted and the pellet was resuspended in MTBE/hexane (1:1 v/v) and centrifuged again. Then, the pellet was dissolved in *t*-BuOH/H_2O (1:1 v/v) and lyophilized. The purity of the peptides was analyzed with analytical HPLC and the peptides were characterized with mass spectrometry.

General procedure for peptide cyclization by azido-bisbromide[22]

To a 1 mM solution of the crude linear peptide in a (1:3 v/v) mixture of MeCN/ NH_4HCO_3 (aq, 20 mM, pH 7.8) a solution of 1-(azidomethyl)-3,5-bis(bromomethyl)benzene (see Chapter 2) (1.25 equiv.) in MeCN (2 mL) was added dropwise. The resulting mixture was stirred at room temperature for 3 hours before being concentrated and lyophilized. The crude cyclic peptide was purified using preparative HPLC. The product-containing fractions were pooled and lyophilized to yield the purified cyclic peptides as white fluffy powder.

Loop 1 (**9**) (cyclic Ac-CGGFGPC-NH_2): 35 mg (42 µmol), 17% (18 steps, 91% per step). Mass calculated $[M + H]^+$: 838.31; MALDI-TOF MS found: 838.41. Rt = 27.00 min.

Loop 2 (**10**) (cyclic Ac-CGERQHC-NH_2): 35.8 mg (35 µmol), 14% (18 steps, 90% per step). Mass calculated $[M + H]^+$: 1030.40; MALDI-TOF MS found: 1030.40. Rt = 17.87 min. Note: Preparative HPLC was performed with 0.1% trifluoroacetic acid in H_2O (buffer A) and 0.1% trifluoroacetic acid in MeCN/H_2O 95:5 (buffer B) using the same protocol as described above.

Loop 3 (**11**) (cyclic Ac-CGDTWDDDC-NH_2): 78 mg (64 µmol), 26% (22 steps, 94% per step). Mass calculated $[M + H]^+$: 1227.24; MALDI-TOF MS found: 1227.24. Rt = 22.98 min.

Alkyne-protected scaffold 2

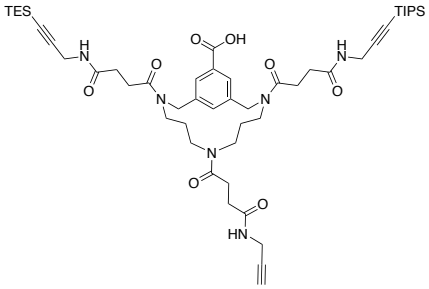

Loading of the resin: To a solution of the Alloc-, Fmoc-, *o*NBS-protected TAC-scaffold[4] (0.4 mmol, 307 mg) in CH_2Cl_2 (10 mL) were added DiPEA (70 µL, 0.4 mmol) and 2-chlorotrityl chloride resin (1 g). The mixture was shaken for 5 minutes after which DiPEA (0.6 mmol, 105 µL) was added. The mixture was shaken overnight after which MeOH

(1 mL) and DiPEA (1.4 mmol, 245 µL) were added and the resulting mixture was shaken for 30 minutes. The mixture was then transferred to a solid-phase tube and the solvent was drained. The resin was washed with CH_2Cl_2 (3x 10 mL), MeOH (3x 10 mL) and Et_2O (3x 10 mL) and dried in vacuo. The loading efficiency was determined by photometric quantification of the absorbance of the dibenzofulvene-piperidine adduct at 300 nm (ε = 7800 M^{-1} cm^{-1}) obtained after piperidine-mediated removal of the Fmoc-group from an aliquot of the resin.

Alloc-removal: The resin was swelled in NMP for 10 minutes after which anilinium p-toluenesulfinate (20 equiv., 1.68 g, 6.3 mmol) and NMP (10 mL) were added. The mixture was bubbled through with argon for 10 min after which $Pd(PPh_3)_4$ (0.3 equiv., 110 mg) was added and the mixture was bubbled through with argon for another 45 minutes under the exclusion of light. The resin was washed with NMP (3x 10 mL), 0.1% diethyldithiocarbamic acid (w/v) in NMP (3x 10 mL) and 20% DiPEA in NMP (3x 10 mL). This Alloc cleavage procedure was repeated once to ensure complete removal of the protecting group.

General procedure for the coupling of succinic anhydride: The resin was washed with NMP (3x 10 mL). Succinic anhydride (10 equiv., 316 mg, 3.2 mmol) and NMP (10 mL) were added to the resin. The mixture was bubbled through with N_2 and DiPEA (10 equiv., 550 µL, 3.15 mmol) was added. The mixture was shaken for 1 hour after which the resin was washed with NMP (3x, 10 mL) and CH_2Cl_2 (3x, 10 mL).

General procedure for the coupling of (protected) propargylamine: The resin was washed with NMP (3x 10 mL) and treated with BOP (560 mg, 1.26 mmol), CH_2Cl_2 (10 mL) and DiPEA (440 µL, 2.53 mmol). After two minutes the (protected) propargylamine (**4**, **5a**, or **5b**, 4 equiv., 1.26 mmol) was added and the resulting mixture was shaken overnight. The resin was washed with CH_2Cl_2 (4x 10 mL) and NMP (3x 10 mL).

Fmoc-removal: The resin was washed with NMP (3x 10 mL). A solution of piperidine in NMP (20%, 10 mL) was added and the mixture was bubbled through with nitrogen for 30 minutes. The resin was washed with NMP (3x 10 mL) and CH_2Cl_2 (10 mL).

oNBS-removal: The resin was washed with DMF (3x 10 mL). 2-Mercapoethanol (221 µL, 3.16 mmol), DBU (1.58 mmol, 236 µL) and DMF (10 mL) were added and the mixture was shaken for 15 minutes. This *o*NBS-removal procedure was repeated once to ensure complete removal of the protecting group. The resin was washed with DMF (3x 10 mL) and CH_2Cl_2 (3x 10 mL).

Cleavage from the resin: The resin was treated with 30% HFIP in CH_2Cl_2 (10 mL) for 30 minutes. The resin was then filtered off and washed with CH_2Cl_2. EtOAc was added To the filtrate and the solvents were evaporated. The residue was redissolved in tBuOH:H_2O (1:1) and lyophilized to give the crude product. Purification was performed by preparative HPLC to yield to product as a white powder (177 mg, 0.32 mmol, 58%, 95% per step)

Mass calculated $[M+Na]^+$: 981.53; MALDI-TOF MS found: 981.58. Rt = 45.85 min.

Compound 12: CuAAC of cyclic peptide 10

In a microwave vessel (0.5-2 mL) alkyne-protected scaffold **2** (10 mg, 10.4 µmol), cyclic peptide **10** (12.6 mg, 10.4 µmol), $CuSO_4.5H_2O$ (0.78 mg, 3.12 µmol), sodium ascorbate (1.85 mg, 9.36 µmol) and TBTA (0.83 mg, 1.56 µmol) were dissolved in DMF/H_2O (2 mL, 3/2 v/v). The microwave vessel was sealed and the resulting mixture was allowed to react in the microwave at 80°C for 25 minutes. The resulting mixture was diluted with a mixture of 0.1% TFA in MeCN/H_2O (1/1, v/v) to a volume of 5 mL, after which it was centrifuged (5 min, 5000 rpm). The supernatant was purified using preparative HPLC and the product-containing fractions were pooled and lyophilized to give the product as a fluffy white solid (9.6 mg, 4.8 µmol, 46%).

Mass calculated $[M + H]^+$: 1988.95; MALDI-TOF MS found: 1988.84. Rt = 33.97 min.

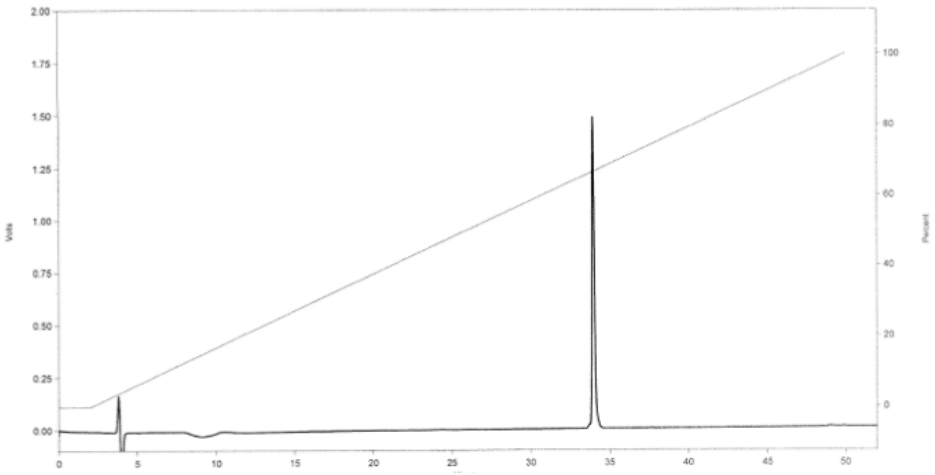

Compound 13: Removal of TES protecting group

TES-protected scaffold **12** (14.4 mg, 7.2 µmol) was dissolved in 20 mL MeOH/H_2O (4/1, v/v) and a solution of $AgNO_3$ (12.2 mg, 72 µmol) in 1 mL H_2O was added. The resulting mixture was stirred for 3 hours and the reaction was followed by LC-MS. The reaction mixture was concentrated to a volume of about 10 mL, after which NaCl (4.2 mg, 72 µmol) was added and the mixture was centrifuged (5 min, 5000 rpm). The supernatant was concentrated *in vacuo* to a volume of approximately 2 mL after which it was diluted with a mixture of 0.1% TFA in MeCN/H_2O (1/1, v/v) to a volume of 5 mL. This mixture was then purified by preparative HPLC and the product-containing fractions were pooled and lyophilized to obtain the product as a fluffy white solid (12.2 mg, 6.5 µmol, 90%).

Mass calculated $[M + H]^+$: 1874.87; MALDI-TOF MS found: 1874.73. Rt = 28.55 min.

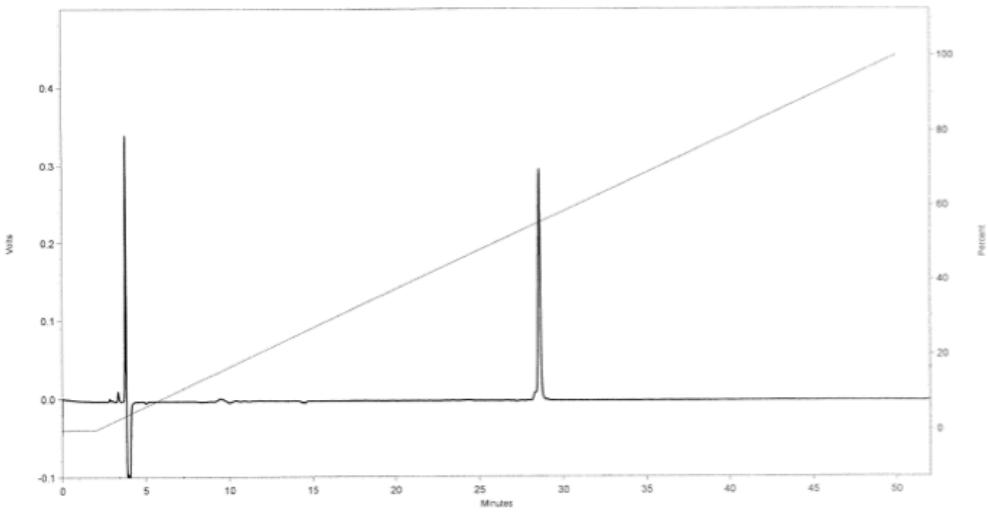

Compound 14: CuAAC of cyclic peptide 11

In a microwave vessel (0.5-2 mL) TES-deprotected scaffold **13** (12.2 mg, 6.5 μmol), cyclic peptide **11** (8.0 mg, 6.5 μmol), $CuSO_4.5H_2O$ (0.49 mg, 1.95 μmol), sodium ascorbate (1.16 mg, 5.85 μmol) and TBTA (0.52 mg, 0.975 μmol) were dissolved in DMF/H_2O (2 mL, 3/2, v/v). The microwave vessel was sealed and the mixture allowed to react in the microwave at 80°C for 25 minutes. The resulting mixture was diluted with a mixture of 0.1% TFA in MeCN/H_2O (1/1, v/v) to a volume of 5 mL, after which it was centrifuged (5 min, 5000 rpm). The supernatant was purified using preparative HPLC and the product-containing fractions were pooled and lyophilized to give the product as a fluffy white solid (6.5 mg, 2.1 μmol, 32%).

Exact mass calculated $[M+2H]^{2+}$: 1551.1242; ESI-TOF MS found: 1551.1212. Rt = 26.83 min.

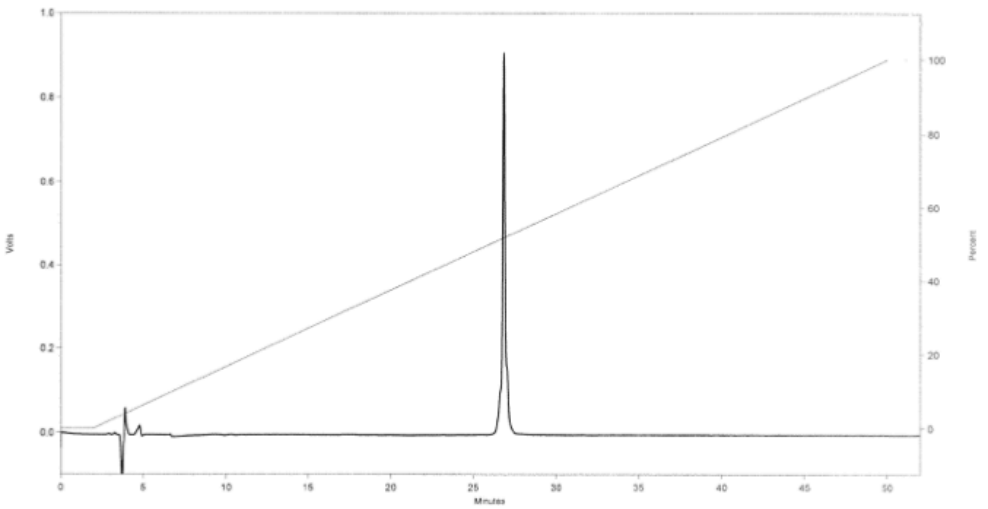

Compound 15: Removal of the TIPS-protecting group

TIPS-protected scaffold **14** (6.5 mg, 2.1µmol) was dissolved in DMF (2 mL) and a solution of TBAF.3H_2O (6.6 mg, 21 µmol) in 0.5 mL DMF was added. The resulting mixture was stirred overnight, after which the progress was checked by LCMS. After completion of the reaction the mixture was purified by preparative HPLC and the product-containing fractions were pooled and lyophilized to give the product as a fluffy white solid (4.1 mg, 1.4 µmol, 67%).

Exact mass calculated $[M+2H]^{2+}$: 1473.0575; ESI TOF MS found: 1473.0506. Rt = 19.47 min.

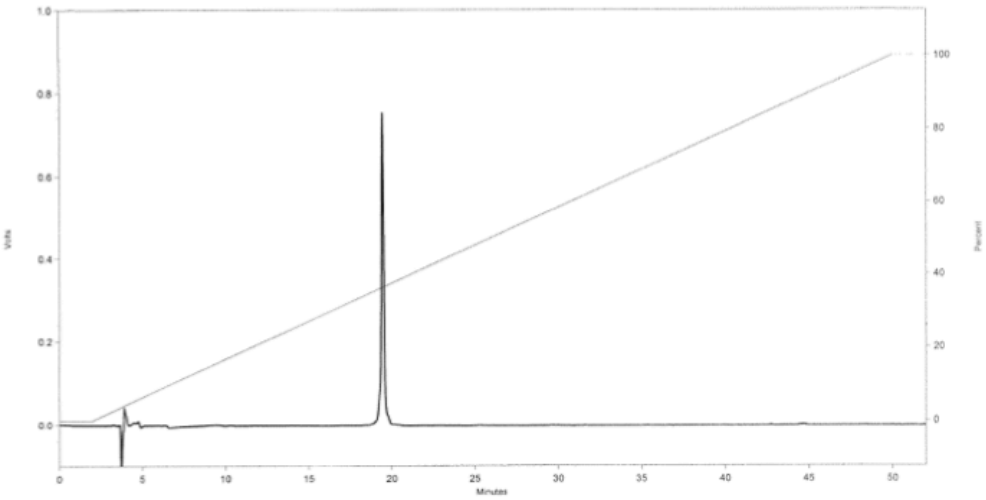

Compound 16: CuAAC of cyclic peptide 9

In a microwave vessel (0.5-2 mL) deprotected scaffold **15** (4.1 mg, 1.4 µmol), cyclic peptide **9** (1.2mg, 1.4 µmol), $CuSO_4.5H_2O$ (0.1 mg, 0.42 µmol) and sodium ascorbate (0.26 mg, 1.29 µmol) and TBTA (0.03 mg, 0.06 µmol) were dissolved in DMF/H_2O (0.5 mL, 3/2. v/v). The microwave vessel was sealed and the mixture was allowed to reacted in the microwave at 80°C for 25 minutes. The resulting mixture was directly purified using preparative HPLC and the product-containing fractions were pooled and lyophilized to give the product as a fluffy white solid (3.4 mg, 0.9 µmol, 64%).

Exact mass calculated $[M+2H]^{2+}$: 1891.7103; ESI TOF MS found: 1891.7154. Rt = 21.47 min.

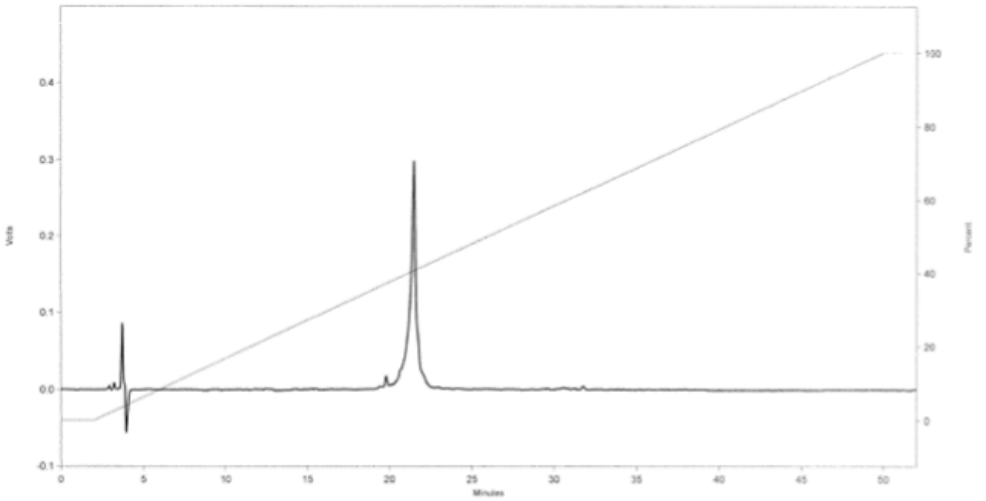

References

1 C. Chamorro, J. A. W. Kruijtzer, M. Farsaraki, J. Balzarini and R. M. J. Liskamp, *Chem. Commun.*, 2009, 821–823.

2 M. Hijnen, D. J. Van Zoelen, C. Chamorro, P. Van Gageldonk, F. R. Mooi, G. Berbers and R. M. J. Liskamp, *Vaccine*, 2007, **25**, 6807–6817.

3 H. S. Park, Q. Lin and A. D. Hamilton, *J. Am. Chem. Soc.*, 1999, **121**, 8–13.

4 T. Opatz and R. M. J. Liskamp, *Org. Lett.*, 2001, **3**, 3499–3502.

5 E. T. Rump, D. T. S. Rijkers, H. W. Hilbers, P. G. De Groot and R. M. J. Liskamp, *Chem. - A Eur. J.*, 2002, **8**, 4613–4621.

6 G. E. Mulder, J. A. W. Kruijtzer and R. M. J. Liskamp, *Chem. Commun.*, 2012, **48**, 10007–10009.

7 G. E. Mulder, H. C. Quarles van Ufford, J. van Ameijde, A. J. Brouwer, J. A. W. Kruijtzer and R. M. J. Liskamp, *Org. Biomol. Chem.*, 2013, **11**, 2676–2684.

8 D. M. Beal and L. H. Jones, *Angew. Chem. Int. Ed.*, 2012, **51**, 6320–6326.

9 M. Mutter and S. Vuilleumier, *Angew. Chem. Int. Ed.,* 1989, **28**, 535–554.

10 P. Dumy, I. M. Eggleston, S. Cervigni, U. Sila, X. Sun and M. Mutter, *Tetrahedron Lett.*, 1995, **36**, 1255–1258.

11 D. Boturyn, J.-L. Coll, E. Garanger, M.-C. Favrot and P. Dumy, *J. Am. Chem. Soc.*, 2004, **126**, 5730–5739.

12 Y. Singh, G. T. Dolphin, J. Razkin and P. Dumy, *ChemBioChem*, 2006, **7**, 1298–1314.

13 X. T. Zhou, A. Rehman, C. Li and P. B. Savage, *Org. Lett.*, 2000, **2**, 3015–3018.

14 S. Pritz, O. Kraetke, A. Klose, J. Klose, S. Rothemund, K. Fechner, M. Bienert and M. Beyermann, *Angew. Chem. Int. Ed.*, 2008, **47**, 3642–5.

15 D. M. Beal, V. E. Albrow, G. Burslem, L. Hitchen, C. Fernandes, C. Lapthorn, L. R. Roberts, M. D. Selby and L. H. Jones, *Org. Biomol. Chem.*, 2012, **10**, 548–554.

16 G. Clavé, H. Volland, M. Flaender, D. Gasparutto, A. Romieu and P.-Y. Renard, *Org. Biomol. Chem.*, 2010, **8**, 4329–4345.

17 M. Galibert, O. Renaudet, P. Dumy and D. Boturyn, *Angew. Chem. Int. Ed.*, 2011, **50**, 1901–1904.

18 I. E. Valverde, A. F. Delmas and V. Aucagne, *Tetrahedron*, 2009, **65**, 7597–7602.

19 A. J. Brouwer, H. Van De Langemheen and R. M. J. Liskamp, *Tetrahedron*, 2014, **70**, 4002.

20 M. Hijnen, F. R. Mooi, P. G. M. Van Gageldonk, P. Hoogerhout, A. J. King and G. A. M. Berbers, *Infect. Immun.*, 2004, **72**, 3716–3723.

21 D. R. Coulson, L. C. Satek and O. Grim, *Inorg. Synth.*, 1972, **XIII**, 121–124.

22 P. Timmerman, J. Beld, W. C. Puijk and R. H. Meloen, *ChemBioChem*, 2005, **6**, 821–824.

4

Chapter 4

Synthesis of a protected trialkyne scaffold and improved sequential ligation

Parts of this chapter have been published in:

P.R. Werkhoven, M. Elwakiel, T.J. Meuleman, H.C. Quarles van Ufford, J.A.W. Kruijtzer, R.M.J. Liskamp Org. Biomol. Chem. 2016, 14, 701-710

4.1 Introduction

In chapter 3, a method for the sequential introduction of cyclic peptides onto a scaffold was described. The scaffold contained three alkynes that were sequentially accessible because two of the alkynes were protected each with a different silyl protecting groups. In this way, different peptides could be sequentially introduced onto the scaffold. This method provides not only great control over the number and identity of the peptides ligated onto the scaffold but also over the relative positioning of the peptides on scaffold. Using the method described in Chapter 3 it was possible to synthesize a mimic of an epitope of the *Bordetella pertussis* protein Pertactin. The versatility of this method was a stimulus to optimize the synthetic route and the scaffold structure. Furthermore, the robustness of the new approach was evaluated by the synthesis of a mimic of a different epitope.

The first adjustment to the scaffold is a shortening of the linker between the scaffold and the alkyne. In chapter 3 (top right Figure 1) succinic anhydride had to be coupled onto the scaffold before the propargylamine derivative could be attached. The new scaffold design (bottom right Figure 1) replaces the succinic anhydride-propargylamine combination with pentynoic acid derivatives. This modification will reduce the number of steps in the synthesis of the required scaffold. Furthermore, the skeleton of the scaffold will be identical to our earlier described scaffold (bottom left Figure 1).[1] In this earlier work, the TAC-scaffold was loaded with three pentynoic acid residues and a mixture of peptides was ligated using CuAAC. Not only will this approach create different peptide combinations on the scaffold but also the relative orientation of a particular peptide combination may differ. The similarity

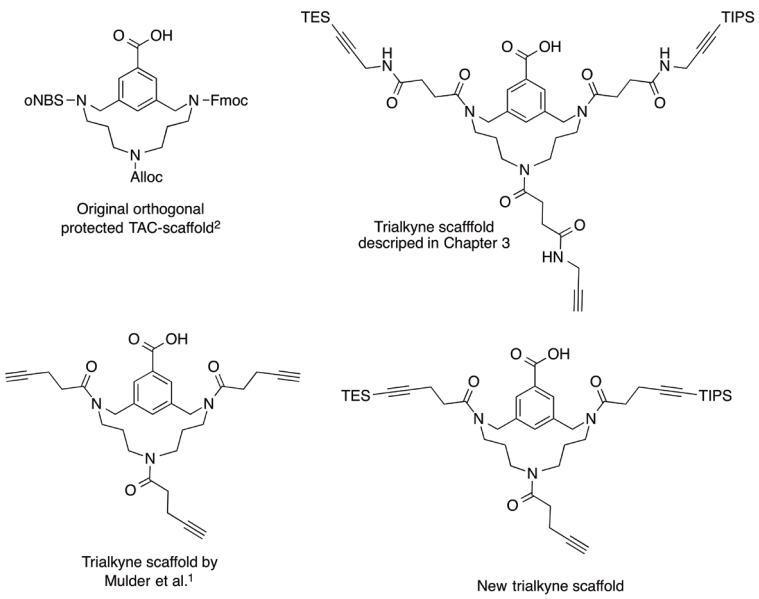

Figure 1. Four generations of the TAC-scaffold Top left: the original TAC-scaffold with three orthogonally protected amines.[2] Bottom left: the three alkyne bearing TAC scaffold by Mulder et al.[1] Top right: The silyl-protected trialkyne scaffold described in chapter 3. Bottom right: Improved scaffold bearing three alkynes through (protected) pentynoic acid moieties.

of the skeleton will enable (re)synthesis of exactly corresponding individual library hits obtained from screening. The approach described in this chapter will enable the controlled introduction of different peptides on the alkyne-functionalized scaffold as well as control over their relative positioning.

The scaffold described in chapter 3 was synthesized from the original Alloc-, Fmoc-, oNBS- protected scaffold (top left Figure 1).[2] The synthesis of this scaffold has been described[2] and optimized in our group.[3] However, for the new pentynoic acid based scaffold an adjusted route could be designed, in which the number of steps was reduced.

This chapter will discuss the complete synthesis of an improved TAC-scaffold bearing three pentynoic acid moieties containing the same orthogonal silyl protecting group strategy as the scaffold in chapter 3. Furthermore, the versatility of the method of sequentially introducing cyclic peptides will be illustrated using the synthesis of a different epitope mimic, namely a mimic of the CD4-binding site of the HIV protein gp120.[4,5]

4.2 Results and discussion

4.2.1 Scaffold synthesis

In the new scaffold, the protected alkynes are introduced as protected pentynoic acid derivatives. The required triethylsilyl and triisopropylsilyl protected pentynoic acid derivatives (**4a** and **4b**) were synthesized in three steps (Scheme 1). Firstly, the carboxylic acid moiety of pentynoic acid (**1**) was protected by conversion to a *tert*-butyl ester (**2**). Next, the silyl-protecting groups were introduced using *n*-BuLi and the appropriate silyl chloride. Both the TIPS- and the TES-protected alkynes (**3a** & **3b**) were obtained in good yields (ca. 70%). Finally, the *tert*-butyl ester was removed by treatment with TFA to afford the silyl-protected pentynoic acid derivatives (**4a** & **4b**). From the modest yield of TES-protected derivative **4a**, compared to the yield of TIPS-protected derivative **4b**, it becomes apparent that the TES-group is less stable under these conditions. For this reason, the TES-protected pentynoic acid had to be introduced onto the scaffold near the end of the synthesis.

The synthesis of the improved tri-alkyne scaffold was based on the synthesis described in earlier work of our group.[3] However, some modifications were made to streamline the

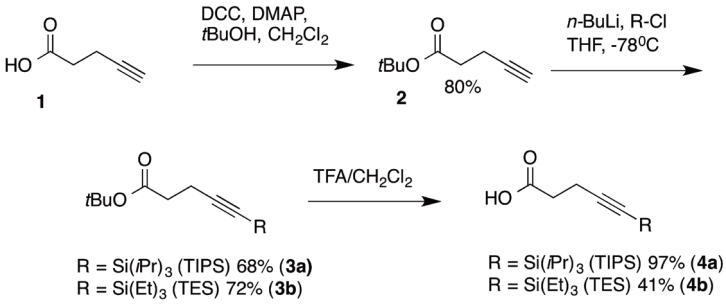

Scheme 1. Synthesis of silyl-protected pentynoic acid derivatives.

synthesis. The main modification in the synthesis route was that the Alloc protecting group on the middle amine was replaced by a pentynoic acid moiety. Pentynoic acid was thus immediately introduced on the desired position and is resistant to all following synthetic steps, which circumvented the Alloc-introduction and deprotection steps.

The synthesis of the optimized scaffold (**13**) is shown in Scheme 2. Starting from 3-bromopropylamine hydrochloride (**5**), the first step was the introduction of the *o*NBS protecting group to afford *o*NBS-protected bromopropylamine (**6**). Next, triamine **7** was prepared by reaction of propylamine **6** and 1,3-diaminopropane in DMA. Then, the primary amine of triamine **7** was protected with a trifluoroacetyl (Tfa) protecting group, using ethyl trifluoroacetate, to afford double-protected triamine **8**. Coupling of pentynoic acid to the

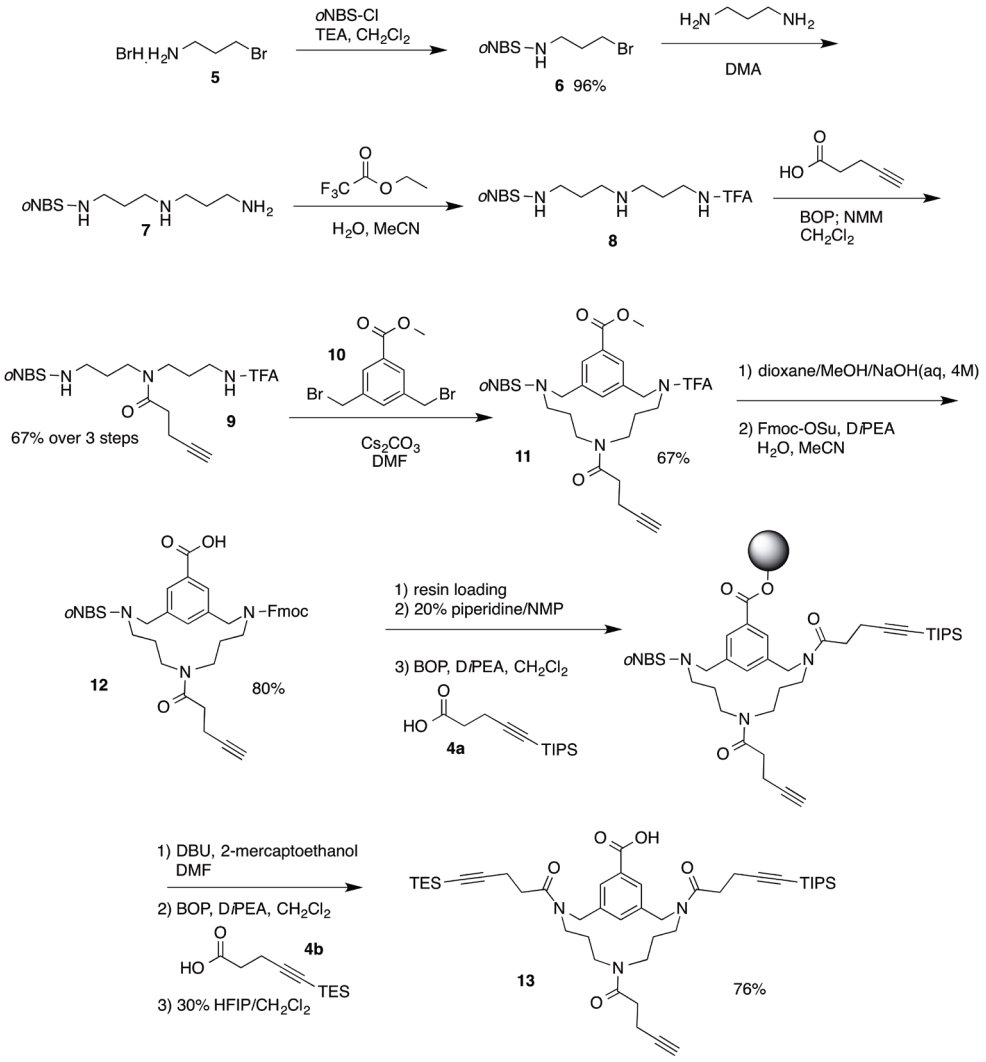

Scheme 2. Synthesis of the protected tri-alkyne scaffold. The synthesis is an adaptation and expansion on the most recent synthesis of the orthogonally protected triamine TAC-scaffold.[3]

secondary amine of triamine **8** using BOP afforded linear triamine **9** with an overall yield of 67% over three steps.

Triamine **9** was cyclized by reaction with dibromide **10**, which was easily synthesized using a literature procedure,[6] to give the TAC-scaffold skeleton (**11**) in a 67% yield. Next, both the methyl ester and the trifluoroacetyl protecting group were hydrolysed by treatment with base. This was followed by the protection of the now free amine with an Fmoc protecting group to afford free carboxylic acid containing TAC-scaffold **12** in a good yield (80%) over two steps.

The scaffold was then loaded onto a 2-chlorotrityl chloride resin. The Fmoc-group was removed by piperidine, followed by the BOP-coupling of TIPS-protected pentynoic acid **4a**. Next, the *o*NBS-group was removed through treatment with DBU and 2-mercaptoethanol, followed by the coupling of TES-protected pentynoic acid **4b**. Finally, the scaffold was cleaved from the resin with HFIP and protected trialkyne scaffold **13** was obtained in a good overall yield (76% over 6 steps).

4.2.2 Cyclic peptides

With the available new scaffold, the next step was the sequential introduction of cyclic peptides onto the scaffold. The cyclic peptides that were used here were based on the discontinuous epitope of the HIV protein gp120, which binds to the CD4-receptor. This is one of the first steps in HIV infection of the cell. The epitope consists of three loops (Figure

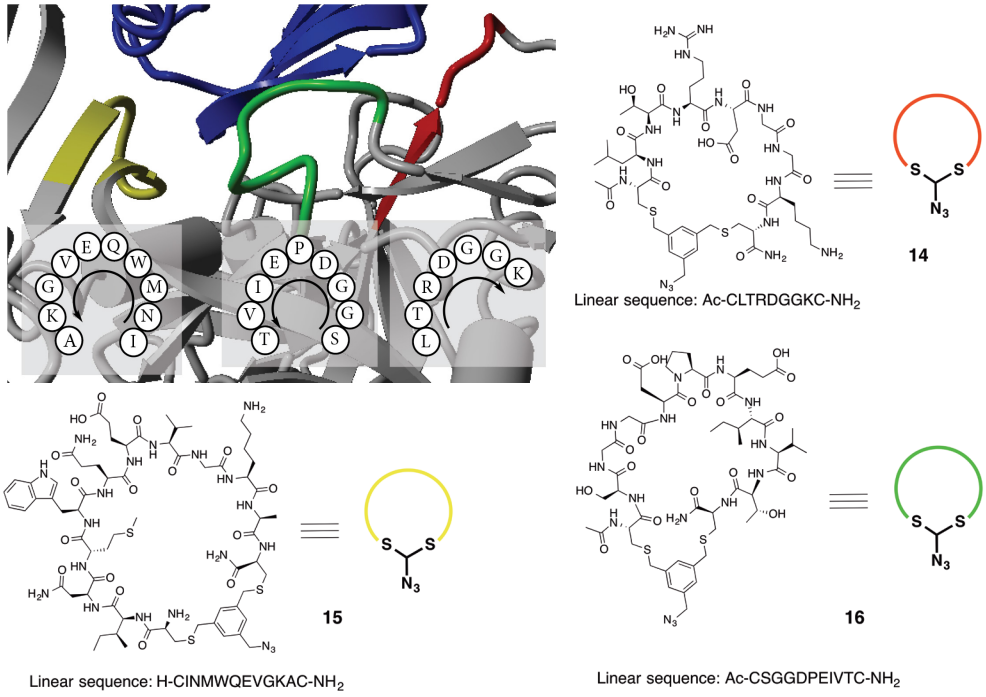

Figure 2. Zoom of the CD4(blue)-binding site of HIV gp120 (gray). The binding loops of the epitope are shown in yellow, green and red and their amino acid sequence is noted. The structures of the azide-bearing cyclic peptides (**14**, **15**, and **16**) that mimic this binding site are also shown.

2),[4,5] which makes it well suited to be mimicked using our system. The binding site to CD4 can be mimicked by three cyclic peptides with amino acid sequences that correspond to the peptide segments in gp120 (Figure 2). The required azide-bearing cyclic peptides were easily accessible using the same synthesis protocol as was described in chapter 2. The desired amino acid sequence was flanked on each side by a cysteine residue. The peptide was cyclized by reacting the thiol moieties of these cysteine residues with our bisbromobenzyl reagent (Chapter 2), which simultaneously introduced the azide required for CuAAC. The azide-bearing cyclic peptides could then be used for the sequential introduction onto the scaffold.

4.2.3 Sequential ligation

The peptides were ligated onto the scaffold using a similar protocol as described in chapter 3 with some improvements (Scheme 3). Firstly, the CuAAC reactions did not require microwave irradiation. In fact, not having to carry out the reaction in the microwave prevented the partial cleavage of the TES-group during the first CuAAC step, which was observed when the reaction was performed in the microwave. As a result, the TES-deprotection step could be combined with the first ligation step. After purification by preparative HPLC the TES-deprotected scaffold (**17**), with the first cyclic peptide (**14**) attached, was obtained in a good yield (50%). Subsequently, the second cyclic peptide was attached to the scaffold again without microwave irradiation to afford two cyclic peptide-bearing scaffold (**18**) in an excellent yield (80%). Next, the TIPS-protecting group was removed with TBAF to provide the scaffold

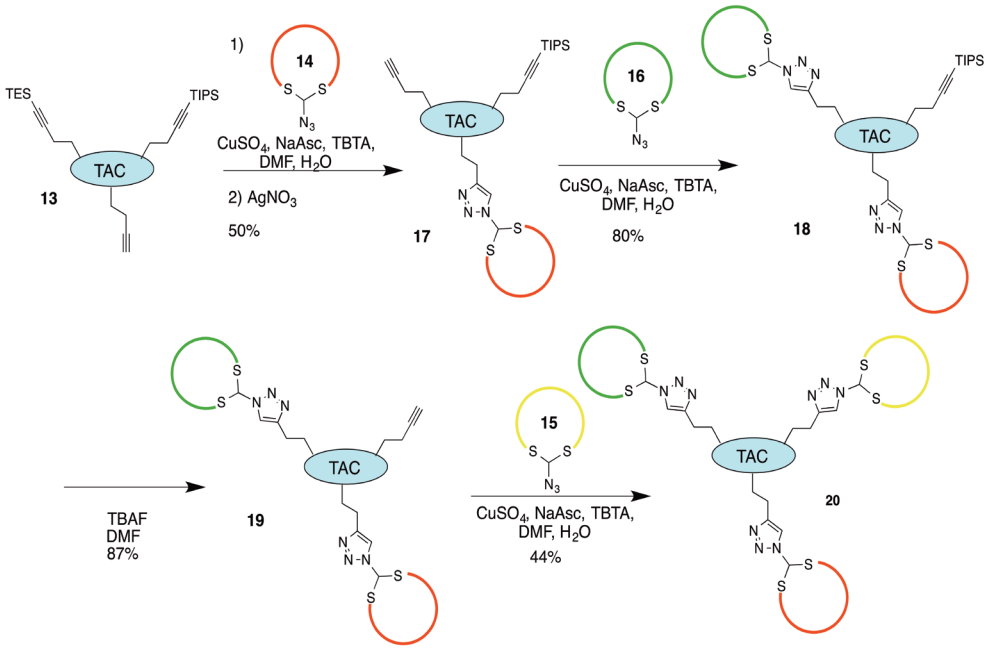

Scheme 3. Sequential ligation of the three cyclic peptides that resemble the CD4-binding sites of HIV gp120 onto the TAC-scaffold.

containing the last remaining alkyne (**19**) in an excellent yield (87%). Finally, the third cyclic peptide was attached to the scaffold to afford the final protein mimic (**20**) in a moderate yield (44%). The overall yield of the procedure for the sequential introduction of three cyclic peptides is 15% (average 68% per step). This is a significant improvement over the 3% yield that was obtained in the sequential introduction described in chapter 3.

This procedure for the sequential introduction of three cyclic peptides has proved to be more efficient than the previously described microwave-assisted procedure. However, the procedure is still laborious and requires multiple purification steps. If the procedure can be streamlined and simplified by reducing the number of purification steps, this will greatly increase the accessibility of mimics of discontinuous epitopes consisting of three loops. A few attempts at eliminating a few purification steps and continuing the procedure were unfortunately unsuccessful. In these attempts, the CuAAC reaction of the second peptide usually showed only low conversion to the desired product. Furthermore, the removal of the TIPS group does not work if too much water is present.

4.3 Conclusions

In this chapter, the synthesis of an improved silyl-protected trialkyne TAC-scaffold has been described. The scaffold was then used for the sequential introduction of cyclic peptides corresponding to the peptide segments of the CD4 binding site of the HIV protein gp120. The procedure for peptide introduction was optimized in comparison with the previously described microwave procedure. This resulted in an increase in overall yield from 3% to 15%. Furthermore, the successful synthesis of the gp120 protein mimic shows that the synthesis method is robust and might be applied to different epitopes.

4.4 Experimental methods

4.4.1 General information

Chemicals were obtained from commercial sources and used without further purification, unless stated otherwise. Peptide grade D*i*PEA, CH_2Cl_2, TFA and HPLC grade solvents were purchased from Biosolve B.V. (Valkenswaard, the Netherlands) and peptide grade NMP and DMF were purchased from Actu-All Chemicals (Oss, the Netherlands). Fmoc-protected amino acids, BOP, and HBTU were purchased from GL Biochem Ltd. (Shanghai, China). Amino acid side chain protecting groups were as follows: Arg(Pbf), Asp(OtBu), Cys(Trt), Gln(Trt), Glu(OtBu), His(Trt), Thr(tBu) and Trp(Boc). TentaGel S RAM resin (particle size 90 μm, capacity 0.25 mmol/g) was purchased from Rapp Polymere GmbH (Tübingen, Germany). Unless stated otherwise, reactions were performed at room temperature.

Solid phase peptide synthesis was performed on an Applied Biosystems 433A peptide synthesizer or a C.S. Bio Co. peptide synthesizer (model CS336X). Unless stated otherwise, reactions were performed at room temperature. TLC analysis was performed on Merck precoated silica gel 60 F-254 plates. Spots were visualized with UV-light, ninhydrin stain (1.5

g ninhydrin and 3.0 mL acetic acid in 100 mL *n*-butanol), Potassium permanganate (1.5 g of $KMnO_4$, 10 g K_2CO_3, and 1.25 mL 10% NaOH in 200 mL water) and/or molybdenum staining agent (12 g ammonium molydate and 0.5 g ammonium cerium(IV) sulfate in 250 mL 10% H_2SO_4). Column chromatography was performed using Silica-P Flash silica gel (60 Å, particle size 40-63 μm) from Silicycle (Canada). Lyophilization was performed on a Christ Alpha 1–2 apparatus. ^{1}H NMR (400 MHz) and ^{13}C NMR (100 MHz) experiments were conducted on a 300 MHz Varian G-300 spectrometer. Chemical shifts are given in ppm (δ) relative to TMS (0.00 ppm) (^{1}H NMR) or relative to $CDCl_3$ (77 ppm) (^{13}C NMR).

Analytical HPLC was performed on a Shimadzu-10Avp (Class VP) system using a Phenomenex Gemini C18 column (110 Å, 5 μm, 250×4.60 mm) at a flow rate of 1 mL min^{-1}. The used buffers were 0.1% trifluoroacetic acid in MeCN/H_2O 5:95 (buffer A) and 0.1% trifluoroacetic acid in MeCN/H_2O 95:5 (buffer B). Runs were performed using a standard protocol: 100% buffer A for 2 min, then a linear gradient of buffer B (0-100% in 48 min) and UV-absorption was measured at 214 and 254 nm. Purification by preparative HPLC was performed on a Prep LCMS QP8000α HPLC system (Shimadzu) using a Phenomenex Gemini C18 column (10 μm, 110 Å, 250×21.2 mm) at a flow rate of 12.5 mL min^{-1}. Runs were performed by a standard protocol: 100% buffer A for 5 min followed by a linear gradient of buffer B (0-100% in 70 min) with the same buffers as were described for analytical HPLC.

ESI-TOF MS spectra were recorded on a microTOF mass spectrometer (Bruker). Samples were diluted with tuning mix (1:1, v/v) and infused at a speed of 300 μl/h using a nebulizer pressure of 5.8 psi, a dry gas flow of 3.0 L/min, a drying temperature of 180°C and a capillary voltage of 5.5 kV. Analytical LC-MS (electrospray ionization) was performed on Thermo-Finnigan LCQ Deca XP Max using same buffers and protocol as described for analytical HPLC. All reported mass values are monoisotopic.

4.4.2 Scaffold synthesis

***tert*-butyl pent-4-ynoate (2)**

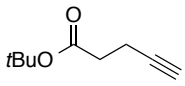

According to a literature procedure,[7] 4-pentynoic acid (**1**, 5.0 g, 51.0 mmol), t-BuOH (9.7 mL, 102 mmol) and DMAP (0.3 g, 2.5 mmol) were dissolved in CH_2Cl_2 (10 mL). The mixture was stirred for 10 min. A solution of DCC (11.55 g, 56.0 mmol) in CH_2Cl_2 (10 mL) was added and the resulting mixture was stirred overnight. Next the formed DCU precipitate was removed by filtration and washed with CH_2Cl_2. The filtrate was washed with 0.5 M HCl (2x 100 mL), 1 M $NaHCO_3$ (2x 100 mL) and dried over Na_2SO_4. After filtration, the solvent was removed by evaporation. The residue was purified by silica gel column chromatography (CH_2Cl_2) to give tert-butyl pent-4-ynoate (2) as a yellowish oil (6.3 g, 40.8 mmol, 80%). Spectroscopic data was in agreement with literature data.[7]

***tert*-butyl 5-(triisopropylsilyl)-pent-4-ynoate (3a)**

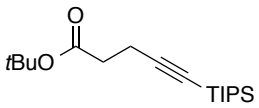

Compound **2** (1.0 g, 6.5 mmol) was dissolved in anhydrous THF (20 mL) and the solution was cooled to -78°C with a dry ice and acetone bath. *n*-BuLi (2.6 mL, 2.5 M in hexane, 6.5 mmol) was added dropwise and the reaction mixture was stirred for 10 minutes. Then the dry ice/acetone bath was replaced with an ice bath (0°C) and TIPS-Cl (1.7 mL, 7.8 mmol) was added dropwise. The reaction mixture was stirred for 3 hours at room temperature, after which it was quenched with 40 mL saturated aqueous NH_4Cl. THF was removed by evaporation *in vacuo* and the resulting aqueous slurry was diluted with H_2O (50 mL). The mixture was extracted with EtOAc (3 x 30 mL) and the combined organic layers were dried over Na_2SO_4. After filtration, the solvent was evaporated. The crude product was purified by silica gel column chromatography (eluent: 10% Et_2O in hexanes) to give tert-butyl 5-(triethylsilyl)pent-4-ynoate (**3a**) as a yellow oil (1.4 g, 4.4 mmol, 68%). R_f = 0.55 (5% EtOAc in petroleum ether 40-60). ^{1}H NMR (400 MHz, $CDCl_3$): δ =1.04 (m, 21H, $Si(CH(CH_3)_2)_3$), 1.44 (s, 9H, $C(CH_3)_3$), 2.44-2.54 (m, 4H, CH_2CH_2). ^{13}C NMR (100 MHz, CDCl3): δ = 11.2 ($Si(\underline{C}H(CH_3)_2)_3$), 15.9 ($C(O)CH_2\underline{C}H_2$), 18.6 ($Si(CH(\underline{C}H_3)_2)_3$), 28.1 ($C(\underline{C}H_3)_3$), 35.1 ($C(O)\underline{C}H_2$) 80.6, 80.8 ($\underline{C}CH_3$, $C\underline{C}Si$), 107.1 ($\underline{C}CSi$), 171.1 (C=O).

***tert*-butyl 5-(triethylsilyl)-pent-4-ynoate (3b)**

Compound **2** (1.4 g, 9.3 mmol) was dissolved in anhydrous THF (20 mL) and the solution was cooled to -78°C with a dry ice and acetone bath. *n*-BuLi (3.7 mL, 2,5 M in hexane, 9.3 mmol) was added dropwise and the reaction mixture was stirred for 10 minutes. Then the dry ice/acetone bath was replaced with an ice bath (0°C) and TES-Cl (1.9 mL, 11.2 mmol) was added dropwise. The reaction mixture was stirred for 3 hours at room temperature, after which it was quenched with 40 mL aqueous saturated NH_4Cl. THF was removed by evaporation *in vacuo* and the resulting aqueous slurry was diluted with H_2O (50 mL). The mixture was extracted with EtOAc (3 x 30 mL) and the combined organic layers were dried over Na_2SO_4. After filtration, the solvent was evaporated. The crude product was purified by silica gel column chromatography (eluent: 2% EtOAc in hexanes) to give *tert*-butyl 5-(triethylsilyl)pent-4-ynoate (**3b**) as a yellow oil (1.8 g, 6.7 mmol, 72%). R_f =0.54 (5% EtOAc in petroleum ether 40-60). ^{1}H NMR (400 MHz, $CDCl_3$): δ = 0.55 (*q*, *J* = 8Hz, 6H, $Si(C\underline{H}_2\text{-}CH_3)_3$), 0.96 (t, *J* = 8Hz, 9H, $Si(CH_2\text{-}C\underline{H}_3)_3$) 1.45 (*s*, 9H, $CC\underline{H}_3$), 2.43-2.53 (*m*, 4H, $CH_2\text{-}CH_2$). ^{13}C NMR (100 MHz, $CDCl_3$): δ = 4.4 ($Si(\underline{C}H_2\text{-}CH_3)_3$), 7.4 ($Si(CH_2\text{-}\underline{C}H_3)_3$), 15.9 ($C(O)CH_2\text{-}\underline{C}H_2$), 28.0 ($C\underline{C}H_3$), 35.0 ($C(O)\underline{C}H_2$) 80.6, 82.2 ($\underline{C}CH_3$, $C\underline{C}Si$), 106.5 ($\underline{C}CSi$), 171.1 (C=O).

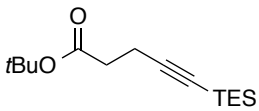

5-(triisopropylsilyl)-4-pentynoic acid (4a)

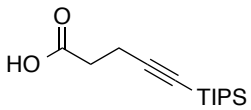

Compound **3a** (1.3 g, 4.3 mmol) was dissolved in 15% TFA in CH_2Cl_2 (50 mL) and the resulting solution was stirred for 2 hours. The mixture was then quenched with 1 M ammonium acetate (100 mL) and extracted with CH_2Cl_2 (2x, 75 mL). The combined organic layers were dried over Na_2SO_4, filtered and evaporated. The crude product was purified using silica gel column chromatography (10% Et_2O in hexanes). 5-(Triethylsilyl)-4-pentynoic acid (**4a**) was obtained as a yellow oil (1.1 g, 4.1 mmol, 97%). R_f = 0.33 (30% EtOAc in hexanes). ^{1}H NMR (400 MHz, $CDCl_3$): δ 1.05 (*m*, 21H, $Si(CH(CH_3)_2)_3$), 2.56-2.64 (*m*, 4H, CH_2-CH_2). ^{13}C NMR (100 MHz, $CDCl_3$): δ 11.2 ($Si(\underline{C}H_2\text{-}CH_3)_3$), 15.6 ($C(O)CH_2\text{-}\underline{C}H_2$), 18.5 ($Si(CH_2\text{-}\underline{C}H_3)_3$), 33.7 ($C(O)\underline{C}H_2$), 81.6 ($C\underline{C}Si$), 106.2 ($\underline{C}CSi$), 177.3 (C=O).

5-(triethylsilyl)-4-pentynoic acid (4b)

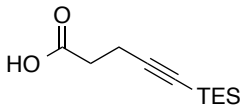

Compound **3b** (1.8 g, 6.7 mmol) was dissolved in 15% TFA in CH_2Cl_2 (50 mL) and the resulting solution was stirred for 2 hours. The mixture was then quenched with 1 M ammonium acetate (100 mL) and extracted with CH_2Cl_2 (2x, 75 mL). The combined organic layers were dried over Na_2SO_4, filtered and evaporated. The crude product was purified by silica gel column chromatography (10% Et_2O in hexanes). 5-(Triethylsilyl)4-pentynoic acid (**4b**) was obtained as a yellow oil (0.55 g, 2.6 mmol, 39%). R_f = 0.34 (10% EtOAc in hexanes). ^{1}H NMR (400 MHz, $CDCl_3$): δ = 0.56 (*q*, *J* = 8Hz, 6H, $Si(C\underline{H}_2\text{-}CH_3)_3$), 0.97 (t, *J* = 8Hz, 9H, $Si(CH_2\text{-}C\underline{H}_3)_3$), 2.53-2.63 (*m*, 4H, CH_2-CH_2). ^{13}C NMR (100 MHz, $CDCl_3$): δ = 4.4 ($Si(\underline{C}H_2\text{-}CH_3)_3$), 7.4 ($Si(CH_2\text{-}\underline{C}H_3)_3$), 15,6 ($C(O)CH_2\text{-}CH_2$), 33.5 ($C(O)CH_2$), 82.9 ($C\underline{C}Si$), 105.6 ($\underline{C}CSi$), 171.1 (C=O).

N-(3-bromopropyl)-2-nitrobenzene-sulfonamide (6)

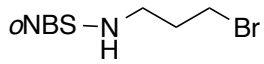

According to a literature procedure,[8] 3-bromo-propylamine hydrobromide (**5**, 15.0 g, 68.5 mmol) and 2-nitrobenzene-sulfonyl chloride (18.2 g, 82.2 mmol) were dissolved in CH_2Cl_2 (180 mL) and cooled to 0°C. After adding TEA (21.9 mL, 164.4 mmol) the mixture was stirred at room temperature for 3 hours. The mixture was washed with 1 M HCl (50 ml), H_2O (50 ml), and brine (50 mL). The organic layer was dried over Na_2SO_4, filtered and the solvent was removed under vacuum to yield the product as a white solid (21.57 g, 66.7 mmol, 97%). Spectroscopic data was in agreement with literature data.[8]

***o*NBS and TFA protected triamine with pentynoic acid residue 9**

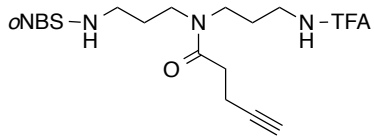

For the synthesis of crude compound **8**, our literature procedure was followed.[3]

To a cooled solution of 1,3 diaminopropane (25.8 mL 309 mmol) in DMA (200 mL) a solution of sulfonamide

bromide **6** (10.0 g, 30.9 mmol) in DMA (50 mL) was added dropwise. The resulting mixture was stirred overnight at room temperature. An aqueous solution of 4 M NaOH (aq, 7.7 mL, 30.9 mmol) was added and the mixture was concentrated *in vacuo* to approximately a third of the volume. DMA (100 mL) was added and again the mixture was concentrated until a third of the volume remained. This co-evaporation was repeated until the collected DMA was not basic anymore due to remaining diaminopropane as shown by pH indicator paper. After evaporation of the remaining DMA triamine **7** was obtained as a yellow oil.

To the crude intermediate (**7**) MeCN (150 mL), H_2O (0.7 mL, 38.8 mmol) and CF_3CO_2Et (18.5 mL, 155.2 mmol) were added. After overnight stirring under reflux, the mixture was concentrated *in vacuo* to afford the crude TFA-protected triamine (**8**) as a yellow oil.

Crude compound **8** was dissolved in CH_2Cl_2 (200 mL). BOP (14.3 g, 32.3 mmol), 4-pentynoic acid (3.0 g, 30,8 mmol) and NMM (10.4 mL, 95.5 mmol) were added and the mixture was stirred overnight. The solvent was evaporated and the residue was dissolved in EtOAc (100 mL) and washed with 5% $NaHCO_3$ (2x 100 mL), 1 M of $KHSO_4$ (2x 100 mL) and brine (100 mL). The organic layer was dried over Na_2SO_4 and filtered and the solvent was removed by evaporation. Silica gel column chromatography (eluent: EtOAc/hexane; 1/1 until removal of the first yellow band, then 6/4 until the product started to elute and 7/3 to complete the elution of the product) afforded triamine **9** as a yellow/orange oil (9.53 g, 19.4 mmol, 63%). R_f = 0.61 (20% hexanes in EtOAc). ^{1}H NMR (400 MHz, $CDCl_3$): δ 1.67-1.76, 1.83-1.92 (2*m*, 4H, N-CH_2-C$\underline{H}_2$), 1.96 (*s*, 1H, CCH), 2.54 (*m*, 4H, C(O)-CH_2-CH_2), 3.05-3.18, 3.22-3.34 (2*m*, 4H, 2x NH-C$\underline{H}_2$-CH_2), 3.38-3.45 (*m*, 4H, CH_2-N-CH_2), 5.51, 6.19, 6.74 (*3m*, 2H, NH), 7.69-7.90, 8.07-8.15 (2*m*, 4H, Ar-H). ^{13}C NMR (100 MHz, $CDCl_3$): δ = 14.7, 14.9, 31.7, 31.9 (N-C(O)$\underline{C}H_2\underline{C}H_2$), 26.8, 28.1, 28.5, 29.0 (2x, CH_2-$\underline{C}H_2$-CH_2), 35.8, 40.8, 41.0, 45.4 (2x, NH-$\underline{C}H_2$-CH_2), 37.4, 42.2, 42.8, 45.0 (2x, CH_2NCH_2), 68.9, 69.2, 82.9, 83.1(C-CH), 114.5, 117.4 (CF_3), 125.1, 125.5, 130.7, 131.0, 132.6, 132.9, 133.2, 133.4, 133.9 (Ar-C), 148.1 (CNO_2), 157.1, 157.5 (CF_3-$\underline{C}$=O), 171.6, 172.5 (($CH_2)_2N\underline{C}$=O). Exact mass calculated [M + H]$^+$: 493.1369. Mass measured: 493.1344.

Triamine cyclization (11)

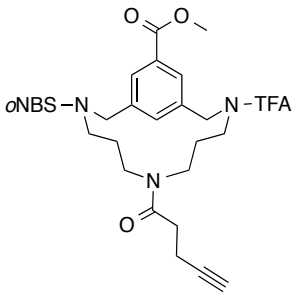

Dibromide **10** was obtained according to a literature procedure.[6]

Triamine **9** (3.0 g, 6.1 mmol), dibromide **10** (2.0 g, 6.1 mmol) and Cs_2CO_3 (8,0 g, 24.4 mmol) were dissolved in DMF (500 mL) and the resulting mixture was stirred overnight. After evaporation of DMF both EtOAc (300 mL) and H_2O (180 mL) were added. The organic layer was washed with an aqueous solution of 1 M $KHSO_4$ (200 mL) and with brine (200 mL), dried over Na_2SO_4 and filtered. Concentration *in vacuo* afforded the crude product as an orange oil, which was purified using silica gel column chromatography (eluent: 2% acetone in CH_2Cl_2). Compound **11** was obtained as a yellow to orange foam (2.7 g, 4.1 mmol,

67%). R_f = 0.38 (EtOAc/Hexanes, 7:3). ^{1}H NMR (400 MHz, $CDCl_3$): δ 1.23-1.45, 1.60-1.70 (2*m*, 4H, 2x N-CH_2-CH_2), 1.92 (*m*, 1H, CCH), 2.435-2.47 (*m*, 4H, C(O)-CH_2-CH_2), 3.93, 3.95 (2*s,* 3H, OCH_3), 4.38-4.53, 4.63-4.80 (2*m*, 4H, 2x Ar-CH_2-N), 7.65-8.11 (*m*, 7H, ArH). Exact mass calculated $[M + H]^+$: 653.1893. Mass measured: 653.1879.

Pentynoic acid amidated TAC-scaffold 12

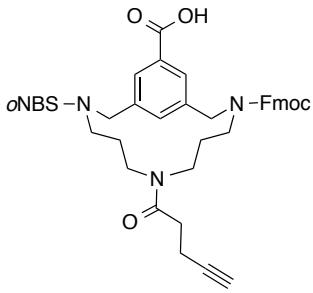

Compound **11** (1.7 g, 2.6 mmol) was dissolved in dioxane/MeOH/aq NaOH (4M) (15:4:1, 91 mL, 18.2 mmol) and the resulting mixture was stirred overnight. 1M HCl was added until the mixture was pH neutral (pH indicator paper), after which MeCN (50 mL) and H_2O (50 mL) were added. The pH was adjusted to approximately 8 using D*i*PEA (using a pH electrode) and a solution of Fmoc-OSu (0.95 g, 2.8 mmol) in MeCN was added. This was followed by the dropwise addition of D*i*PEA to maintain the pH at 8. The reaction was considered complete when no more D*i*PEA was needed to keep the pH above 7.5 for 10 min. Addition of aqueous solution of HCl (1M, 30 mL) and H_2O (200 mL) was followed by extraction with EtOAc (2x, 200 mL). The combined organic layers were washed with brine and dried over Na_2SO_4. Evaporation of the solvents gave the crude compound which was purified using silica gel column chromatography (gradient from EtOAc/Hexanes/AcOH 8/2/0.1 to 0.1% AcOH in EtOAc to give the Fmoc-protected TAC-scaffold (**12**) (1.6 g, 2.1 mmol, 80%) R_f = 0.37 (6% MeOH/ CH_2Cl_2). Exact mass calculated $[M + H]^+$: 765.2594. Mass measured: 765.2618.

Orthogonally protected trialkyne TAC-scaffold 13

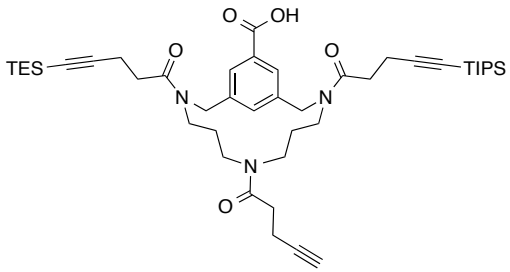

TAC-scaffold **12** (0.3 g, 0.4 mmol) was dissolved in CH_2Cl_2 (20 mL), and D*i*PEA (70 µL, 0.4 mmol) and 2-chlorotrityl chloride resin (1.0 g, 3.2 mmol) were added. After 5 minutes D*i*PEA (105 µL, 0.6 mmol) was added and the mixture was stirred overnight. D*i*PEA (1 mL) and MeOH (4 mL) were added and the mixture was stirred for 30 minutes. The resin was transferred to a solid phase synthesis tube and washed with MeOH (3 x 20 mL) and Et_2O (3 x 20 mL). After drying for 30 minutes, 5 mg of resin was transferred to a 20 mL volumetric flask and 20% piperidine in NMP (2 mL) was added. The flask was shaken for 30 minutes after which MeOH was added until a volume of 20 mL. UV-absorption was measured at 300 nm (ε = 7800 M^{-1} cm^{-1}) resulting in a loading of 0.25 mmol/g resin (loading yield of 63%). The resin was washed with CH_2Cl_2 (3 x 20 mL), NMP (3 x 20 mL) and 20% piperidine/NMP (20 mL) was added. The mixture was bubbled through with N_2 for 30 minutes, followed by washing with NMP (3 x 20 mL) and CH_2Cl_2 (3 x 20 mL). A positive

Bromophenol Blue-test indicated Fmoc removal.

Next, BOP (0.22 g, 0.5 mmol), CH_2Cl_2 (20 mL), TIPS-protected pentynoic acid **4a** (0.13 g, 0.5 mmol), D*i*PEA (1.7 mL, 1.0 mmol) were added respectively. The mixture was bubbled through with N_2 for 2 hours. Then the resin was washed with CH_2Cl_2 (3 x 20 mL). A negative Bromophenol Blue-test indicated coupling of the pentynoic acid derivative.

The resin was washed with DMF (3 x 20 ml). DMF (20 mL), β-mercaptoethanol (175 µL, 2.5 mmol) and DBU (187 µL, 1.25 mmol, 5 equiv.) were added subsequently. The mixture was bubbled through with N_2 for 15 minutes. The deprotection step was repeated once. The resin was washed with DMF (3 x 20 mL) and CH_2Cl_2 (3 x 20 mL). A positive Bromophenol Blue-test indicated *o*NBS removal.

Next, BOP (0.22 g, 0.5 mmol), CH_2Cl_2 (20 ml), TES-protected pentynoic acid **4b** (0.11 g, 0.5 mmol) and D*i*PEA (166.8 µL, 1.0 mmol) were added and the mixture was bubbled through with N_2 for 2 hours. The resin was washed with CH_2Cl_2 (3 x 20 mL) and a negative Bromophenol Blue-test indicated coupling of the pentynoic acid derivative. The resin was transferred to a round-bottom flask and 30% HFIP in CH_2Cl_2 (20 mL) was added. The mixture was allowed to stir for 45 minutes. After filtration and washing of the residue with CH_2Cl_2, EtOAc (30 mL) was added to the filtrate. The solvents were removed through evaporation. Silica gel column chromatography (6% MeOH in CH_2Cl_2) afforded scaffold **13** as a colorless oil. The oil was dissolved in *t*-BuOH/H_2O and lyophilized to obtain a white solid (0.15 g, 0.19 mmol, 76%). R_f = 0.55 (10% MeOH in CH_2Cl_2). ^{1}H NMR (400 MHz, $CDCl_3$): δ = 0.57 (*q*, *J* = 7.9Hz, 6H, $Si(C\underline{H}_2CH_3)_3$), 0.97 (*t*, *J*= 7.9Hz, 9H, $Si(CH_2C\underline{H}_3)_3$), 1.04 (*m*, 21H, $Si(CH(CH_3)_2)_3$), 1.32-1.60 (*m*, 4H, N-CH_2-$C\underline{H}_2$-CH_2-N), 1.92 (*m*, 1H, CCH), 2.44 (*m*, 4H, $C\underline{H}_2C\underline{H}_2CCH$), 2.60-2.78 (*m*, 8H, 2x $C\underline{H}_2C\underline{H}_2CCSi$), 2.81-3.08, 3.40-3.50 (2*m*, 8H, N-$C\underline{H}_2$-CH_2-$C\underline{H}_2$-N), 4.59-4.72 (*m*, 4H, 2x N-CH_2-Ar). ^{13}C NMR (100 MHz, $CDCl_3$): δ = 4.4 ($Si(CH_2CH_3)_3$), 7.5 ($Si(CH_2\underline{C}H_3)_3$), 11.2 (SiCH), 14.5, 14.5 ($\underline{C}H_2CCH$), 16.3, 16.4 ($\underline{C}H_2CCSi$), 18.6 ($Si(CH(\underline{C}H_3)_2)_3$), 28.0, 28.0, 28.3 ($CH_2\underline{C}H_2CH_2$), 31.9, 31.9 ($\underline{C}H_2CH_2CCH$), 32.8, 33.1, 33.1 ($\underline{C}H_2CH_2CCSi$), 43.5, 45.5, 45.6, 45.7, 46.0, 48.2, 48.3 ($NCH_2CH_2\underline{C}H_2N$), 52.0, 52.1, 53.8, 53.8 ($Ar\underline{C}H_2N$), 68.8 ($C\underline{C}H$), 81.2, 81.3, 82.7, 82.7, 83.1, 83.2 ($\underline{C}CH$, $C\underline{C}Si$), 106.4, 106.4, 107.0, 107.0 ($\underline{C}CSi$), 128.8, 130.0, 130.0, 130.1, 130.3, 131.1, 131.2, 131.5, 131.6, 138.2, 140.5 (ArC), 168.9, 170.7, 172.0, 172.5 (C=O). Exact mass calculated $[M + H]^+$: 788.4854. Mass measured: 788.4831.

4.4.3 Peptide synthesis

Solid phase peptide synthesis

Linear peptides were synthesized on a C.S. Bio Co. peptide synthesizer using Tentagel S RAM resin (rink amide linker) on a 0.25-mmol scale. Removal of the Fmoc-group was performed using 20% piperidine in NMP. Amino acids were coupled using 4 equiv. of amino acid and HBTU as an activating agent with D*i*PEA as a base and NMP as solvent. Capping was performed using acetic anhydride (12 mL), HOBt (0.5 g) and D*i*PEA (5.5 ml) in NMP (250 mL). Note: In the synthesis of linear loop 1 (**14**), the glycine residue adjacent to the aspartic acid residue was coupled as Fmoc-(Dmb)-Gly-OH to prevent aspartimide formation.

General procedure for the cleavage and deprotection of the peptide from the solid support

The sidechain-protected linear peptide was cleaved from the resin and deprotected using a mixture of TFA:H_2O:EDT:TIS (90:5:2.5:2.5) (v/v/v/v), 10 mL per gram resin. The reaction mixture was stirred for 3 hours, after which the mixture was filtered and concentrated to a volume of 2 mL, followed by precipitation of the peptides from MTBE/hexane (1:1 v/v). After centrifugation (3500rpm, 5 min), the supernatant was decanted and the pellet was resuspended in MTBE/hexane (1:1 v/v) and centrifuged again. The pellet was dissolved in *t*-BuOH/H_2O (1:1 v/v) and lyophilized. The purity of the peptides was analyzed using analytical HPLC and the peptides were characterized by spectrometry.

Cyclic peptide synthesis

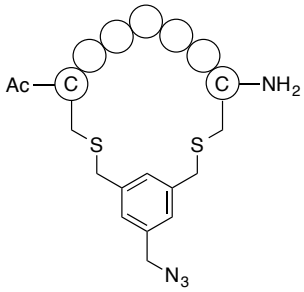

To a 1 mM solution of the crude linear peptide in a (1:3 v/v) mixture of MeCN/NH_4HCO_3 (aq, 20 mM, pH 7.8) a solution of 1-(azidomethyl)-3,5-bis(bromomethyl)benzene (see Chapter 2) (1.25 equiv.) in MeCN (2 mL) was added dropwise. The resulting mixture was stirred at room temperature for 3 hours before being concentrated and lyophilized. The crude cyclic peptide was purified using preparative HPLC. The product-containing fractions were pooled and lyophilized to yield the purified cyclic peptides as white fluffy powder.

Cyclic Ac-CLTRDGGKC-NH_2 (**14**): 69 mg (60 µmol), 34%, (21 steps, average 95% per step). Exact mass calculated $[M + H]^+$: 1150.5250; ESI-TOF MS found: 1150.5263. Rt = 19.90 min.

Cyclic H-CINMWQEVGKAC-NH_2 (**15**): 65 mg (42 µmol), 17%, (26 steps, average 93% per step). Exact mass calculated $[M + 2H]^{2+}$: 769.3472; ESI-TOF MS found: 769.3464. Rt = 22.05 min.

Cyclic Ac-CSGGDPEIVTC-NH_2 (**14**): 92 mg (72 µmol), 29%, (25 steps, average 95% per step). Exact mass calculated $[M + H]^+$: 1278.5247; ESI-TOF MS found: 1278.5269. Rt = 22.58 min.

4.4.4 Sequential ligation

First cycloaddition and subsequent TES-removal 17

Solutions of TAC-scaffold **13** (10.0 mg, 12.7 µmol) in 100 µL DMF, peptide loop **14** (11.5 mg,10 µmol) in 100 µL DMF, $CuSO_4.5H_2O$ (3.8 µmol, 0.95 mg) in 100 µL H_2O, NaAsc (11.4 µmol, 2.3 mg) in 100 µL H_2O and TBTA (1.9 µmol, 1.0 mg) in 100 µL DMF were prepared. The five solutions were combined and DMF (0.9 mL) and H_2O (0.6 mL) were added to obtain a final volume of 2 mL of DMF/H_2O 3/2 (v/v). The resulting mixture was stirred at room temperature for 3 hours and the progress of the reaction was monitored using LC-MS. When the reaction was complete, a solution of $AgNO_3$ (127 µmol, 21.6 mg) in H_2O (0.5 mL) was

added and the mixture was stirred at room temperature for 1 hour. The mixture was then diluted to a volume of 5 mL with MeCN/H_2O/TFA (50/50/0.1), followed by the addition of NaCl (127 µmol, 7.4 mg) in order to remove Ag^+ as an AgCl precipitate. The formed suspension was centrifuged (5 min, 5000 rpm) and the supernatant was purified using preparative HPLC. The product-containing fractions were pooled and lyophilized to obtain the TES-deprotected scaffold as a white solid.

Exact mass calculated $[M + 2H]^{2+}$: 912.4620; ESI-TOF MS found: 912.4684.

Rt = 30.42 min.

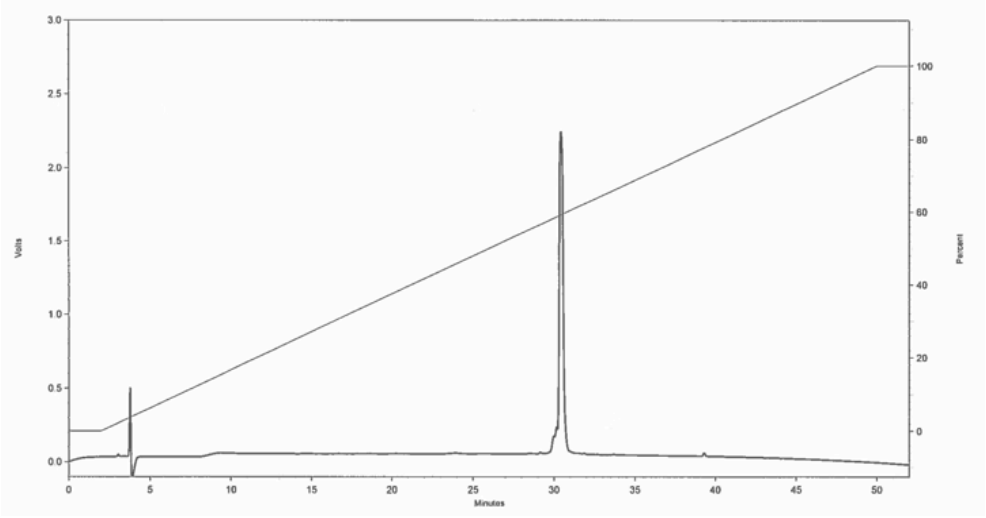

CuAAC of the second peptide onto the scaffold (18)

Solutions of scaffold **17** -containing one peptide sequence as well as one free and one protected alkyne- (3.3 µmol, 6.0 mg) in 200 µL DMF and of the peptide (**16**) (3.3 µmol, 4.2 mg) in 200 µL DMF were prepared. Stock solutions of $CuSO_4.5H_2O$ (9.9 µmol, 2.5 mg, 3 equiv. in 1 mL H_2O), NaAsc (30 µmol, 5.9 mg, 9 equiv. in 1 mL H_2O) and TBTA (5.0 µmol, 2.7 mg 1.5 equiv. in 1 mL DMF) were prepared. The solutions of the scaffold and the peptide were combined and 100 µL each of the $CuSO_4$, the NaAsc and TBTA solutions was added. To the resulting mixture DMF (0.4 mL) and H_2O (0.4 mL) were added to obtain a final volume of 1.5 mL of DMF/H_2O 3:2 (v/v). The resulting mixture was stirred at room temperature for 3h and the progress of the reaction was monitored using LC-MS. When the reaction was complete, the mixture was diluted to a volume of 5 mL with MeCN/H_2O/TFA (50/50/0.1). The resulting mixture was centrifuged (5 min, 5000 rpm) and the supernatant was purified using preparative HPLC. The product-containing fractions were pooled and lyophilized to obtain the TAC-scaffold with as a white solid (2.5 mg, 2.6 µmol, 80%).

Exact mass calculated $[M + 3H]^{3+}$: 1034.4829; ESI-TOF MS found: 1034.4842.

Rt = 27.95 min.

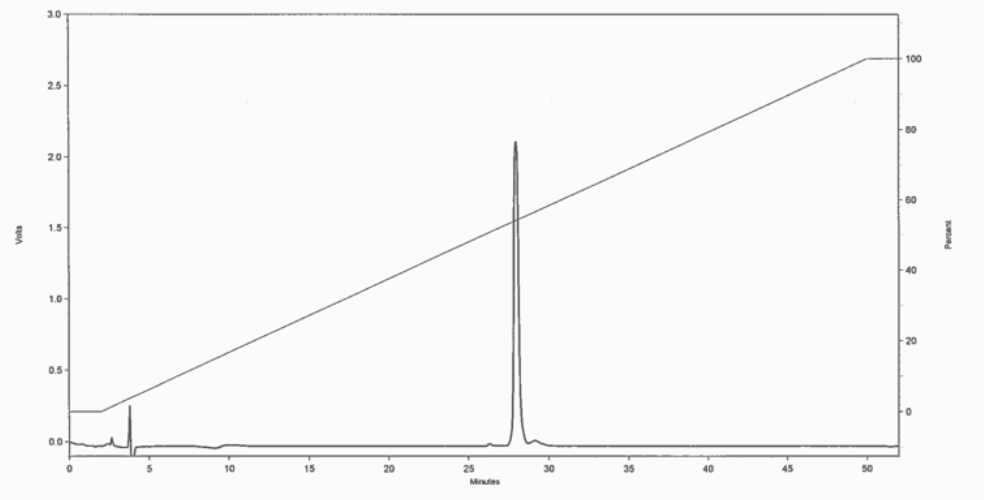

Removal of the TIPS-protecting group (19)

TIPS-protected scaffold **18** (2.8 µmol, 8.7 mg) was dissolved in DMF (1 mL) and a solution of TBAF.3H_2O (28 µmol, 8.8 mg, 10 equiv). The resulting mixture was stirred at room temperature and the progress was monitored using LC-MS. When the reaction was complete (usually after stirring overnight), the mixture was diluted to a volume of 5 mL with MeCN/H_2O/TFA (50/50/0.1). The resulting mixture was centrifuged (5 min, 5000 rpm) and the supernatant was purified using preparative HPLC. The product-containing fractions were pooled and lyophilized to obtain the product as a white solid (7.3 mg, 2.5 µmol, 87%).

Exact mass calculated $[M + 2H]^{2+}$: 1473.1537; ESI-TOF MS found: 1473.1494.

Rt = 21.03 min.

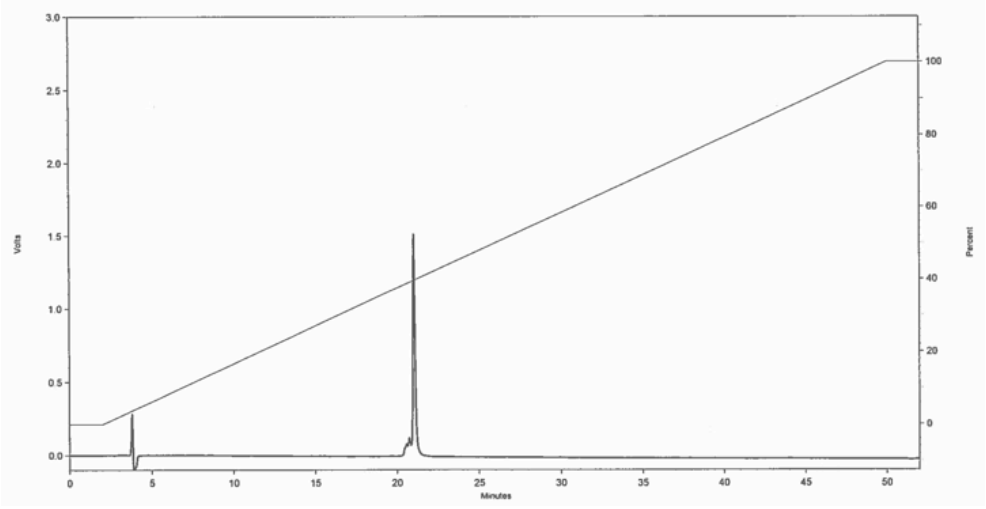

CuAAC of the third peptide onto the scaffold (20)

Solutions of the scaffold (**19**) -containing two peptides and one free alkyne- (2.5 µmol 7.4 mg) in 200 µL DMF and of peptide **15** (2.5 µmol, 3.8 mg) in 200 µL DMF were prepared. Stock solutions of $CuSO_4.5H_2O$ (7.5 µmol, 1.9 mg, 3 equiv. in 1 mL H_2O), NaAsc (22.5 µmol, 4.5 mg, 9 equiv. in 1 mL H_2O) and TBTA (3.75 µmol, 2.0 mg, 1.5 equiv. in 1 mL DMF) were prepared. The solutions of the scaffold and the peptide were combined and 100 µL each of the $CuSO_4$, the NaAsc and TBTA solutions was added. To the resulting mixture, DMF (0.4 mL) and H_2O (0.4 mL) were added to obtain a final volume of 1.5 mL of DMF/H_2O 3:2 (v/v). The resulting mixture was stirred at room temperature for 3h and the progress of the reaction was monitored using LC-MS. When the reaction was complete, the mixture was diluted to a volume of 5 mL with MeCN/H_2O/TFA (50/50/0.1). The resulting mixture was centrifuged (5 min, 5000 rpm) and the supernatant was purified using preparative HPLC. The product-containing fractions were pooled and lyophilized to obtain the product as a white solid (4.9 mg, 1.1 µmol, 44%).

Exact mass calculated $[M + 3H]^{3+}$: 1034.4829; ESI-TOF MS found: 1034.4842.

Rt = 20.72 min.

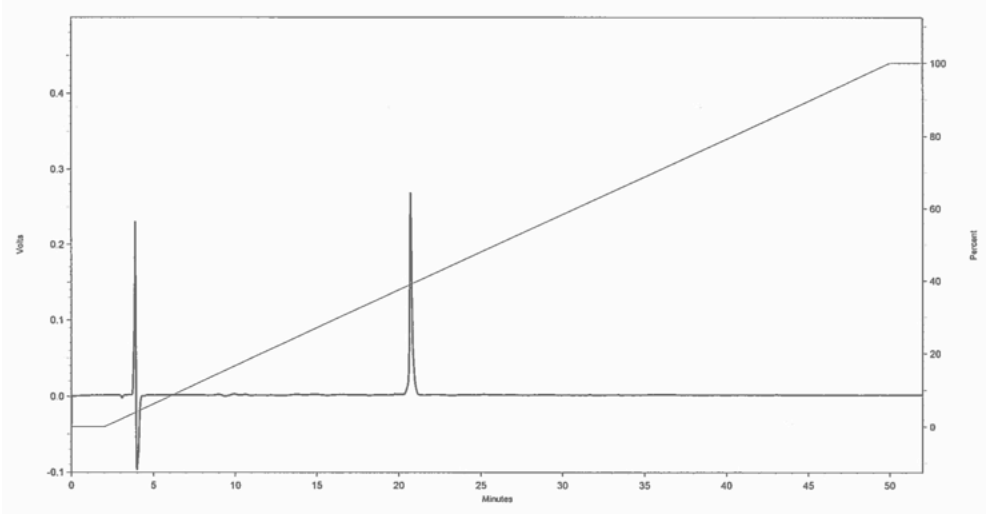

References

1 G. E. Mulder, J. A. W. Kruijtzer and R. M. J. Liskamp, *Chem. Commun.*, 2012, **48**, 10007–10009.

2 T. Opatz and R. M. J. Liskamp, *Org. Lett.*, 2001, **3**, 3499–3502.

3 A. J. Brouwer, H. Van De Langemheen and R. M. J. Liskamp, *Tetrahedron*, 2014, **70**, 4002.

4 P. D. Kwong, R. Wyatt, S. Majeed, J. Robinson, R. W. Sweet, J. Sodroski and W. A. Hendrickson, *Structure*, 2000, **8**, 1329–39.

5 P. D. Kwong, R. Wyatt, J. Robinson, R. W. Sweet, J. Sodroski and W. A. Hendrickson, *Nature*, 1998, **393**, 648–59.

6 K. Kurz and M. W. Göbel, *Helv. Chim. Acta*, 1996, **79**, 1967–1979.

7 G. M. Fischer, C. Jüngst, M. Isomäki-Krondahl, D. Gauss, H. M. Möller, E. Daltrozzo and A. Zumbusch, *Chem. Commun.*, 2010, **46**, 5289–5291.

8 S. N. Georgiades and J. Clardy, *Org. Lett.*, 2005, **7**, 4091–4094.

5

Chapter 5

Molecular construction of CD4-binding site mimics and evaluation of their activity and stability

Parts of this chapter have been published in:

P.R. Werkhoven, M. Elwakiel, T.J. Meuleman, H.C. Quarles van Ufford, J.A.W. Kruijtzer, R.M.J. Liskamp Org. Biomol. Chem. 2016, 14, 701-710

5.1 Introduction

Despite major research efforts dedicated to finding a vaccine for HIV, an effective vaccination to prevent against infection remains elusive.[1–4] The glycoprotein gp120 of HIV-1 has been of particular interest as a therapeutic target.[4] Gp120 is one of HIV's envelope proteins and its main function is binding to the human T-cell receptor CD4, which is the first step of HIV's entry into the cell.[5] Its involvement in this first step of the infection makes gp120 an interesting therapeutic target. Many small molecule and peptide inhibitors that target this protein and its interactions thereby inhibiting the entry of the virus have been reported.[5–8] Because of its accessibility as an envelope protein, g120 is also an interesting candidate for the vaccine development.

Structural studies of the ternary complex of gp120, CD4, and an anti-gp120 antibody have indicated that gp120 binds to CD4 through a conserved binding site. The site is discontinuous and consists of three loops: loop 1 ^{454}LTRDGGK^{460}, loop 2 ^{424}INMWQEVGKA^{433}, and loop 3 ^{365}SGDDPEIVT^{373} (Figure 1).[9] Residues that contribute the most to the binding were identified to be Trp^{427}, Asp^{368}, and Glu^{370}, which are all highly conserved over primate immunodeficiency viruses.[10] The conservation of the CD4-binding site of gp120, together with its relative accessibility, makes it an attractive target for an immune response, and many broadly neutralizing antibodies target this site.[10] However, the conserved binding site is shielded by the more readily accessible and highly variable V1/V2 loop.[10] These characteristics cause the V1/V2 loop to attract the attention of the immune system over the conserved site, making it an immuno-dominant epitope. The accessibility and variability of the V1/V2 loop shield the CD4-binding site from the immune system and prevent an immunogenic response to the conserved site. The antibody included in the ternary complex (Figure 1) binds to this variable V1/V2 loop. It is important to mention that gp120 epitopes, including the CD4-binding site, are also shielded from the immune system by its glycans.[11]

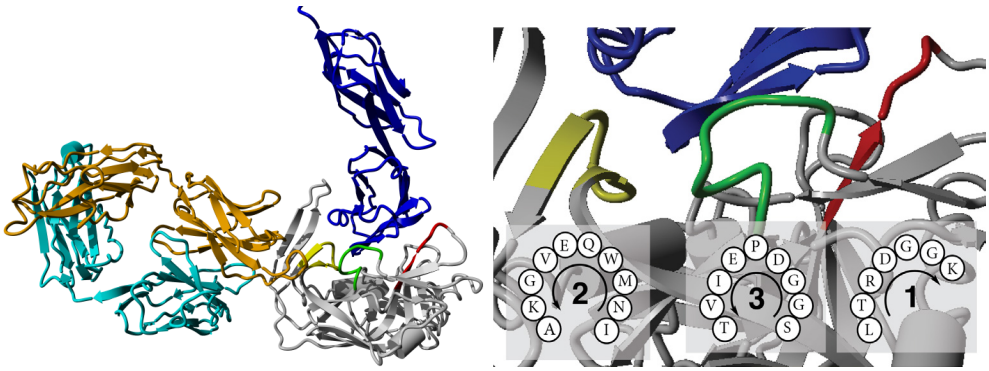

Figure 1. Left: X-ray structure of gp120-CD4-antibody complex. CD4 (blue) binds to gp120 (gray) through interactions with three conserved loops (yellow, green and red). The antibody (cyan & orange) binds to the variable, immuno-dominant V1/V2 loop, which due to its relative accessibility is the dominant site for binding of antibodies.[12] Right: Zoom of the conserved CD4-binding site on gp120. The binding loops are highlighted in color and their amino-acid sequence including the N to C direction is noted. For clarity we have numbered the loops 1, 2, and 3.

Synthetic epitope mimics can circumvent viral immune evasion strategies, like immunodominant epitopes and glycan shielding. A synthetic mimic omits the bulk of the protein and should only display the desired epitope without inference of the remainder of the protein. Mimicry of a conserved binding site will greatly increase the effectiveness of the mimic, especially for vaccination purposes. Therefore, a synthetic mimic of the conserved CD4-binding site of gp120 might lead to an effective synthetic vaccine that remains effective despite new mutations that arise during HIV replication. For this reason, several epitope mimics, mimicking this binding site, have been investigated in the literature.[13–17] However, synthesis of discontinuous epitope mimics remains challenging and it is difficult to predict exactly what is needed to design and construct the best possible mimic.

In the previous chapters, a new and efficient procedure for the synthesis of mimics of discontinuous epitopes through the sequential introduction of three different cyclic peptides onto a molecular scaffold was described. This method enabled the construction of epitope mimics based on the CD4 binding site of HIV protein gp120, as well as mimics based on the Pertactin epitope from *Bordetella Pertussis*. In this chapter, the first steps are described towards investigation of the characteristics of an epitope mimic that are essential for an optimal mimic. Using the control over the position of the peptides on the scaffold, which is inherent to our new synthesis procedure, the influence of the peptide's positioning on the mimic's ability to bind to CD4 was investigated. Furthermore, the influence of the cyclization of the peptides was investigated to corroborate the expectation that cyclic peptides might be better epitope mimics than linear peptides.

5.2 Results and discussion

5.2.1 Relative positioning of cyclic peptides on the TAC-scaffold

The procedure for the synthesis of discontinuous epitope mimics described in the previous chapter allowed for absolute control of the position of the peptides on the scaffold because the peptides were introduced on the scaffold sequentially. This control therefore allowed investigation of the effect of the relative positioning of the peptides on the mimic's binding affinity to the natural target of the epitope, i.e. CD4.

Mimics of the CD4-binding site of the HIV protein gp120 were constructed using three cyclic peptides: loop 1, loop 2, and loop 3 with linear sequences Ac-CLTRDGGKC-NH_2, H-CINMWQEVGKAC-NH_2, and Ac-CSGGDPEIVTC-NH_2 respectively. These sequences correspond to the natural CD4-binding site of gp120 (Figure 1)[9] and have been previously used for the construction of epitope mimics.[13–17] The cyclic peptides were synthesized as described in chapter 2 by side chain-to-side chain cyclization of the cysteine residues using a new alkylating agent, which simultaneously introduced the azide moiety needed for introduction onto the scaffold by CuAAC (Figure 2).

The epitope mimics were synthesized using the earlier developed tri-alkyne functionalized scaffold and the sequential introduction procedure that is described in chapter 4 (Scheme

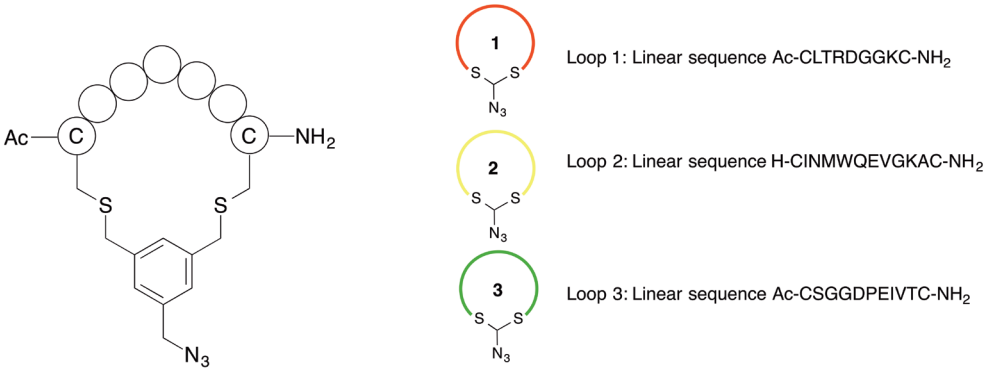

Figure 2 Left: General structure of the azide-functionalized cyclic peptides. Right: Linear sequences of the three peptides (**1**, **2**, and **3**) that correspond to the CD4-binding site of HIV gp120.

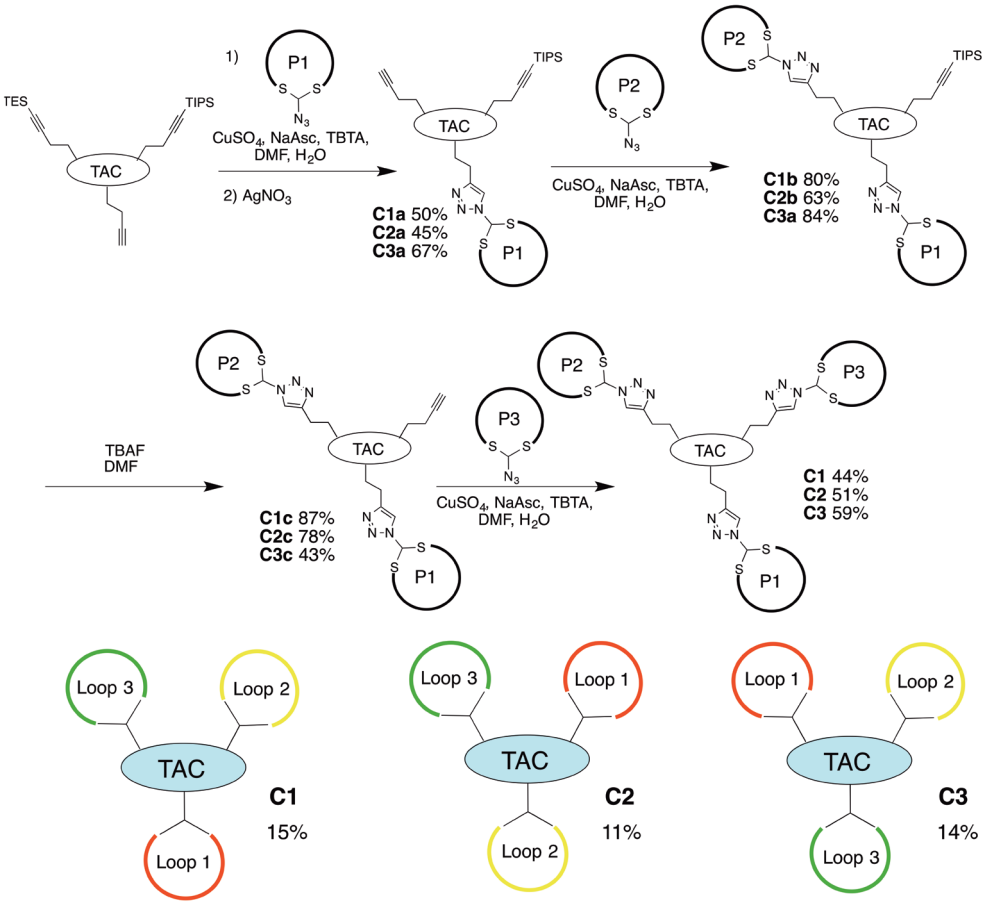

Scheme 1. Top: General procedure for the sequential introduction of azide-functionalized cyclic peptides on peptides. Bottom: The three constructs that were synthesized (**C1**, **C2**, and **C3**) differing only in the relative positioning of the cyclic peptides, including the overall yield of the syntheses starting from the scaffold.

1). To investigate the influence of the relative positioning of the peptides, three constructs mimicking the CD4-binding site of gp120 were synthesized (**C1**, **C2**, and **C3**; Scheme 1). The only difference between them is the sequence in which they were ligated onto the scaffold during the synthesis. This results in different positioning of the peptides in space and relative to one another. The overall yields of the constructs are comparable with the yield described in chapter 4 (between 11% and 15%), underlining once more that the procedure is highly reproducible.

In order to evaluate the mimics and to investigate the difference between the relative positioning of the peptides, the ability of the mimics to interfere with the binding of gp120 and CD4 in a gp120-capture ELISA experiment was investigated.[13,16–19] The ability of a construct to interfere with this binding may provide information about how well the construct is mimicking the binding site. Using this easily available assay the best gp120 mimic may be uncovered, which then could be used in subsequent immunization studies.

In the gp120-capture ELISA experiment (Figure 3) 96-wells plates, coated with the extracellular domain of CD4, were incubated with different concentrations of the mimic in the presence of recombinant monomeric gp120. After washing away the unbound gp120, the amount of bound gp120 was labeled using horseradish peroxidase(HRP)-conjugated murine anti-gp120. The antibodies were visualized using 3,3',5,5'-tetramethylbenzidine (TMB) as a substrate for HRP, which yields a blue color that can be quantified by measuring the absorbance at 450 nm. The potency of the constructs was measured relative to binding of gp120 in the absence of any mimic to give a percentage of inhibition.

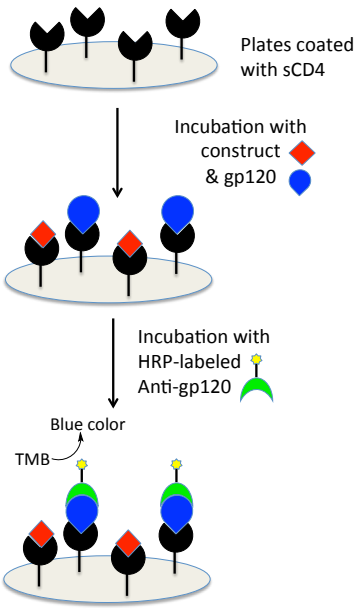

Figure 3. Schematic representation of the gp120-capture ELISA experiment.

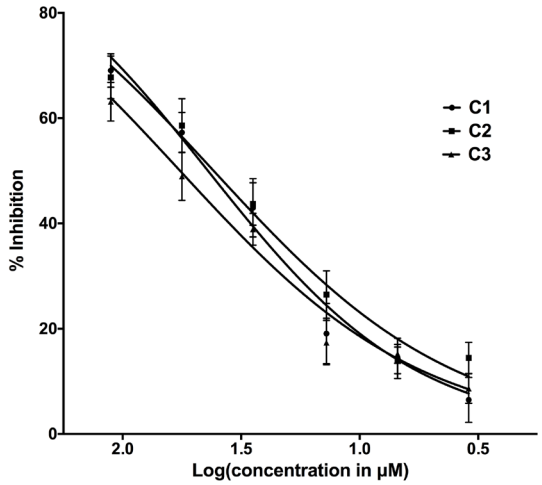

	IC_{50} (µM)	$\log(IC_{50})$
C1	43.7	1.64 ± 0.081
C2	41.3	1.62 ± 0.086
C3	57.3	1.76 ± 0.084

Figure 4. Results of the competitive gp120-capture ELISA from three constructs (**C1**, **C2**, and **C3**) differing only in the relative position of the peptides.

The results of the ELISA experiments are shown in Figure 4. All three mimics were able to inhibit the binding of gp120 to CD4 with IC_{50} values between 41 and 57 µM. Interestingly, there is little difference between the three mimics. This suggests that the relative positioning of the peptides in these three gp120 protein mimics relative to the CD4-receptor is similar. Possibly, the flexibility of the TAC-scaffold is at least partly responsible for a similar orientation of the three loops. However, it must be noted that the lack of difference between the relative positioning constructs is not necessarily generally true for other constructs or peptide combinations. Mulder et al. have shown that, when using the more rigid CTV scaffold, also active epitope mimics were obtained.[19] It is possible that epitope mimics based on the CTV scaffold will show a difference in activity based on the relative positioning of the peptides. However, to investigate this, the CTV scaffold would have to be modified with three alkynes bearing the orthogonal silyl protecting group strategy. Synthesis of this modified scaffold is currently under development. The individual peptides, a mixture of the three non-ligated peptides, as well as the unreacted scaffold were also tested and did not show any inhibition.

5.2.2 The importance of peptide cyclization

Cyclic peptides are generally assumed to be better mimics of the loop-like structures found in epitopes than their linear counterparts. In order to investigate the importance of peptide cyclization, an epitope mimic was synthesized that resembled cyclic peptide-based construct **C1** as closely as possible but now contained linear variants of the peptides.

For the best comparison, the linear peptides were synthesized with an azide-bearing alkylating agent (**5**) which resembled the cyclization linker described in chapter 2, and was accessible from the benzylic dibromide **4** (Scheme 2). This mono-bromide was used to alkylate a single cysteine residue. Mono-bromide alkylating agent **5** was obtained as a crude mixture with diazide **6**. Despite numerous attempts, purification of the desired product (**5**)

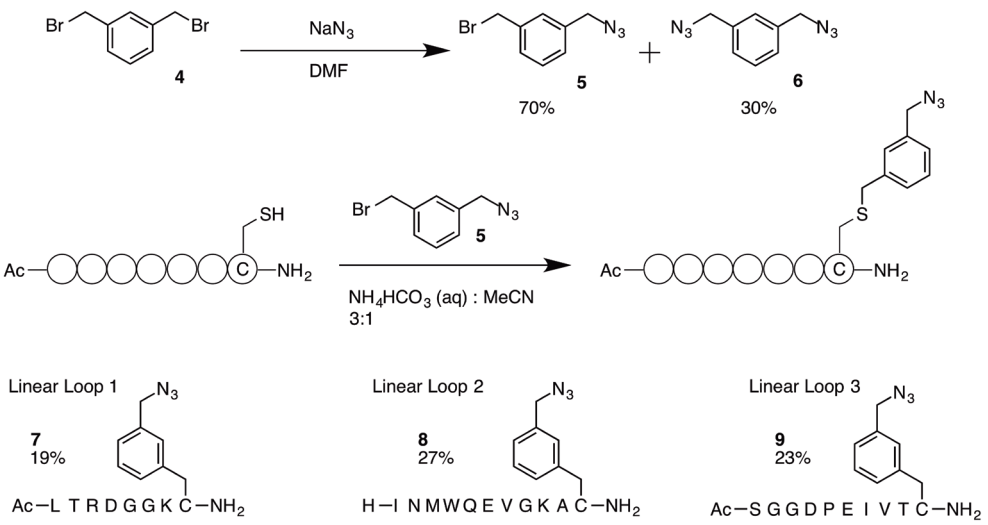

Scheme 2. Top: Synthesis of alkylating agent **5**. Middle: Alkylation of single cysteine bearing peptides by alkylating agent **5**. Bottom: the three synthesized linear peptides (**7**, **8**, and **9**) that represent the CD4-binding site of gp120.

was unsuccessful. However, the diazide was not expected to interfere with the alkylation reaction, so a known mixture of mono-azide **5** and diazide **6** was used for alkylation of the peptides. ^{1}H-NMR analysis showed that the ratio between mono-azide **5** and diazide **6** was 7:3. The alkylation of peptides was performed under the same conditions as the cyclization reaction discussed in chapter 2 (Scheme 2).

Azide-functionalized linear peptides **7**, **8**, and **9** were then used for sequential introduction onto the TAC-scaffold as we have described above and in chapter 4 (Scheme 3). The final linear peptide-based epitope mimic containing three linear peptides on the scaffold (**C4**) was obtained in a good overall yield (23%).

The construct based on linear peptides was also tested for its ability to inhibit the binding of gp120 to CD4 (Figure 5 left). The construct was able to interfere with the binding (91 μM, Log IC_{50}: 1.96 ± 0.139), however to a lesser extent than its cyclic counterpart (44 μM). This suggests that the use of cyclic peptides in protein mimics offers a small benefit over the use of linear peptides. This might be explained by an improved resemblance of cyclic peptides to the corresponding peptide segments in the binding site, which are present in loop-like segments in the context of a protein. If more generally true, this will improve mimicry possibilities of a protein binding site and therefore the development of reliable protein mimics. However, if the benefit of cyclic peptides on the activity is small, the accessibility of the cyclic peptides also has to be taken into account.

It is generally accepted that cyclic peptides have an improved proteolytic stability over linear peptides.[20] To investigate whether this is true for the scaffolded peptides in epitope mimics, we tested the proteolytic stability of both linear and cyclic peptide-based constructs. Constructs **C1** and **C4** were incubated with human serum and analyzed using HPLC. Cyclic peptide-based construct **C1** proved to be very stable and had hardly degraded after 24 hours,

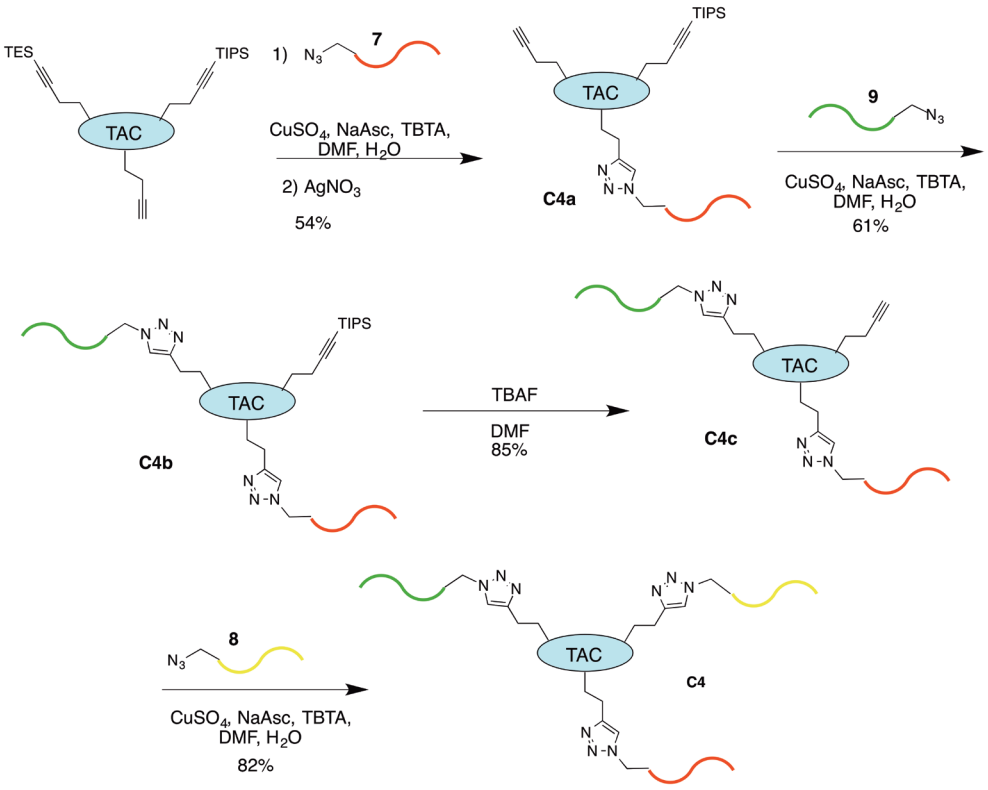

Scheme 3. Sequential introduction of linear peptides **4**, **5**, and **6** on the TAC-scaffold.

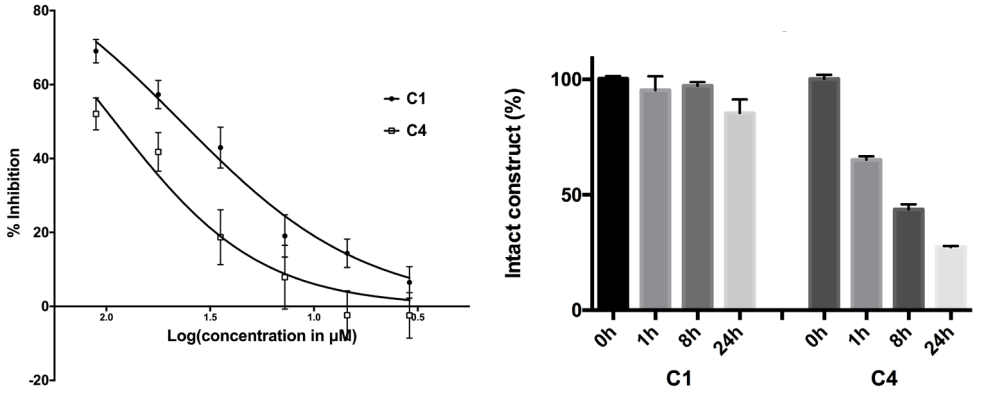

Figure 5. Comparison between the construct based on cyclic peptides (C1) and the construct based on linear peptides (C4). Left: Results from the competitive gp120-CD4 ELISA. Right: Result from the serum stability assay.

while linear peptide-based construct **C4** started to degrade already after 1 hour of incubation and after 24 hours only 25% remained intact (Figure 5 right). This result further underlines the importance of the use of cyclic peptides over linear peptides in order to obtain optimal epitope mimics.

In conclusion, the bio-activity results for the linear versus cyclic peptide based epitope mimics showed the benefits of using cyclic peptides over linear peptides for epitope mimicry. Firstly, epitope mimics based on cyclic peptides have a better biological activity than mimics based on linear peptides. Secondly, mimics based on cyclic peptides have better proteolytic stability in serum. Especially the latter makes them more attractive as protein mimics than mimics based on linear peptides.

5.2.3 Preparation of smart libraries by mixture ligation

Recently, Mulder et al. described a method for the ligation of a mixture of peptides onto the TAC-scaffold to create a smart library of epitope mimics.[13] In this work the TAC-scaffold, equipped with three alkyne moieties, was reacted with an equimolar mixture of the three azide-functionalized peptides representing the CD4-binding site of gp120. This combinatorial approach provided easy access to a fairly large amount of epitope mimics bearing a variety of peptide combinations (e.g. 2-2-3 and 1-1-1). This allowed for the assessment of the importance of each peptide combination. However, no discrimination could be made with regard to the relative positioning of the peptides, although considering the results shown above this probably does not have a large influence on the bio-activity of the TAC-scaffolded peptides.

The synthesis of the smart library can be combined with the method for sequential introduction in order to find an optimal protein mimic. The random library can identify 'hit' peptide combinations, which can then be re-synthesized using sequential introduction of the different cyclic peptides to investigate the optimal relative positioning. Furthermore, the sequential introduction method offers a more robust and efficient way to obtain large quantities of a single desired mimic.

Two smart libraries were synthesized (Scheme 4), one using linear peptides **7**, **9**, and **11** and the other using cyclic peptides **1**, **2**, and **3**. The only difference between linear peptide **8**, which was used in the sequential introduction, and linear peptide **11** that was used here, was that peptide **11** was acetylated on the N-terminus and peptide **8** was not. A mixture of scaffold **10**, peptides, copper sulfate, sodium ascorbate, and TBTA was reacted using the microwave to prepare smart libraries **12**, based on cyclic peptides, and **13**, based on linear peptides.

The reaction mixture was analyzed using LC-MS and individual protein mimics bearing a single peptide combination could be identified based on their mass. The HPLC traces of the reaction mixture for the linear and the cyclic libraries are shown in Figure 6. The synthesis for both the linear and the cyclic peptide based smart libraries was reproducible and yielded many of the same combinations in comparable yield per combination (based on LC-MS analysis).

The reaction mixtures were then purified using preparative HPLC. Separation of the linear peptide based protein mimics was easy and supplied a variety of pure mimics with specific

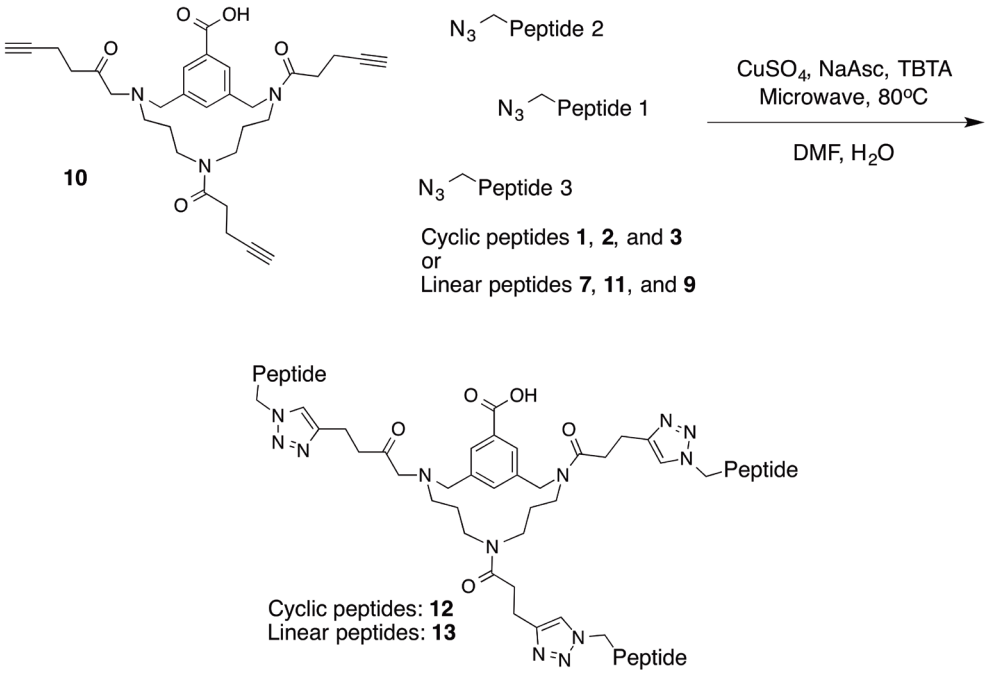

Scheme 4. Synthesis of a smart library of epitope mimics, based on cyclic peptides (**12**) or linear peptides (**13**) through ligation of a mixture of peptides.

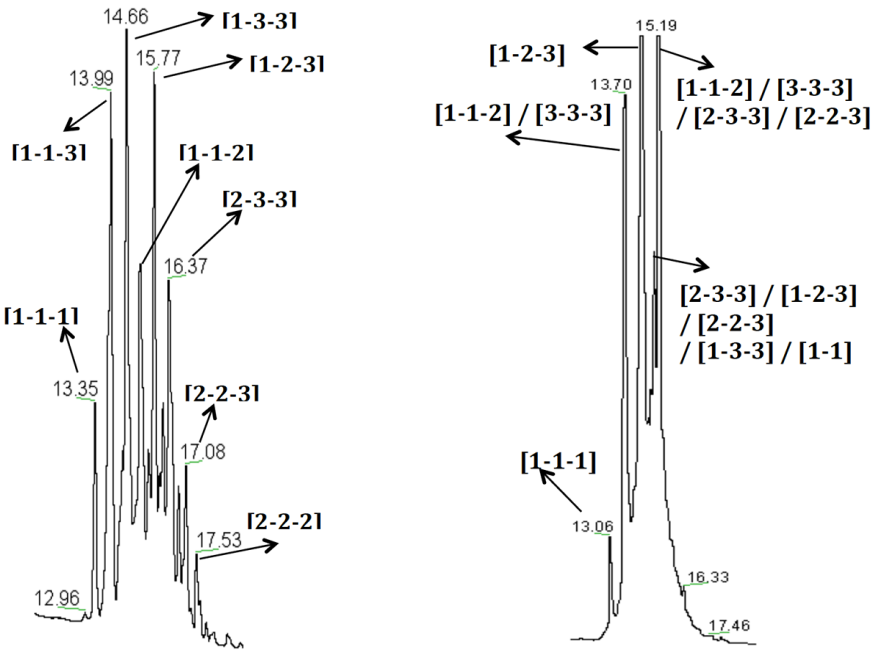

Figure 6. Chromatogram of the reaction mixtures of the generation of smart libraries of epitope mimics based on linear (left) and cyclic (right) peptides.

peptide combinations. In contrast, the individual protein mimics obtained from the cyclic peptides were not easily separated on preparative HPLC. The retention times on HPLC of the cyclic peptides were also very similar (especially loop 2 and 3), as compared to those of the linear peptides (Figure 7). This probably caused the synthesized mimics in the smart library to also have similar retention times (Figure 6), which made separation of individual protein mimics difficult. Unfortunately, efforts to optimize the purification through using different columns and/or eluent systems have proved unsuccessful.

After purification using preparative HPLC, the individual fractions were analyzed by LC-MS to identify the specific epitope mimics. The obtained fractions from the linear peptide smart library were all pure, in contrast to the fractions obtained from the cyclic peptide smart library. The fractions from the cyclic peptide library that were to be tested were chosen and identified with respect to the most dominant peptide combination present according to the mass spectra.

The mimics were tested in the same ELISA assay as described earlier at a single concentration (500 μg/mL or 250 μg/mL if not enough material was available). The results are shown in Figure 8. Most of the mimics measured show good inhibition of the interaction between CD4 and gp120. Interestingly, the combination of loops 1, 2, and 3 shows good inhibition from the linear library, but the same peptide combination from the cyclic library shows poor inhibition. This is in strong contrast to the results obtained with the mimics synthesized through the

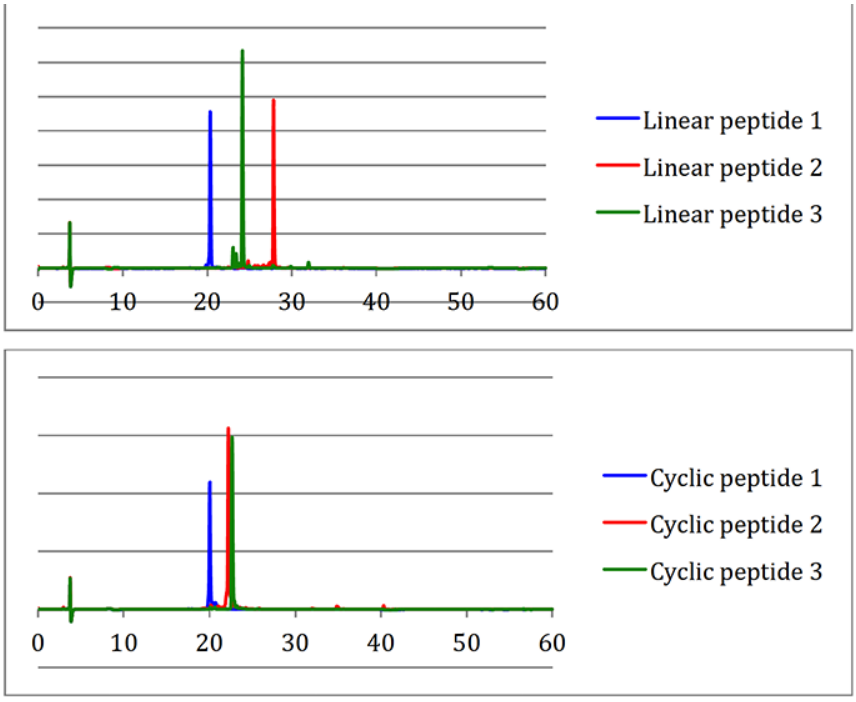

Figure 7. Merged chromatograms of purified linear (top) and cyclic (bottom) peptides representing the gp120 epitope.

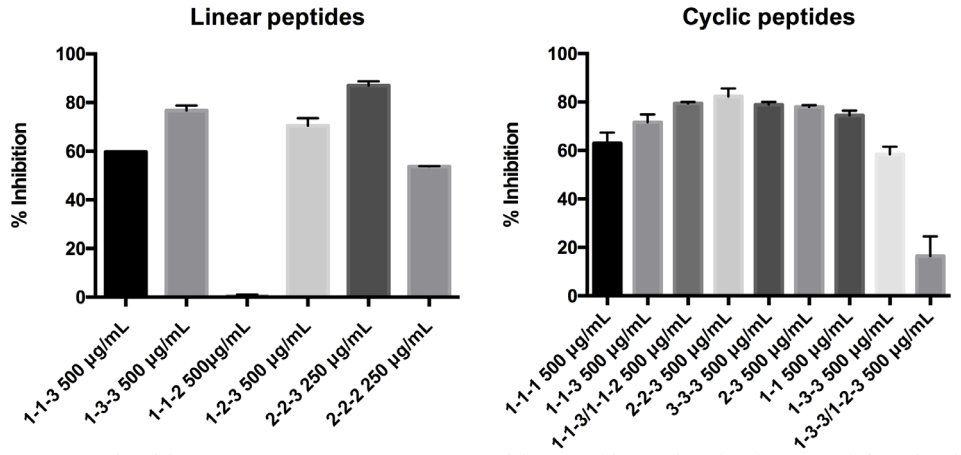

Figure 8. Results of the gp120-capture ELISA experiments of the smart libraries based on linear (**13**, left) and cyclic (**12**, right) peptides.

sequential introduction, where each combination of loops 1, 2, and 3 showed good inhibition. However, due to the difficult separation of the cyclic mixture, the fraction containing the 1-2-3 combination was not pure and the contaminants probably caused this drop in inhibition.

Three peptide combinations were present in both the cyclic and the linear libraries, 1-1-3, 1-3-3, and 2-2-3. For the 1-1-3 and the 2-2-3 combinations, the inhibition was similar when comparing the linear and cyclic libraries. For the 1-3-3 combination, the construct from the linear library showed a better inhibition than the one from the cyclic library (77% versus 58%). Based on these results, no preference for either of the cyclic or linear peptide library can be given for which library provides better mimics.

In conclusion, the generation of smart libraries of epitope mimics through mixture ligation enables quick access to collections of active mimics bearing either linear or cyclic peptides. The individual protein mimics bearing linear peptides could be easily separated and purified. However, protein mimics based on linear peptides have some disadvantages, as has been shown by the serum stability assay above. In contrast, the purification of individual mimics based on cyclic peptides was far more difficult. Therefore, the combinatorial approach is rather limited in obtaining and screening individual mimics using these cyclic peptides. After combining these results with the results of Mulder et al., it is concluded that the success of the combinatorial approach is largely dependent on the characteristics of the peptides, such as amino acid sequence and cyclization method.

5.2.4 Evaluating discontinuous epitope mimics using Isothermal Titration Calorimetry

So far, mimics of the CD4-binding site of gp120 have been evaluated based on their inhibitory activity in an ELISA assay. Although this method provided considerable insights into the characteristics needed to obtain the best possible mimic, it is not optimal. The ELISA experiments often afforded variable results and sometimes gave values far below 0% or above 100%. This makes the ELISA assay unreliable and therefore Isothermal Titration Calorimetry

(ITC) was explored as an alternative technique for the evaluation of the binding of the protein mimics.

ITC measures the liberated or consumed energy of a chemical reaction or binding triggered after mixing of two binding partners. ITC operates on the heat compensation principle, measuring the amount of power needed to keep the temperature difference between the reaction and reference cell constant. The reaction cell contains one of the binding partners and the second binding partner is titrated into the cell, which may generate heat. This causes a drop in the power needed to keep the temperature difference constant, which is measured and can be translated to binding characteristics like enthalpy (ΔH), entropy (ΔS) and the dissociation constant K_d.[21] ITC has been successfully used for the investigation of the interaction between gp120 and CD4, as well as for interactions between antibodies/inhibitors and gp120.[22–25]

Both recombinant gp120 and soluble CD4 (sCD4), the latter of which consists of the two N-terminal domains of CD4, were commercially available, albeit very expensive. For the preparation of the proteins for ITC-experiments, they were thoroughly dialyzed against the same PBS-buffer. This minimized the heat of dilution when the two solutions were mixed. Furthermore, the final dialysis buffer was saved so that it could be used for control experiments and dissolving the protein mimic. The construct (**C1**) was dissolved in the dialysis buffer. All solutions were degassed before use.

Two ITC-experiments were performed. The first was the titration of recombinant gp120 (18 μM) into a solution of sCD4 (1.93 μM), including a control experiment where recombinant gp120 (18 μM) was titrated into dialysis buffer. The data of the control experiment was subtracted from the data of the gp120-CD4 experiment to correct for any heat of dilution. The second experiment was the titration of a solution of epitope mimic **C1** (40 μM) into a solution of sCD4 (3.86 μM), including a control where epitope mimic **C1** (40 μM) was titrated into dialysis buffer. Results of the two experiments are shown in Figure 9.

The top half of the result figure shows the thermograms of the titration experiment, which are raw data and uncorrected. The bottom parts show the binding curve after integration and subtraction of the control titration. Both experiments showed a binding curve indicating that the binding of **C1**/gp120 to CD4 can be measured using ITC. However, the signal is in both cases very low and there is no plateau reached, so no reliable K_d could be determined. To remedy this, the concentration of both the sample cell and the titrant should be increased. Unfortunately, due to the high costs of the proteins, we were unable to repeat these experiments at higher concentrations and using commercial proteins for future experiments is not financially viable. Therefore, protein expression efforts for the production of sCD4 and gp120 should be pursued. Nevertheless, these pilot experiments indicated that ITC might prove very informative on the quality of the gp120 protein mimics capable of binding to CD4. Progress of future research in this area may greatly benefit from an improved and optimized ITC.

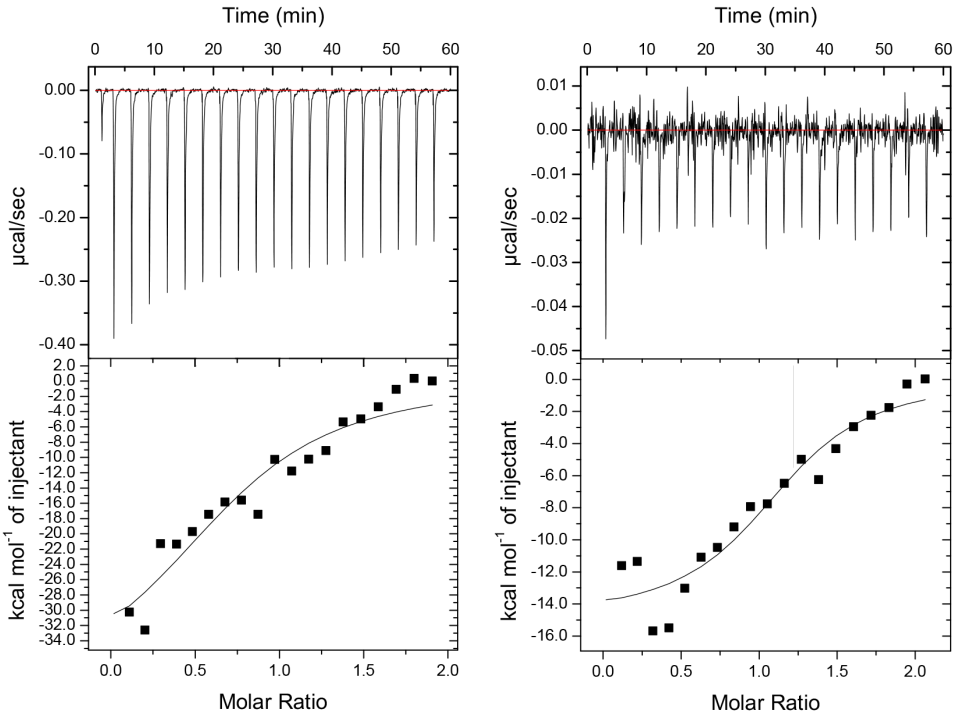

Figure 9. Results from the ITC pilot experiments. Left: Titration of gp120 to CD4. Right: Titration of **C1** to CD4.

5.3 Conclusions

In chapter 4, a procedure for the synthesis of three cyclic peptide-containing discontinuous epitope mimics has been described. Using control over the relative positioning of the peptides presented in this chapter, the influence of the position of the peptides on the scaffold was investigated. Three molecular constructs mimicking the CD4-binding site of gp120 were synthesized that differed only in the relative position of the peptides. These protein mimics were evaluated for their ability to inhibit the interaction between CD4 and gp120. Interestingly, all three mimics were equally potent, which suggests that the relative positioning of the peptides in the three gp120 protein mimics with respect to the CD4-receptor is similar. Possibly, the flexibility of the TAC-scaffold is at least partly responsible for a similar orientation of the three loops.

Furthermore, the influence of cyclization of the peptides on the activity and stability of the resulting protein mimics was investigated. Two mimics were synthesized, one composed of cyclic peptides and one composed of linear peptides. The protein mimic composed of cyclic peptides had a somewhat better biological activity and a better proteolytic stability compared to its linear equivalent. These results, especially the latter, underline the importance of using cyclic peptides in order to obtain the best protein mimic.

Two smart libraries of epitope mimics were also synthesized, one based on linear peptides and one on cyclic peptides. The individual protein mimics from the linear library were easily

purified and showed good activity. However, the separation of the individual mimics from the cyclic library was poor and it was impossible to obtain pure mimics. However, the success of the combinatorial approach is highly dependent on the sequence and cyclization pattern of the peptides and might be more effective for ligation of peptides consisting of other amino acid sequences.

To improve the biological evaluation of the gp120 mimics, Isothermal Titration Calorimetry was also explored to measure the binding affinity of the mimics to CD4. The results of the ITC pilot experiment were encouraging and suggest that ITC can be of great value to this research.

5.4 Experimental procedures

5.4.1 General information

Chemicals were obtained from commercial sources and used without further purification, unless stated otherwise. Peptide grade D*i*PEA, CH_2Cl_2, TFA and HPLC grade solvents were purchased from Biosolve B.V. (Valkenswaard, the Netherlands) and peptide grade NMP and DMF were purchased from Actu-All Chemicals (Oss, the Netherlands). Fmoc-protected amino acids, HBTU, and BOP were purchased from GL Biochem Ltd. (Shanghai, China). Used amino acids with side chain protecting groups were as follows: Fmoc-Arg(Pbf), Fmoc-Asp(OtBu), Fmoc-Cys(Trt), Fmoc-Gln(Trt), Fmoc-Glu(OtBu), Fmoc-His(Trt), Fmoc-Thr(tBu) and Fmoc-Trp(Boc). TentaGel S RAM resin (particle size 90 μm, capacity 0.25 mmol/g) was purchased from Rapp Polymere GmbH (Tübingen, Germany).

Solid phase peptide synthesis was performed on a C.S. Bio Co. peptide synthesizer (model CS336X). Unless stated otherwise, reactions were performed at room temperature. TLC analysis was performed on Merck precoated silica gel 60 F-254 plates. Spots were visualized with UV-light, ninhydrin stain (1.5 g ninhydrin and 3.0 mL acetic acid in 100 mL *n*-butanol), Potassium permanganate (1.5 g of $KMnO_4$, 10 g K_2CO_3, and 1.25 mL 10% NaOH in 200 mL water) and/or molybdenum staining agent (12 g ammonium molydate and 0.5 g ammonium cerium(IV) sulfate in 250 mL 10% H_2SO_4). Column chromatography was performed using Silica-P Flash silica gel (60 Å, particle size 40-63 μm) from Silicycle (Canada). Lyophilization was performed on a Christ Alpha 1–2 apparatus. ^{1}H NMR (400 MHz) and ^{13}C NMR (100 MHz) experiments were conducted on a 300 MHz Varian G-300 spectrometer. Chemical shifts are given in ppm (δ) relative to TMS (0.00 ppm) (^{1}H NMR) or relative to $CDCl_3$ (77 ppm) (^{13}C NMR).

Analytical HPLC was performed on a Shimadzu-10Avp (Class VP) system using a Phenomenex Gemini C18 column (110 Å, 5 μm, 250×4.60 mm) at a flow rate of 1 mL min^{-1}. The used buffers were 0.1% trifluoroacetic acid in MeCN/H_2O 5:95 (buffer A) and 0.1% trifluoroacetic acid in MeCN/H_2O 95:5 (buffer B). Runs were performed using a standard protocol: 100% buffer A for 2 min, then a linear gradient of buffer B (0-100% in 48 min) and UV-absorption was measured at 214 and 254 nm. Purification using preparative HPLC was performed on a Prep LCMS QP8000α HPLC system (Shimadzu) using a Phenomenex

Gemini C18 column (10 µm, 110 Å, 250×21.2 mm) at a flow rate of 12.5 mL min^{-1}. Runs were performed by a standard protocol: 100% buffer A for 5 min followed by a linear gradient of buffer B (0-100% in 70 min) with the same buffers as were described for analytical HPLC.

ESI-TOF MS spectra were recorded on a microTOF mass spectrometer (Bruker). Samples were diluted with tuning mix (1:1, v/v) and infused at a speed of 300 µl/h using a nebulizer pressure of 5.8 psi, a dry gas flow of 3.0 L/min, a drying temperature of 180°C and a capillary voltage of 5.5 kV. Analytical LC-MS (electrospray ionization) was preformed on Thermo-Finnigan LCQ Deca XP Max using same buffers and protocol as described for analytical HPLC. All reported mass values are monoisotopic.

The microtiterplate reader used in the ELISA assays was a BioTek µQuant (Beun de Ronde, Abcoude, the Netherlands).

ITC experiments were carried out on a MicroCal ITC200 (MicroCal Inc.).

5.4.2 Experimental procedures and analytical data

1-(azidomethyl)-3-(bromomethyl)-benzene (2)

1,3-bis(bromomethyl)-benzene (1.32 g, 5.00 mmol) was dissolved in DMF (40 ml), followed by the dropwise addition of a suspension of NaN_3 (0.29 g, 4.46 mmol, 0.9 eq) in DMF (10 ml). The resulting mixture was stirred for 3 h and the reaction was monitored using TLC (10 % EtOAc in hexanes). Upon completion of the reaction, the mixture was concentrated *in vacuo*, which yielded a yellow oil that contained a NaBr-salt precipitate. The oil was dissolved in EtOAc and the resulting mixture was filtered. The filtrate was concentrated *in vacuo* and purified using silica gel column chromatography (0.5% EtOAc in hexanes), which yielded the product as a clear light yellow oil. Despite multiple purification attempts, 1,3-bis(azidomethyl)-benzene remained as an impurity. Analysis by ^{1}H-NMR provided a ratio of 70:30 for 1-(azidomethyl)-3-(bromomethyl)-benzene (**2**) and 1,3-bis(azidomethyl)-benzene (**3**), respectively. Yield: 0.72 g (of which 0.53 g monoazide). Rf (monoazide: 0.63 (10 % EtOAc in PE). ^{1}H-NMR (400 MHz, $CDCl_3$): δ = 4.35, 4.36 (s, 2H, CH_2N) 4.49 (s, 2H, CH_2Br), 7.23 – 7.40 (m, 4H, Ar-*H*). ^{13}C-NMR (100 MHz, $CDCl_3$): δ = 32.97 (CH_2Br), 54.43, 54.50 (CH_2N_3), 127.80, 128.01, 128.10, 128.66, 128.90, 129.31, 129.34, 136.13, 136.15, 138.47 (Ar-*C*).

Peptide synthesis

Solid phase peptide synthesis

Linear peptides were synthesized on a C.S. Bio Co. peptide synthesizer using Tentagel S RAM resin (rink amide linker) on a 0.25-mmol scale. Removal of the Fmoc-group was performed using 20% piperidine in NMP. Amino acids are coupled using 4 equiv. of amino acid and HBTU as an activating agent with D*i*PEA as a base and NMP as solvent. Capping was performed using acetic anhydride (12 mL), HOBt (0.5 g) and D*i*PEA (5.5 ml) in NMP (250 mL). Note: In the synthesis of both cyclic and linear loop 1 (**1** and **7**) the glycine residue adjacent to the aspartic acid residue was coupled as Fmoc-(Dmb)-Gly-OH to prevent aspartimide formation.

General procedure for the cleavage and deprotection of the peptide from the solid support

The sidechain-protected linear peptide was cleaved from the resin and deprotected using a mixture of TFA:H_2O:EDT:TIS (90:5:2.5:2.5) (v/v/v/v), 10 mL per gram resin. The reaction mixture was stirred for 3 hours after which the mixture was filtered and concentrated to a volume of 2 mL, followed by precipitation of the peptides from MTBE/hexane (1:1 v/v). After centrifugation (3500rpm, 5 min), the supernatant was decanted and the pellet was resuspended in MTBE/hexane (1:1 v/v) and centrifuged again. The pellet was dissolved in *t*-BuOH/H_2O (1:1 v/v) and lyophilized. The purity of the peptides was analyzed using analytical HPLC and the peptides were characterized by mass spectrometry.

Cyclic peptide synthesis

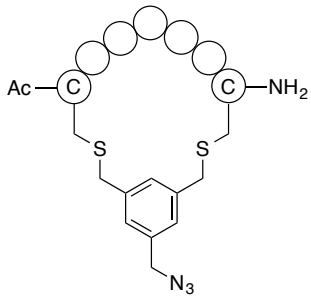

To a 1 mM solution of the crude linear peptide in a (1:3 v/v) mixture of MeCN/ NH_4HCO_3 (aq, 20 mM, pH 7.8) a solution of 1-(azidomethyl)-3,5-bis(bromomethyl)benzene (see Chapter 2) (1.25 equiv.) in MeCN (2 mL) was added dropwise. The resulting mixture was stirred at room temperature for 3 hours before being concentrated and lyophilized. The crude cyclic peptide was purified using preparative HPLC. The product-containing fractions were pooled and lyophilized to yield the purified cyclic peptides as white fluffy powder.

Cyclic Ac-CLTRDGGKC-NH_2 (**1**): 69 mg (60 µmol), 34%, (21 steps, average 95% per step). Exact mass calculated $[M + H]^+$: 1150.5250; ESI-TOF MS found: 1150.5263. Rt = 19.90 min.

Cyclic H-CINMWQEVGKAC-NH_2 (**2**): 65 mg (42 µmol), 17%, (26 steps, average 93% per step). Exact mass calculated $[M + 2H]^{2+}$: 769.3472; ESI-TOF MS found: 769,3464. Rt = 22.05 min.

Cyclic Ac-CSGGDPEIVTC-NH_2 (**3**): 92 mg (72 µmol), 29%, (25 steps, average 95% per step). Exact mass calculated $[M + H]^+$: 1278.5247; ESI-TOF MS found: 1278.5269. Rt = 22.58 min.

Functionalized linear peptide synthesis

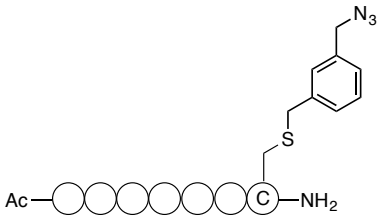

Crude peptide was dissolved in 20 mM NH_4HCO_3 (aq)/MeCN (3/1 (v/v)) (80 mL). Crude 1-azido-3-bromo-xylene (**5**) was dissolved in MeCN (5 mL) and the resulting solution was added to the crude peptide solution. The resulting mixture was stirred for 3 h and the reaction was monitored using LC-MS. Upon completion of the reaction, the mixture was concentrated *in vacuo*.

The mixture was lyophilized overnight, which yielded the crude product as a fluffy white powder. The crude product was purified using preparative HPLC.

Linear loop 1 (**7**, sequence Ac-LTRDGGKC-NH_2) 36 mg (34 µmol), 19%, (19 steps, average 92% per step). Exact mass calculated $[M + H]^+$: 1035.5158; ESI-TOF MS found: 1035.5170. Rt = 20.19 min.

Linear loop 2 (**8**, sequence H-INMWQEVGKAC-NH_2) 95 mg (34 µmol), 27%, (24 steps, average 95% per step). Exact mass calculated $[M + H]^+$: 1422.6775; ESI-TOF MS found: 1422.6839. Rt = 27.89 min.

Linear loop 3 (**9**, sequence Ac-SGGDPEIVTC-NH_2) 52 mg (44 µmol), 23%, (23 steps, average 94% per step). Exact mass calculated $[M + H]^+$: 1163.5155; ESI-TOF MS found: 1163.5139. Rt = 24.12 min.

Linear acetylated loop 2 (**11**, sequence Ac-INMWQEVGKAC-NH_2) 34 mg (23 µmol), 11%, (24 steps, average 91% per step). Exact mass calculated $[M + H]^+$: 1464.6880; ESI-TOF MS found: 1464.6874. Rt = 27.9 min.

Sequential introduction of peptides onto the TAC-scaffold

The procedure for the sequential introduction of peptides onto the TAC-sacffold is identical to the procedure described in chapter 4. The yields, scale, and analytical data for the four synthesized constructs and their intermediates are given below.

Constructs bearing one peptide and a free alkyne

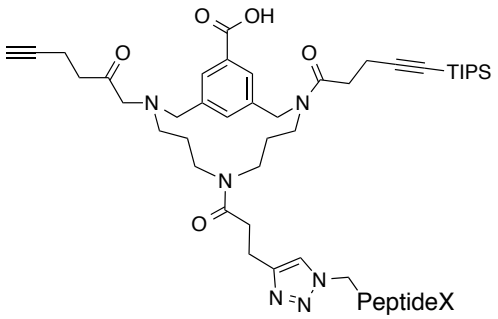

C1a Peptide X = cyclic loop 1 (12.7 µmol scale) yield: 11.5 mg (6.3 µmol), 50%. Exact mass calculated $[M + 2H]^{2+}$: 912.4620; ESI-TOF MS found: 912.4684. Rt = 30.42 min.

C2a Peptide X = cyclic loop 2 (5 µmol scale) 5.0 mg (2.3 µmol), 45%. Exact mass calculated $[M + 2H]^{2+}$: 1106.0428; ESI-TOF MS found: 1106.0408. RT = 31.14 min.

C3a Peptide X = cyclic loop 3 (10 µmol scale) yield: 13 mg (6.7 µmol), 67%. Exact mass calculated $[M + 2H]^{2+}$: 976.4618; ESI-TOF MS found: 976.4619. Rt = 34.54 min.

C4a Peptide X = linear loop 1 (12.7 µmol scale) yield: 11.8 mg (6.9 µmol), 54%. Exact mass calculated $[M + H]^{+}$: 1708.9069; ESI-TOF MS found: 1708.9070. Rt = 30.91 min.

Constructs bearing two peptides and one protected alkyne

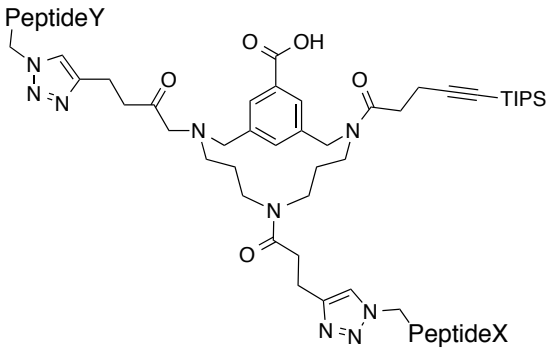

C1b Peptide X = cyclic loop 1**,** Peptide Y = cyclic loop 3 (3.3 µmol scale) yield: 2.5 mg (2.6 µmol), 80%. Exact mass calculated $[M + 3H]^{3+}$: 1034.4829; ESI-TOF MS found: 1034.4842. Rt = 27.95 min.

C2b Peptide X = cyclic loop 2**,** Peptide Y = cyclic loop 3 (2.0 µmol scale) 4.5 mg (1.3 µmol), 63%. Exact mass calculated $[M + 2H]^{2+}$: 1744.8012; ESI-TOF MS found: 1744.7973. Rt = 28.89 min.

C3b Peptide X = cyclic loop 3**,** Peptide Y = cyclic loop 1 (5.0 µmol scale) yield: 13 mg (4.2 µmol), 84%. Exact mass calculated $[M + 2H]^{2+}$: 1551.2204; ESI-TOF MS found: 1551.2168. Rt = 28.03 min.

C4b Peptide X = linear loop 1**,** Peptide Y = linear loop 3 (6.9 µmol scale) yield: 12 mg (4.2 µmol), 61%. Exact mass calculated $[M + 3H]^{3+}$: 957.8101; ESI-TOF MS found: 957.8010. Rt = 28.38 min.

Constructs bearing two peptides and a free alkyne

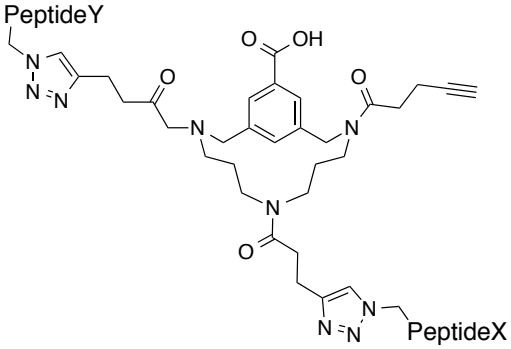

C1c Peptide X = cyclic loop 1**,** Peptide Y = cyclic loop 3 (2.8 µmol scale) yield: 7.3 mg (2.5 µmol), 87%. Exact mass calculated $[M + 2H]^{2+}$: 1473.1537; ESI-TOF MS found: 1473.1494. Rt = 21.03 min.

C2c Peptide X = cyclic loop 2**,** Peptide Y = cyclic loop 3 (1.2 µmol scale) yield: 3.0 mg (0.9 µmol), 78%. Exact mass calculated $[M + 2H]^{2+}$: 1666.7345; ESI-TOF MS found: 1666.7269. Rt = 21.37 min.

C3c Peptide X = cyclic loop 3**,** Peptide Y = cyclic loop 1 (3.6 µmol scale) yield: 4.6 mg (1.6 µmol), 43%. Exact mass calculated $[M + 2H]^{2+}$: 1473.1537; ESI-TOF MS found: 1473.1518. Rt = 21.03 min.

C4c Peptide X = linear loop 1**,** Peptide Y = linear loop 3 (4.2 µmol scale) yield: 9.7 mg (3.6 µmol), 85%. Exact mass calculated $[M + 2H]^{2+}$: 1358,1445; ESI-TOF MS found: 1358.1403. Rt = 21.47 min.

Final constructs bearing three peptides

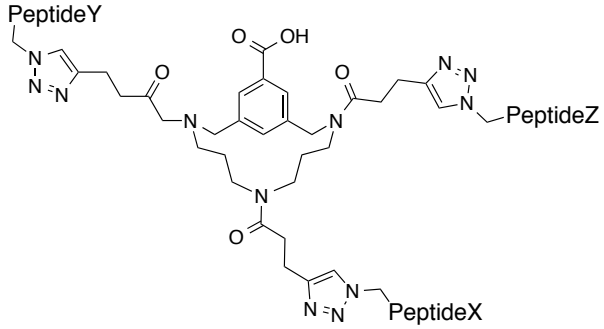

C1 Peptide X = cyclic loop 1**,** Peptide Y = cyclic loop 3, Peptide Z = cyclic loop 2 (2.5 μmol scale) yield: 4.9 mg (1.1 μmol), 44%. Exact mass calculated $[M + 3H]^{3+}$: 1034.4829; ESI-TOF MS found: 1034.4842. Rt = 20.72 min.

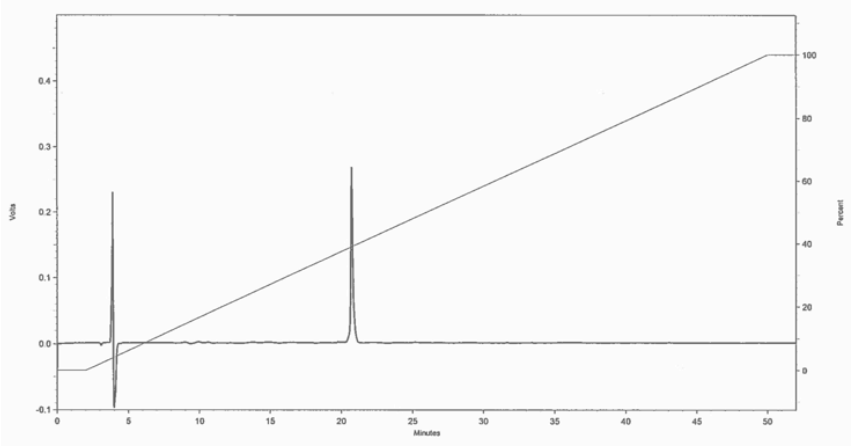

C2 Peptide X = cyclic loop 2**,** Peptide Y = cyclic loop 3, Peptide Z = cyclic loop 1 (0.75 μmol scale) yield: 1.7 mg (0.38 μmol), 51%. Exact mass calculated $[M + 2H]^{2+}$: 1744.8012; ESI-TOF MS found: 1744.7973. Rt = 20.85 min.

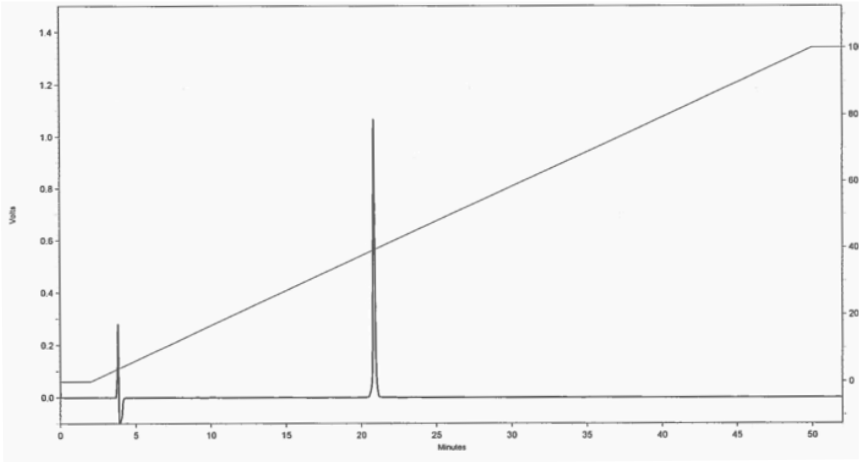

C3 Peptide X = cyclic loop 3**,** Peptide Y = cyclic loop 1, Peptide Z = cyclic loop 2 (1.4 µmol scale) yield: 3.6 mg (0.8 µmol), 59%. Exact mass calculated $[M + 2H]^{2+}$: 1551.2204; ESI-TOF MS found: 1551.2168. Rt = 20.89 min.

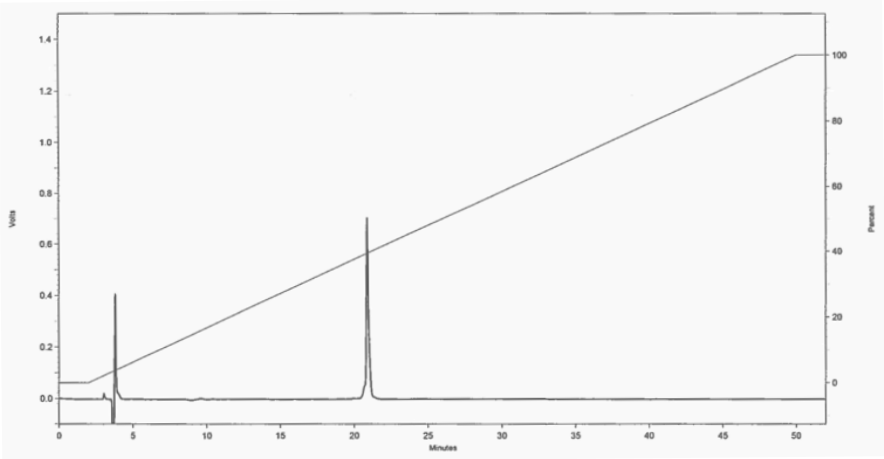

C4 Peptide X = linear loop 1**,** Peptide Y = linear loop 3, Peptide Z = linear loop 2 (1.5 µmol scale) yield: 2.2 mg (0.54 µmol), 36%. Exact mass calculated $[M + 3H]^{3+}$: 1379.6555; ESI-TOF MS found: 1379.6620. Rt = 23.41 min.

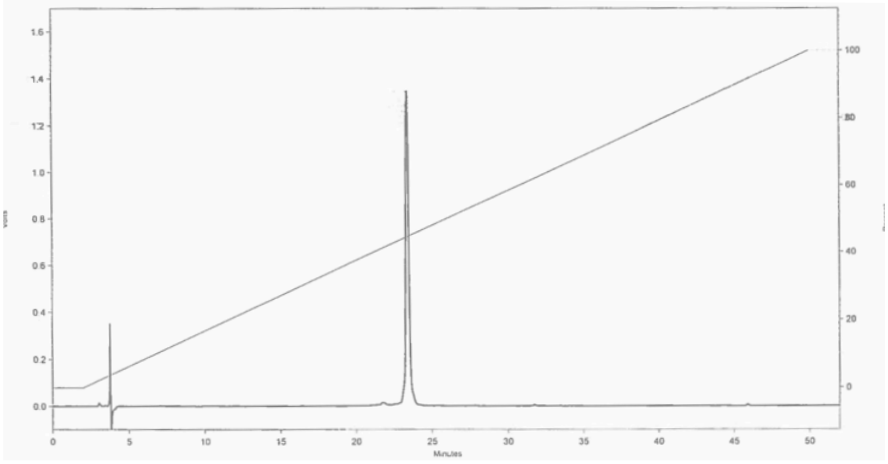

Synthesis of smart libraries through mixture ligation (12 & 13)

The procedure for the synthesis of the smart library of epitope mimics is based on a literature procedure.[13]

Cyclic peptide based smart library (**12**)

Stock solutions of $CuSO_4.5H_2O$ and sodium ascorbate were prepared: $CuSO_4.5H_2O$ (3.2 mg, 13 µmol) was dissolved in H_2O (283 µL) and sodium ascorbate (5.6 mg, 28 µmol) was dissolved in H_2O (315 µL). Solutions of the three linear peptides were prepared: Loop 1 (**1**, 8.6 mg, 7.5 µmol) was dissolved in DMF (200 µL), loop 2 (**2**, 12 mg, 7.5 µmol) was dissolved in DMF (200 µL), and loop 3 (**3**, 9.6 mg, 7.5 µmol) was dissolved in DMF (200 µL). The resulting peptide solutions were pooled in a microwave vessel and the resulting mixture was stirred. A solution of pentynoic acid functionalized TAC-scaffold **10** (3.9 mg, 7.5 µmol) in DMF (200 µL) was added, followed by the addition of 100 µL of the $CuSO_4.5H_2O$ stock solution (1.1 mg, 4.5 µmol), 100 µL of the sodium ascorbate solution (4.3 mg, 9.0 µmol), and a solution of TBTA (0.55 mg, 1.0 µmol, 0.14 eq) in DMF (200 µL). The reaction mixture was diluted with H_2O (0.47 mL) to achieve a DMF/H_2O ratio of 3/2 (v/v). The resulting mixture was stirred for 25 minutes at 80°C in the microwave, after which the mixture was purified using preparative HPLC. The separate fractions were analyzed by LC-MS to identify the epitope mimics, after which the fractions were lyophilized. The fraction identity and their LC-MS data are tabulated below. Retention times are given based on the following LC protocol: 100% buffer A for 2 min, then a linear gradient of buffer B (0-100% in 16 min).

Fraction	Dominant loop combination	Calculated m/z $[M+XH]^{x+}$	Found m/z $[M+XH]^{x+}$	Rt (min) LC-MS
12a	1-1-1	1322.94 [3+] 992.46 [4+]	1322.16 [3+] 991.88 [4+]	10.03
12b	1-1-3	1365.61 [3+] 1024.46 [4+]	1365.04 [3+] 1023.94 [4+]	10.66
12c	1-1-3	1365.61 [3+] 1024.46 [4+]	1364.67 [3+] 1023.73 [4+]	10.79
	1-1-2	1451.99 [3+] 1089.25 [4+]	1450.83 [3+] 1088.63 [4+]	10.79
12d	2-2-3	1623.71 [3+] 1218.04 [4+]	1622.74 [3+] 1217.39 [4+]	11.47
12e	2-3-3	1537.33 [3+] 1153.25 [4+]	1536.51 [3+] 1152.88 [4+]	11.59
12f	3-3-3	1450.94 [3+]	1450.11 [3+]	11.68
12g	2-3	1666.73 [2+] 1111.49 [3+]	1665.22 [2+] 1111.13 [3+]	11.71
12h	1-1	1409.15 [2+] 939.77 [3+]	1407.89 [2+] 939.03 [3+]	10.73
12i	1-3-3	1408.27 [3+]	1407.69 [3+]	11.20
12j	1-3-3	1408.27 [3+]	1407.55 [3+]	11.16
	1-2-3	1494.66 [3+] 1121.24 [4+]	1493.59 [3+] 1120.59 [4+]	11.16

Linear peptide based smart library (**13**)

Stock solutions of $CuSO_4.5H_2O$ and sodium ascorbate were prepared: $CuSO_4.5H_2O$ (4.6 mg, 18 µmol) was dissolved in H_2O (200 µL) and sodium ascorbate (5.3 mg, 27 µmol) was dissolved in H_2O (200 µL).

Solutions of the three linear peptides were prepared: Loop 1 (**7**, 7.7 mg, 7.5 µmol) was dissolved in DMF (200 µL), loop 2 (**11**, 11 mg, 7.5 µmol) was dissolved in DMF (600 µL), and loop 3 (**9**, 8.8 mg, 7.5 µmol) was dissolved in DMF (600 µL). The resulting peptide solutions were pooled in a microwave vessel and the resulting mixture was stirred. A solution of pentynoic acid functionalized TAC-scaffold **10** (3.9 mg, 7.5 µmol) in DMF (200 µL) was added, followed by the addition of 49 µL of the $CuSO_4.5H_2O$ stock solution (1.2 mg, 4.5 µmol), 67 µL of the sodium ascorbate solution (1.8 mg, 9.0 µmol), and a solution of TBTA (1.0 µmol, 0.55 mg) in DMF (200 µL). The reaction mixture was diluted with H_2O (1.2 mL) to achieve a DMF/H_2O ratio of 3/2 (v/v). The resulting mixture was stirred for 25 minutes at 80°C in the microwave, after which the mixture was purified using preparative HPLC. The separate fractions were analyzed by LC-MS to identify the epitope mimics, after which the fractions were lyophilized. The fraction identity and their LC-MS data are tabulated below. Retention times are given based on the following LC protocol: 100% buffer A for 2 min, then a linear gradient of buffer B (0-100% in 28 min).

Fraction	Loop combination	Calculated m/z $[M+XH]^{x+}$	Found m/z $[M+XH]^{x+}$	Rt (min) LC-MS
13a	1-1-1	1207.93 [3+] 906.20 [4+]	1207.41 [3+] 905.63 [4+]	13.12
13b	1-1-3	1250.60 [3+]	1250.03 [3+]	13.82
13c	1-3-3	1293.26 [3+]	1292.81 [3+]	14.56
13d	1-1-2	1350.99 [3+] 1013.49 [4+]	1350.46 [3+] 1012.84 [4+]	15.03
13e	1-2-3	1393.65 [3+]	1393.10 [3+]	15.60
13f	1-2	1508.73 [2+] 1006.15 [3+]	1507.71 [2+] 1005.56 [3+]	15.97
13g	2-3-3	1436.32 [3+]	1435.71 [3+]	16.30
13h	2-2-3	1536.71 [3+] 1152.78 [4+]	1535.96 [3+] 1152.00 [4+]	16.96
13i	2-2-2	1637.10 [3+] 1228.08 [4+]	1635.94 [3+] 1227.36 [4+]	17.39

HIV-1 gp120 capture ELISA

Recombinant HIV-1IIIB gp120 protein (referred to as rgp120 hereafter unless otherwise noted) capture ELISA was performed according to the manufacturer's instructions (ImmunoDiagnostics, Inc., Woburn, MA, U.S.A.). A solution of the test compound, diluted in sample buffer (50 µL 0,1% BSA in PBS) and 2% DMSO, was added to the CD4-coated plate, which was immediately followed by the addition of 50 µL 2 µg/ml rgp120 (final concentration 1 µg/mL). After 4 hours of incubation at room temperature, the plate was washed with wash

buffer (0.1% Tween 20 in PBS) followed by incubation with peroxidase-conjugated murine anti-gp120 MAb to detect the amounts of captured rgp120. Any unbound material was washed away using wash buffer, and the plates were developed by adding 100 µL/well substrate solution (0.1 mg/mL TMB in 0.1 N NaOAc buffer pH 5.5, containing 0.003% H_2O_2). The reaction was stopped by adding 100 µL 4N sulfuric acid. Absorbances (ODs) were read at 450 nm using a microtiterplate reader. All assays were performed in duplicate and all compounds were tested independently at least three times.

Serum stability assay

4 mg/mL construct solutions were prepared in MilliQ. Duplicate samples were prepared with 100 µL peptide solution and 500 µL human serum. The samples were incubated at 37°C, and samples were taken at t = 0, 1, 8 and 24 h as follows: To 100 µL serum solution, 200 µL MeOH (containing 0.075 mg/mL ethylparaben as an internal standard) was added to precipitate the proteins. The sample was vortexed briefly and allowed to stand for 10 min at RT. The samples were then centrifuged at 12,000 RPM for 5 min, and the supernatant was taken and stored at -20°C until analysis. Each sample was analyzed by HPLC, on a C18 column. The peaks were integrated and normalized to the internal standard.

Isothermal Titration Calorimetry

Sample preparation

Commercially available sCD4 (Life Technologies, Bleiswijk, the Netherlands) (250 µg, 28kD) was dissolved in H_2O (1.2 mL) and the solution was thoroughly dialyzed against PBS (10 kD cut-off), after which the volume was determined to be 1.54 mL to a final concentration of 3.86 µM.

Commercially available recombinant gp120 (Life Technologies, Bleiswijk, the Netherlands) (250 µg, 54.6 kD) was dissolved in H_2O (400 µL) and thoroughly dialyzed simultaneously with the sCD4 solution (10 kD cut-off). After dialysis, the volume of the gp120 solution was determined to be 735 µL (6.2 µM). The solution was concentrated by spin filter to a concentration of 18 µM.

Epitope mimic **C1** (approx. 0.4 mg) was dissolved in aqueous NH_4HCO_3 (20 mM) and the resulting solution was lyophilized. The white solid (0.36 mg, 0.08 µmol) was dissolved in dialysis buffer (1 mL) to afford a final concentration of 80 µM.

ITC experiments

The titrant (100 µL), either gp120 (18 µM) or **C1** (40 µM) was titrated into the sample cell (400 µL) containing either PBS or sCD4 (1.93 or 3.86 µM). The titration started with an initial delay of 60 seconds, followed by a first injection of 0.4 µL. After 120 seconds, the rest was titrated in 19 injections of 2 µL 180 seconds apart. All experiments were carried out at 25°C. Data was analyzed with Microcal ORIGIN software using a one-site binding model.

References

1 M. Rolland, S. Manocheewa, J. V. Swain, E. C. Lanxon-Cookson, M. Kim, D. H. Westfall, B. B. Larsen, P. B. Gilbert and J. I. Mullins, *J. Virol.*, 2013, **87**, 5461–5467.

2 L. M. Walker, M. Huber, K. J. Doores, E. Falkowska, R. Pejchal, J.-P. Julien, S.-K. Wang, A. Ramos, P.-Y. Chan-Hui, M. Moyle, J. L. Mitcham, P. W. Hammond, O. A. Olsen, P. Phung, S. Fling, C.-H. Wong, S. Phogat, T. Wrin, M. D. Simek, P. G. Principal Investigators, W. C. Koff, I. A. Wilson, D. R. Burton and P. Poignard, *Nature*, 2011, **477**, 466–470.

3 S. Z. Shapiro, *AIDS Res. Hum. Retroviruses*, 2014, **30**, 325–329.

4 D. V. Glidden, *Nature*, 2012, **490**, 350–351.

5 C. Guarise, S. Shinde, K. Kibler, G. Ghirlanda, L. J. Prins and P. Scrimin, *Tetrahedron*, 2012, **68**, 4346–4352.

6 W. Shi, L. Cai, L. Lu, C. Wang, K. Wang, L. Xu, S. Zhang, H. Han, X. Jiang, B. Zheng, S. Jiang and K. Liu, *Chem. Commun.*, 2012, **48**, 11579–81.

7 W. Liu, J. Tan, M. M. Mehryar, Z. Teng and Y. Zeng, *Med. Chem. Comm*, 2014.

8 V. Briz, E. Poveda and V. Soiano, *J. Antimicrob. Chemother.*, 2006, **57**, 619–627.

9 P. D. Kwong, R. Wyatt, S. Majeed, J. Robinson, R. W. Sweet, J. Sodroski and W. A. Hendrickson, *Structure*, 2000, **8**, 1329–39.

10 P. D. Kwong, R. Wyatt, J. Robinson, R. W. Sweet, J. Sodroski and W. A. Hendrickson, *Nature*, 1998, **393**, 648–59.

11 R. Pejchal, K. J. Doores, L. M. Walker, R. Khayat, P.-S. Huang, S.-K. Wang, R. L. Stanfield, J.-P. Julien, A. Ramos, M. Crispin, R. Depetris, U. Katpally, A. Marozsan, A. Cupo, S. Maloveste, Y. Liu, R. McBride, Y. Ito, R. W. Sanders, C. Ogohara, J. C. Paulson, T. Feizi, C. N. Scanlan, C.-H. Wong, J. P. Moore, W. C. Olson, A. B. Ward, P. Poignard, W. R. Schief, D. R. Burton and I. A. Wilson, *Science*, 2011, **334**, 1097–1103.

12 P. D. Kwong, R. Wyatt, J. Robinson, R. W. Sweet, J. Sodroski and W. A. Hendrickson, *Nature*, 1998, **393**, 648–659.

13 G. E. Mulder, J. A. W. Kruijtzer and R. M. J. Liskamp, *Chem. Commun.*, 2012, **48**, 10007–10009.

14 R. Franke, T. Hirsch, H. Overwin and J. Eichler, *Angew. Chem. Int. Ed.*, 2007, **46**, 1253–1255.

15 R. Franke, T. Hirsch and J. Eichler, *J. Recept. Signal Tr. R.*, 2006, **26**, 453–460.

16 H. van de Langemheen, H. L. C. Quarles van Ufford, J. A. W. Kruijtzer and R. M. J. Liskamp, *Org. Lett.*, 2014, 10–13.

17 H. van de Langemheen, M. van Hoeke, H. C. Quarles van Ufford, J. A. W. Kruijtzer and R. M. J. Liskamp, *Org. Biomol. Chem.*, 2014, **12**, 4471–8.

18 Q. Yang, A. G. Stephen, J. W. Adelsberger, P. E. Roberts, W. Zhu, M. J. Currens, B. J. Crise, R. J. Gorelick, A. R. Rein, R. J. Fisher, R. H. Shoemaker, S. Sei and Y. Feng, *J. Virol.*, 2005, **79**, 6122–6133.

19 G. E. Mulder, H. C. Quarles van Ufford, J. van Ameijde, A. J. Brouwer, J. A. W. Kruijtzer and R. M. J. Liskamp, *Org. Biomol. Chem.*, 2013, **11**, 2676–2684.

20 L. Y. Chan, V. M. Zhang, Y. H. Huang, N. C. Waters, P. S. Bansal, D. J. Craik and N. L. Daly, *ChemBioChem*, 2013, **14**, 617–624.

21 S. Leavitt and E. Freire, *Curr. Opin. Struct. Biol.*, 2001, **11**, 560–566.

22 E. Falkowska, A. Ramos, Y. Feng, T. Zhou, S. Moquin, L. M. Walker, X. Wu, M. S. Seaman, T. Wrin, P. D. Kwong, R. T. Wyatt, J. R. Mascola, P. Poignard and D. R. Burton, *J. Virol.*, 2012, **86**, 4394–4403.

23 Y. Liu, A. Schön and E. Freire, *Chem. Biol. Drug Des.*, 2013, **81**, 72–78.

24 A. Schön, N. Madani, J. C. Klein, A. Hubicki, D. Ng, X. Yang, A. B. Smith, J. Sodroski and E. Freire, *Biochemistry*, 2006, **45**, 10973–10980.

25 D. G. Myszka, R. W. Sweet, P. Hensley, M. Brigham-Burke, P. D. Kwong, W. A. Hendrickson, R. Wyatt, J. Sodroski and M. L. Doyle, *Proc. Natl. Acad. Sci. U. S. A.*, 2000, **97**, 9026–9031.

6

Chapter 6

Towards synthetic vaccines

6.1 Introduction

Vaccination is one of the most effective methods to combat infectious diseases.[1–4] The prophylactic approach of vaccination may provide the ultimate protection strategy against pathogens and toxic proteins since it is able to induce lasting immunological memory.

Epitope mimics representing antigenic proteins of pathogens may possess the ability to induce the production of antibodies, making them possible candidates for synthetic vaccines. The possibility of synthetic preparation of vaccines is very attractive because these vaccines may have distinct advantages over traditional vaccines. One major advantage of synthetic mimics as vaccines may be that they only display the desired epitope(s) and do not include the remainder of the protein. This may circumvent pathogenic defences like genetically variable immuno-dominant epitopes and glycan shielding. In this way, conserved epitopes that are normally missed by the immune system can be targeted specifically.

Moreover, (modified) proteins or other constituents of a pathogen or even complete (attenuated) pathogens are traditionally used for vaccination purposes. Although these methods have proven to be very effective, they are associated with various risks, like genetic instability, the use of potentially harmful components and residual virulence.[2,3] Moreover, during preparation of the vaccine, the original pathogen (or parts thereof) is used, which in principle creates a biohazardous situation. When these issues are taken into consideration, the advantages of possible synthetic vaccines become evident. Since a synthetic vaccine is accessible through chemical synthesis, there is no risk of exposure to and contamination by (parts of) the pathogen. A chemical process for its preparation may also be easier to scale up compared to a corresponding biotechnological process for vaccine production involving pathogens. For this reason considerable research efforts have been spent on the development of synthetic vaccines, for example by epitope mimicry (of both T-cell and B-cell epitopes).[1,2,5,6]

Several peptides have entered clinical trials to be investigated with regards to their synthetic vaccine prospects. In recent reviews, it was stated that of the 125 peptides that were enrolled in clinical trial phase I, only 30 survived to enter phase II and none went on to phase III.[7,8] Most of these were single, linear, peptides, thus mimicking either a continuous epitope or only one of the peptide segments of a discontinuous epitope. The failure to proceed to phase III trials all the more showed that there are significant hurdles to overcome when designing a synthetic peptide vaccine. The reliance on continuous epitopes and their mimics has so far not yielded any good vaccine candidates. Research is therefore increasingly focused on mimicry of discontinuous epitopes. However, the major hurdle with respect to this is probably the considerable effort required for adequate mimicry of a discontinuous epitope. Altogether potential applications of such vaccines may be very attractive, for tackling diseases like cancer, influenza, HIV, malaria.[9,10] Other important issues to consider are the (not always justified) confidence in the specificity of antibodies and underestimation of the difference between antigenicity and immunogenicity.[7] Especially intriguing is the necessity of coupling of peptide epitope mimics to carrier proteins such as the often-used keyhole limpet hemocyanin (KLH) and tetanus toxoid.[11–13] These proteins are extensively used to increase the immunogenicity

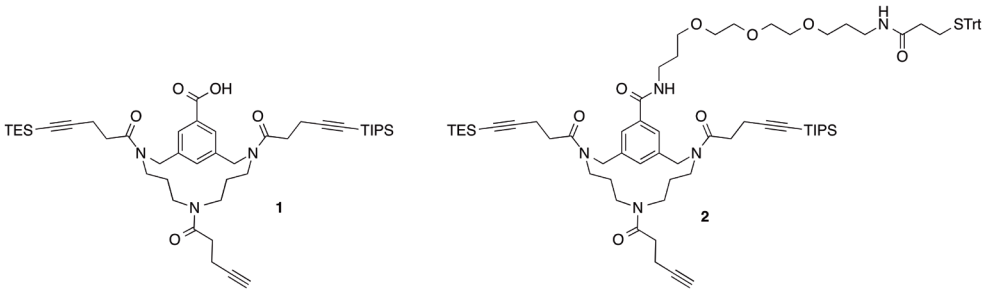

Figure 1. Left: TAC-scaffold suitable for the sequential introduction of peptides as described in chapter 4 and 5 (**1**). Right: modified scaffold suitable for conjugation to a carrier protein (**2**)

and to induce immunogenic memory and therefore protection of their cargo.

In the previous chapters, a new method was described for the synthesis of discontinuous epitope mimics through the sequential introduction of cyclic peptides onto a molecular scaffold. Using this method, we synthesized mimics of a conserved binding site of the HIV protein gp120. These mimics were capable of inhibition of the binding of CD4 and gp120, which points toward correct mimicry of the natural epitope. Furthermore, the discontinuous epitope mimics showed excellent serum stability. These two characteristics make these discontinuous epitope mimics good candidates for synthetic vaccination.

However, the described mimics are not yet ready for immunization studies. As mentioned above, most peptide-based vaccines have to be conjugated to a carrier protein like KLH or tetanus toxoid. This is usually carried out using a thiol-maleimide conjugation reaction to a commercially available maleimide-functionalized carrier protein. As a consequence, a thiol moiety has to be incorporated in the scaffold to make it suitable for conjugation. Therefore a modified scaffold (**2**) was designed which can be synthesized from the scaffold described in chapter 4 (**1**) (Figure 1). The carboxylic acid of the original scaffold (**1**) was used to attach a spacer with a thiol moiety at the end.

6.2 Results and discussion

The trityl group was used as a protecting group for the thiol moiety. The synthesis of the adapted scaffold (Scheme 1) started with coupling of trityl-protected thiopropionic acid (**3**) to the diamine spacer (**4**). Using EDCI as a coupling reagent and an excess of diamine **4**, the product (**5**) was obtained in 60% yield. The thiol-functionalized spacer was then coupled to protected trialkyne TAC-scaffold **1**, again using EDCI as a coupling reagent to afford modified scaffold **2** in a 42% yield.

The scaffold was then used for the sequential introduction of cyclic peptides. The peptides that were used for this purpose were the same as the peptides described in chapter 4 and 5 (Figure 2). These peptides correspond to the CD4 binding site of the HIV protein gp120 and, when mounted on the TAC-scaffold, they are able to bind to CD4 and inhibit the interaction between CD4 and gp120. The peptides (**6**, **7**, and **8**) were synthesized, cyclized, and functionalized with an azide handle as described in chapter 2.

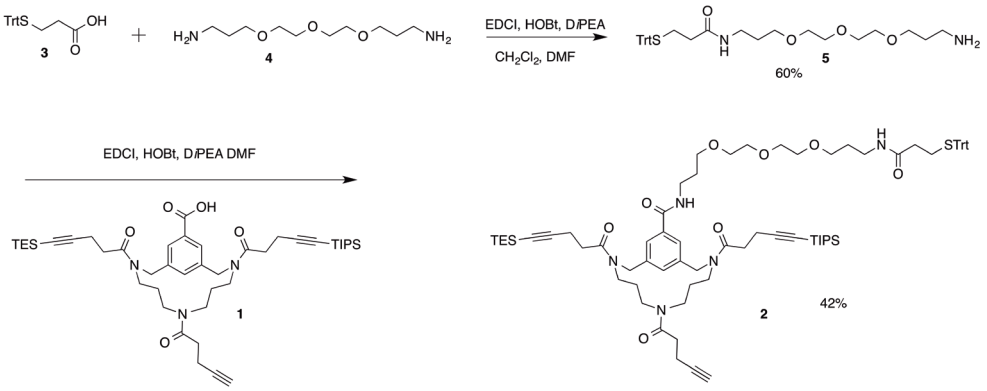

Scheme 1. Synthesis of adapted scaffold **2**.

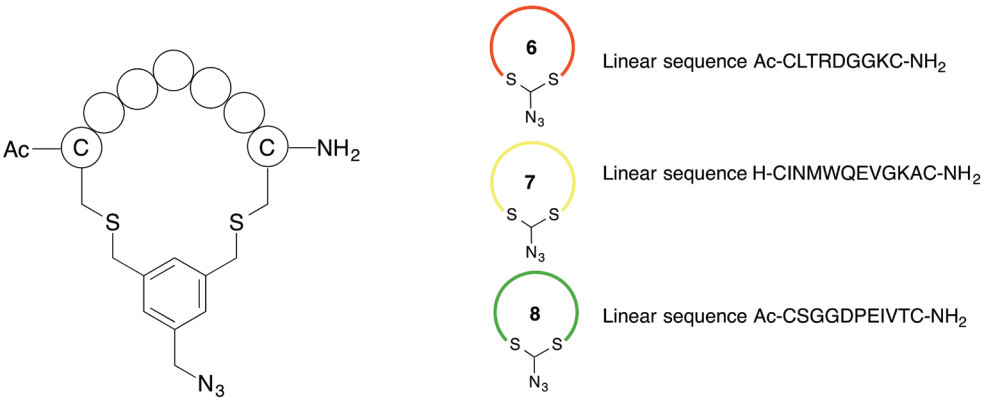

Figure 2. Left: General structure of the azide-functionalized cyclic peptides. Right: Linear sequences of the three peptides (**6**, **7**, and **8**) that correspond to the CD4-binding site of HIV gp120

In the first attempt at the sequential introduction of the three cyclic peptides the same protocol was used as was described in chapters 4 and 5. The first step was the attachment of the first peptide (**6**) onto scaffold **2** and the subsequent TES-removal by $AgNO_3$ to afford partially deprotected scaffold **9** (Scheme 2). However, the trityl protection group proved to be incompatible with the TES-deprotection by treatment with $AgNO_3$. To remedy this, another method for the removal of the TES-group was attempted, namely treatment with a large excess of K_2CO_3.[14] Although this method did remove the TES-group from the alkyne, it had some disadvantages. Firstly, the reaction time was very long and the reaction did not reach full completion even after 6 days. Secondly, the yield of the reaction was disappointing, especially compared to the TES-removal by $AgNO_3$ (90%, see chapter 3). Finally, in contrast to the $AgNO_3$ procedure, it could not be combined with the first ligation step and required an extra purification step of ligation product **10**. Nevertheless, using this deprotection procedure the desired product (**9**) was obtained, albeit in low yield (16% over 2 steps).

After the removal of the TES-group, the standard procedure for the sequential introduction of the cyclic peptides was followed (Scheme 2) as was described in chapters 4 and 5. Peptide

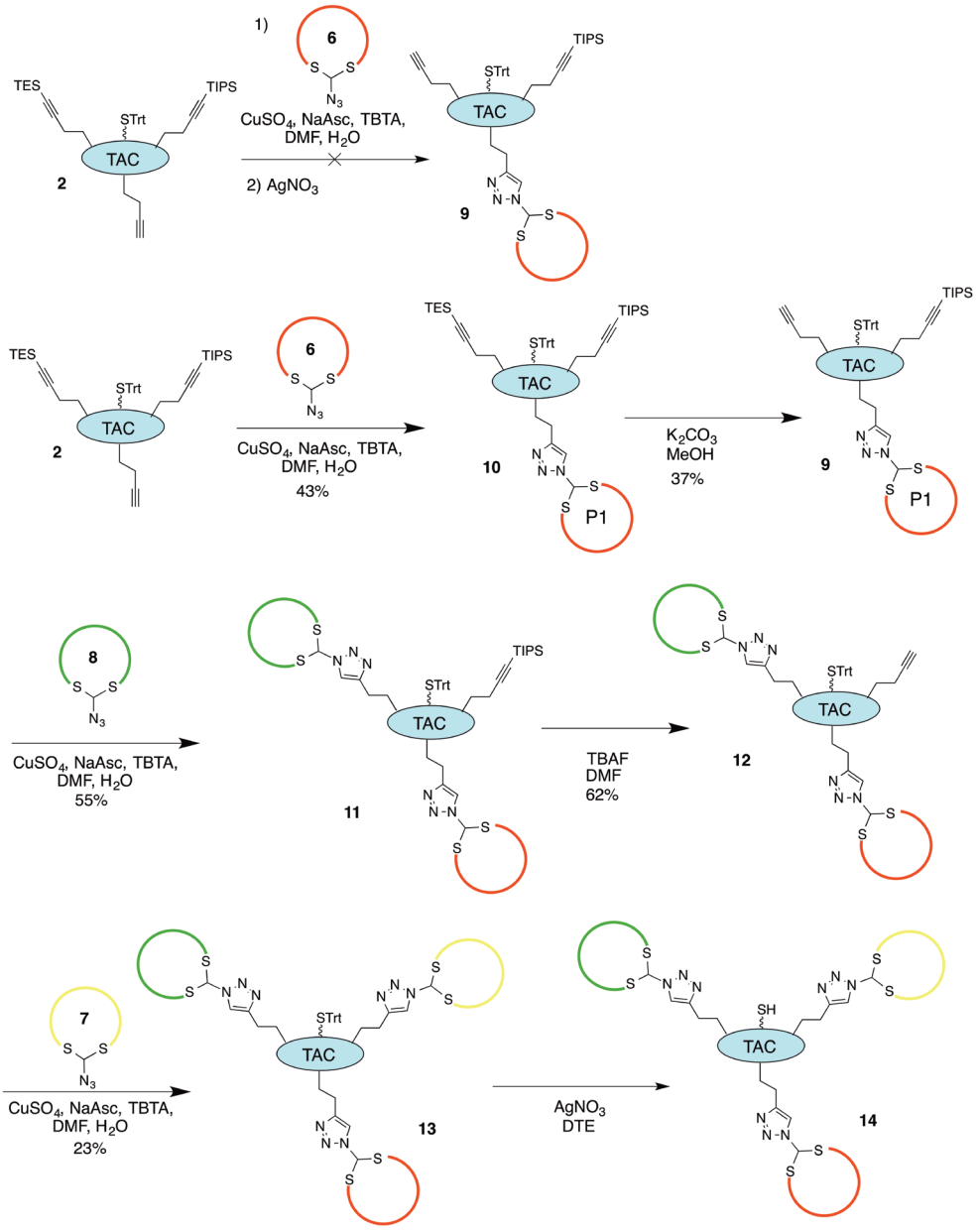

Scheme 2. Synthesis of construct **14** bearing three cyclic peptides and a free thiol functionality which can be used for the ligation to a carrier protein.

8 was attached next to prepare two cyclic peptide containing scaffold **11**, followed by the deprotection of the third alkyne by TBAF. Peptide **7** could then be added to be ligated to the free alkyne scaffold **12** to form three cyclic peptide-containing construct **13**. Due to disappointing yields, construct **13** was obtained in a small quantity (< 1 mg). The overall yield of the sequential introduction is only 1% compared to 10-15% of the constructs described in chapter 5.

The final step was the removal of the trityl protecting group to final construct **14**. The removal of the trityl group was previously encountered as a side-reaction during treatment with $AgNO_3$. Therefore, we wondered if this side-reaction could be applied to fully deprotect the thiol functionality. Construct **13** was therefore treated with $AgNO_3$ and the reaction was monitored using LC-MS, which showed a quick conversion of the trityl protected construct **13** to desired construct **14** (Figure 3). Then, dithioerythritol was added to reduce any disulfide bridges and break up possibly formed silver mercaptides. Due to the low amount of starting material (**13**) we were unable to obtain appreciable quantities of the purified final construct (**14**). However, the LC-MS traces of the reaction mixture do confirm the formation of the product (Figure 3).

Although it was possible to confirm formation of the construct based on the new scaffold derivative, it was not possible to isolate the construct in appreciable quantities. The main reason for this was the sub-optimal TES-removal by potassium carbonate. The low yield and long reaction time are in strong contrast to the TES-removal by $AgNO_3$. Unless this reaction can be optimized, another route where the $AgNO_3$ step does not have to be replaced would be more desirable. Changing the protecting group on the thiol functionality to a protecting group that is compatible with $AgNO_3$ would be the easiest approach. However, both thioether-based (like trityl) and disulfide-based (like S*t*Bu) protecting groups were not compatible with the $AgNO_3$ treatment. A test reaction with a cysteine derivative protected as a thiazolidine ring

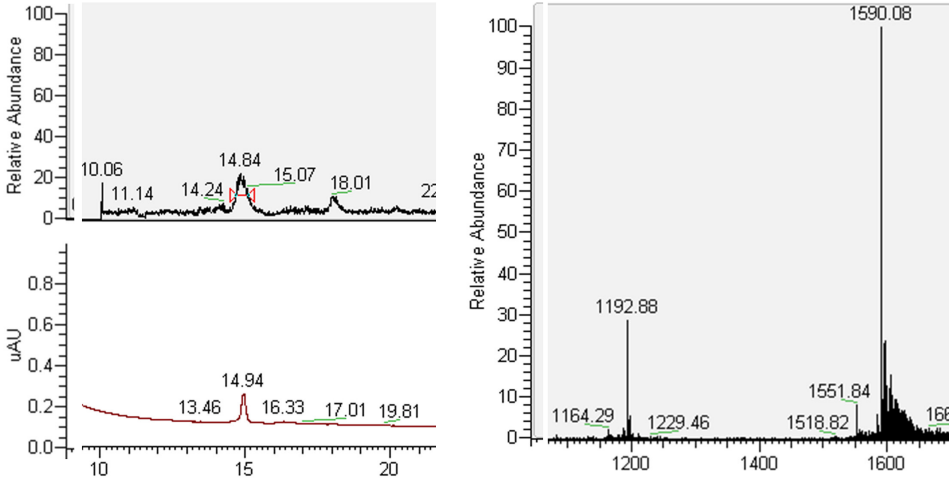

Figure 3. LC-MS data of the crude reaction mixture of the deprotection of construct **13** by $AgNO_3$ to final construct **14**. Left top: Total ion current trace of the reaction mixture. Left bottom: UV-trace of the reaction mixture. Right: Mass spectrum of final construct **14**.

also showed this protecting group was not stable to the conditions of the CuAAC reaction. Another option is to protect the thiol as a thioester, for example by acetylation. This method has been successfully used in the work of Beal et al., in which they attached two different labels and a protein (BSA) to a linear scaffold.[15] However, since a thioester is prone to hydrolysis, it should be first investigated whether it is compatible with the conditions of the used sequential introduction of the cyclic peptides.

6.3 Conclusions

One of the most attractive applications for epitope mimics might be as synthetic vaccines. To increase the effectiveness of peptide-based vaccines, they have to be conjugated to a carrier protein. In this chapter the synthesis of an epitope mimic of gp120 containing a free thiol group for ligation to a carrier protein was explored. The scaffold discussed in earlier chapters was easily modified on the free carboxylic acid with a spacer that contained a protected thiol at the end. However, the protecting group on the thiol functionality (trityl) proved to be incompatible with a downstream reaction. Although an alternative route was used and the formation of the final construct was demonstrated, the synthesis was not optimal and will have to be modified and/or optimized.

6.4 Experimental procedures

6.4.1 General information

Chemicals were obtained from commercial sources and used without further purification, unless stated otherwise. Peptide grade CH_2Cl_2 and TFA and HPLC grade solvents were purchased from Biosolve B.V. (Valkenswaard, the Netherlands) and peptide grade NMP and DMF were purchased from Actu-All Chemicals (Oss, the Netherlands). Unless stated otherwise, reactions were performed at room temperature. TLC analysis was performed on Merck precoated silica gel 60 F-254 plates. Spots were visualized with UV-light, ninhydrin stain (1.5 g ninhydrin and 3.0 mL acetic acid in 100 mL *n*-butanol) and/or potassium permanganate (1.5 g of $KMnO_4$, 10 g K_2CO_3, and 1.25 mL 10% NaOH in 200 mL water). Column chromatography was performed using Silica-P Flash silica gel (60 Å, particle size 40-63 μm) from Silicycle (Canada). Lyophilization was performed on a Christ Alpha 1–2 apparatus. ^{1}H NMR (400 MHz) and ^{13}C NMR (100 MHz) experiments were conducted on a 300 MHz Varian G-300 spectrometer. Chemical shifts are given in ppm (δ) relative to TMS (0.00 ppm) (^{1}H NMR) or relative to $CDCl_3$ (77 ppm) (^{13}C NMR).

Analytical HPLC was performed on a Shimadzu-10Avp (Class VP) system using a Phenomenex Gemini C18 column (110 Å, 5 μm, 250×4.60 mm) at a flow rate of 1 mL min^{-1}. The used buffers were 0.1% trifluoroacetic acid in MeCN/H_2O 5:95 (buffer A) and 0.1% trifluoroacetic acid in MeCN/H_2O 95:5 (buffer B). Runs were performed using a standard protocol: 100% buffer A for 2 min, then a linear gradient of buffer B (0-100% in 48 min) and UV-absorption was measured at 214 and 254 nm. Purification by preparative HPLC

was performed on a Prep LCMS QP8000α HPLC system (Shimadzu) using a Phenomenex Gemini C18 column (10 µm, 110 Å, 250×21.2 mm) at a flow rate of 12.5 mL min^{-1}. Runs were performed using a standard protocol: 100% buffer A for 5 min followed by a linear gradient of buffer B (0-100% in 70 min) with the same buffers as were described for analytical HPLC.

ESI-TOF MS spectra were recorded on a microTOF mass spectrometer (Bruker). Samples were diluted with tuning mix (1:1, v/v) and infused at a speed of 300 µl/h using a nebulizer pressure of 5.8 psi, a dry gas flow of 3.0 L/min, a drying temperature of 180°C and a capillary voltage of 5.5 kV. Analytical LC-MS (electrospray ionization) was preformed on Thermo-Finnigan LCQ Deca XP Max using same buffers and protocol as described for analytical HPLC. All reported mass values are monoisotopic.

6.4.2 Synthetic procedures and analytical data

Trityl protected spacer 5

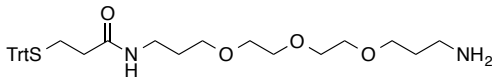

At 0°C Trityl-3-thiopropionic acid (**3**, 0.90 g, 2.6 mmol), EDC (0.43 g, 2.8 mmol), and HOBt (0.43 g, 2.8 mmol) were dissolved in CH_2Cl_2 (200 mL). DMF (10 mL) was added to achieve complete dissolution. The resulting mixture was stirred for 30 minutes at 0°C, after which the diamine (**4**, 3 mL, 13.0 mmol) and D*i*PEA (0.1 mL, 0.58 mmol) were added. The resulting mixture was stirred overnight at r.t., after which it was washed with $KHSO_4$ (aq, 1M, 200 mL), $NaHCO_3$ (aq, 1M, 200 mL) and brine (200 mL). The organic layer was dried over $MgSO_4$ and concentrated *in vacuo*. The crude product was purified by silica gel column chromatography (MeOH/EtOAc (1/1, v/v containing 0.1% D*i*PEA) to afford the product as a yellow oil (1.6 mmol, 0.87 g, 60%).

^{1}H-NMR (400 MHz, CD_3OD): δ = 1.71 (p, *J* = 6.5 Hz, 2H, $CH_2C\underline{H}_2CH_2$) 1.83 (p, *J* = 6.0 Hz, 2H, $CH_2C\underline{H}_2CH_2$), 2.18, 2.38 (2t, *J* = 7.0 Hz and 7.4 Hz, 4H, SCH_2CH_2), 2.94, 3.21 (2t, *J* = 6.5 Hz and 6.8 HZ, 4H, NCH_2), 3.47, (t, *J* = 6.1 Hz, 2H, $OC\underline{H}_2CH_2OCH_2CH_2N$), 3.53 (m, 2H, $OC\underline{H}_2CH_2OCH_2CH_2N$), 3.60 (m, 8H, $OCH_2CH_2OCH_2CH_2O$), 7.15-7.40 (m, 15H, Ar-H) ^{13}C-NMR (100 MHz, CD_3OD): δ = 28.2, 29.0 ($NCH_2\underline{C}H_2CH_2O$), 27.7, 34.5 ($SCH_2CH_2$), 36.3, 38.6 ($NCH_2$), 68.3, 69.0, 69.6, 69.7, 69.8, 70.0 (OCH_2) 126.4, 127.5, 129.3 ($(C_6H_5)_3$) 144.7 ($\underline{C}(C_6H_5)_3$), 172.3 (C=O)

Derivatized TAC-scaffold 2

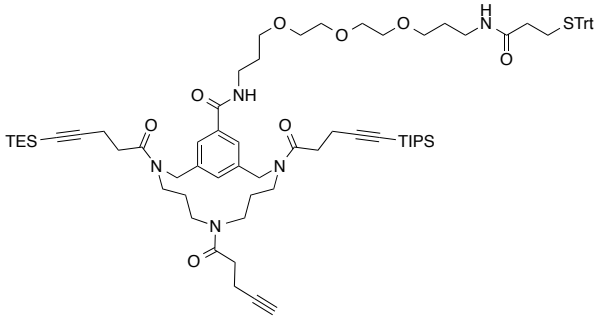

TAC-scaffold **1** (78 mg, 0.1 µmol), EDC (21 mg, 0.11 µmol), and HOBt (17 mg, 0.11 µmol) were dissolved in DMF (3 mL) and the resulting mixture was stirred for 30 minutes. Trityl-protected linker **5** (83 mg, 0,15 µmol) was added and the resulting mixture was stirred overnight. The solvent

was evaporated and the crude product was purified using silica gel column chromatography (4% MeOH in CH_2Cl_2). The purified product was dissolved in *t*BuOH/H_2O (1/1, v/v) and was lyophilized to yield the product as a white fluffy powder (55 mg, 0,042 µmol, 42%).

^{1}H NMR (400 MHz, $CDCl_3$): δ = 0.56 (*q*, *J* = 7.9Hz, 6H, 3x $SiCH_2CH_3$), 0.96 (*t*, *J*= 7.9Hz, 9H, 3x $SiCH_2CH_3$), 1.04 (*m*, 21H, 3x $SiCH(CH_3)_2$), 1.28-1.55 (*m*, 4H, $NCH_2CH_2CH_2N$), 1.67 (p, *J* = 6.1 Hz, 2H, $NCH_2CH_2CH_2O$) 1.86 (m, 2H, $NCH_2CH_2CH_2O$), 1.91 (*m*, 1H, CCH), 2.06, (t, *J* = 7.4 Hz, 2H, SCH_2CH_2), 2.45 (*m*, 6H, CH_2CH_2CCH and SCH_2CH_2), 2.57-2.76 (*m*, 8H, 2x CH_2CH_2CCSi), 2.83-2.98, 3.19-3.27, 3.35-3.65 (3*m*, 24H, $NCH_2CH_2CH_2N$, $NHCH_2CH_2CH_2O$, OCH_2CH_2O), 4.52-4.65 (m, 4H, 2x NCH_2Ar), 6.14, 7.25 (2m, 2H, 2x NH), 7.13-7.29, 7.34-7.41, 7.68-7.74 (3m, 18H, ArH). ^{13}C NMR (100 MHz, $CDCl_3$): δ = 4.4 ($SiCH_2$), 7.5 ($SiCH_2CH_3$), 11.2 (SiCH), 14.5 (CH_2CCH), 16.3, 16.3 (CH_2CCSi), 18.6 ($SiCH(CH_3)_2$), 27.7, 35.4 (SCH_2CH_2), 28.9, 29.0, 29.7 ($CH_2CH_2CH_2$), 31.8 (CH_2CH_2CCH), 32.8, 33.0 (CH_2CH_2CCSi), 37.4, 38.3, 43.4, 45.4, 45.9 ($NCH_2CH_2CH_2$) 53.8, 53.8 ($ArCH_2N$), 69.5, 69.8, 69.8, 69.9, 70.1, 70.2 (OCH_2), 126.6, 127.9, 129.5 136.0, 138.2, 140.2 (ArC) 144.6 ($C(C_6H_5)_3$) 166.2, 170.5, 171.0, 171.0 (C=O)

Scaffold containing one cyclic peptide 10

Solutions of TAC-scaffold **2** (23 µmol, 30 mg) in 500 µL DMF, peptide loop **6** (23 µmol, 26 mg) in 500 µL DMF, $CuSO_4.5H_2O$ (6.8 µmol, 1.7 mg) in 500 µL H_2O, NaAsc (20 µmol, 4.0 mg) in 500 µL H_2O and TBTA (3.4 µmol, 1.8 mg) in 500 µL DMF were prepared. These five solutions were combined and DMF (1.5 mL) and H_2O (1.0 mL) were added to obtain a final volume of 5 mL of DMF/H_2O 3/2 (v/v). The resulting mixture was stirred at room temperature for 3 hours and the progress of the reaction was monitored using LC-MS. When the reaction was complete, the mixture was diluted to a volume of 10 mL with MeCN/H_2O/TFA (50/50/0.1). The resulting mixture was centrifuged (5 min, 5000 rpm) and the supernatant was purified using preparative HPLC. The product-containing fractions were pooled and lyophilized to obtain the TAC-scaffold with as a white solid (22 mg, 9.0 µmol, 40%).

Exact mass calculated $[M + 2H]^{2+}$: 1235.6432; ESI-TOF MS found: 1235.6414.

Rt = 42.25 min.

Free alkyne scaffold containing one cyclic peptide 9

TES-protected scaffold **10** (2.9 µmol, 7.1 mg) was dissolved in MeOH (5 mL) and K_2CO_3 (145 µmol, 20 mg, 50 equiv.) was added. The resulting mixture was stirred at r.t. for 6 days, after which the mixture was diluted to a total volume of 10 mL with MeCN/H_2O/TFA (50/50/0.1). The resulting mixture was centrifuged (5 min, 5000 rpm) and the supernatant was purified using preparative HPLC. The product-containing fractions were pooled, lyophilized and the TES-deprotected TAC-scaffold was obtained as a white solid (1.1 µmol, 2.5 mg, 37%)

Exact mass calculated $[M + 2H]^{2+}$: 1178.5999; ESI-TOF MS found: 1178.5938.

Rt = 32.47 min.

Scaffold containing two cyclic peptides 11

Solutions of scaffold **9** (0.8 µmol, 2.0 mg) in 200 µL DMF and of peptide **8** (1.5 µmol, 2.0 mg) in 200 µL DMF were prepared. Stock solutions of $CuSO_4.5H_2O$ (2.4 µmol, 0.6 mg, 3 equiv. in 1 mL H_2O), NaAsc (7.2 µmol, 1.4 mg, 9 equiv. in 1 mL H_2O) and TBTA (1.2 µmol, 0.64 mg, 1.5 equiv. in 1 mL DMF) were prepared. The solutions of the scaffold and the peptide were combined and 100 µL of each $CuSO_4$, NaAsc, and TBTA solutions were added. To the resulting mixture DMF (0.4 mL) and H_2O (0.4 mL) were added to obtain a final volume of 1.5 mL of DMF/H_2O 3:2 (v/v). The resulting mixture was stirred at room temperature for 3h and the progress of the reaction was monitored using LC-MS. When the reaction was complete, the mixture was diluted to a volume of 5 mL with MeCN/H_2O/TFA (50/50/0.1). The resulting mixture was centrifuged (5 min, 5000 rpm) and the supernatant was purified using preparative HPLC. The product-containing fractions were pooled and lyophilized to obtain the TAC-scaffold with as a white solid (1.6 mg, 0.44 µmol, 55%).

Exact mass calculated $[M + 3H]^{3+}$: 1817.3584; ESI-TOF MS found: 1817.3567.

Rt = 32.94 min.

Free alkyne scaffold containing two cyclic peptides 12

TIPS-protected scaffold **11** (0.41 µmol, 1.5 mg) was dissolved in DMF (1 mL) and a solution of TBAF.$3H_2O$ (6.2 µmol, 2.0 mg, 15 equiv). The resulting mixture was stirred at room temperature and the progress was monitored by LC-MS. When the reaction was complete (usually after stirring overnight), the mixture was diluted to a volume of 5 mL with MeCN/H_2O/TFA (50/50/0.1). The resulting mixture was centrifuged (5 min, 5000 rpm) and the supernatant was purified using preparative HPLC. The product-containing fractions were pooled and lyophilized to obtain the product as a white solid (0.86 mg, 0.25 µmol, 62%).

Exact mass calculated $[M + 2H]^{2+}$: 1739.2917; ESI-TOF MS found: 1739.2750.

Rt = 27.68 min.

Scaffold containing three cyclic peptides 13

Solutions of scaffold **12** (0.25 µmol, 0.86 mg) in 200 µL DMF and of peptide **7** (0.3 µmol, 0.46 mg) in 200 µL DMF were prepared. Stock solutions of $CuSO_4.5H_2O$ (1.8 µmol, 0.45 mg, 6 equiv. in 1 mL H_2O), NaAsc (5.4 µmol, 1.1 mg, 18 equiv. in 1 mL H_2O) and TBTA (0.9 µmol, 0.48 mg, 3 equiv. in 1 mL DMF) were prepared. The solutions of the scaffold and the peptide were combined and 50 µL of each $CuSO_4$, NaAsc, and TBTA solutions were added. To the resulting mixture DMF (0.5 mL) and H_2O (0.5 mL) were added to obtain a final volume of 1.5 mL of DMF/H_2O 3:2 (v/v). The resulting mixture was stirred at room temperature for 3h and the progress of the reaction was monitored using LC-MS. When the reaction was complete, the mixture was diluted to a volume of 5 mL with MeCN/H_2O/TFA (50/50/0.1). The resulting mixture was centrifuged (5 min, 5000 rpm) and the supernatant was purified using preparative HPLC. The product-containing fractions were pooled and lyophilized to obtain the product as a white solid (0.29 mg, 0.058 µmol, 23%).

Exact mass calculated $[M + 3H]^{3+}$: 1672.0900; ESI-TOF MS found: 1672.0871.
Rt = 25.70 min.

Attempted final construct bearing three peptides and a free thiol 14

Three cyclic peptide containing construct **13** (0.16 µmol, 0.82 mg) was dissolved in MeOH/H_2O (1/1 , v/v, 2 mL) and a solution of $AgNO_3$ (1.6 µmol 0.26 mg, 10 equiv.) in H_2O (1 mL) was added. The resulting mixture was stirred for 90 minutes and monitored by LC-MS. After complete conversion of the starting material as determined using LC-MS, dithioerythritol (0.49 mg, 20 equiv.) was added to the mixture and the mixture was diluted to a volume of 5 mL with MeCN/H_2O/TFA (50/50/0.1). The resulting mixture was centrifuged (5 min, 5000 rpm) and it was attempted to purify the supernatant using preparative HPLC. However, no appreciable quantities were obtained.

References

1 P. R. Dormitzer, G. Grandi and R. Rappuoli, *Nat. Rev. Microbiol.*, 2012, **10**, 807–813.
2 P. Moyle and I. Toth, *ChemMedChem*, 2013, **8**, 360–376.
3 S. A. Plotkin, *Clin. Vaccine Immunol.*, 2009, **16**, 1709–1719.
4 R. Rappuoli, C. W. Mandl, S. Black and E. De Gregorio, *Nat. Rev. Immunol.*, 2011, **11**, 865–872.
5 J. Neefjes and H. Ovaa, *Nat. Chem. Biol.*, 2013, **9**, 769–75.
6 D. R. Flower, *Nat. Chem. Biol.*, 2013, **9**, 749–53.
7 M. Van Regenmortel, *Open Vaccine J.*, 2009, **2**, 33–44.
8 D. Hans, P. Young and D. Fairlie, *Med. Chem.*, 2006, **2**, 627–646.
9 R. Knittelfelder, A. B. Riemer and E. Jensen-Jarolim, *Expert Opin. Biol. Ther.*, 2009, **9**, 493–506.
10 A. B. Riemer and E. Jensen-Jarolim, *Immunol. Lett.*, 2007, **113**, 1–5.
11 M. Hijnen, D. J. Van Zoelen, C. Chamorro, P. Van Gageldonk, F. R. Mooi, G. Berbers and R. M. J. Liskamp, *Vaccine*, 2007, **25**, 6807–6817.
12 T. T. Wang, G. S. Tan, R. Hai, N. Pica, L. Ngai, D. C. Ekiert, I. A. Wilson, A. García-Sastre, T. M. Moran and P. Palese, *Proc. Natl. Acad. Sci. U. S. A.*, 2010, **107**, 18979–18984.
13 N. Gaidzik, U. Westerlind and H. Kunz, *Chem. Soc. Rev.*, 2013.
14 I. E. Valverde, A. F. Delmas and V. Aucagne, *Tetrahedron*, 2009, **65**, 7597–7602.
15 D. M. Beal, V. E. Albrow, G. Burslem, L. Hitchen, C. Fernandes, C. Lapthorn, L. R. Roberts, M. D. Selby and L. H. Jones, *Org. Biomol. Chem.*, 2012, **10**, 548–554.

Summary

Samenvatting

Summary

Interactions between proteins are an essential aspect of all biological processes. The interaction sites on these proteins are often large and complex in structure. Although the term epitope originates from the field of immunology, where it is used to designate the part of an antigen that is recognized by the immune system, it is nowadays increasingly used outside immunology for any protein-protein interaction site. The simplest structure of an interaction site, the continuous epitope, is a single contiguous stretch of amino acids. However, the more common discontinuous epitope is far more complex and is composed of multiple peptide segments that are remote in the protein's sequence but are brought together by the folding of the protein.

Synthetic mimics of epitopes may have a wide range of therapeutic applications. They may be used as protein-protein interaction inhibitors, synthetic vaccines, or synthetic antibodies. However, the synthesis of these mimics remains challenging. The large and complex discontinuous epitopes in particular are difficult to mimic accurately. The approach described in this thesis is to mimic discontinuous epitopes by attachment of peptides that correspond to the amino acid sequences of the epitope onto a molecular scaffold. An optimal molecular scaffold should present these essential parts of the epitope in a spatial structure that resembles that of the native protein.

More specifically, the research described in this thesis aimed at the development of a general method for the synthesis of discontinuous epitopes through the sequential introduction of peptides onto a molecular scaffold.

In **chapter 2**, two approaches for the cyclization of peptides containing two cysteine residues were described. In both approaches, an azide functionality was present in the linker connecting the cysteine residues, which allowed the introduction of the cyclized peptide onto a scaffold through a copper-catalyzed azide-alkyne cycloaddition reaction. In the first approach, a benzylic dibromide derivative was developed. This benzylic dibromide derivative allowed a fast and efficient cyclization of unprotected peptides. Using this approach, six peptides were synthesized that corresponded either to a part of an epitope of the HIV protein gp120 or a part of an epitope of the Pertussis protein Pertactin. The second approach involved the use of a bromomaleimide derivative for the cyclization of the peptides. However, due to the instability of the products, this approach was not suitable for the preparation of cyclic peptides in a reliable manner.

Chapter 3 described the development of a new scaffold for the sequential introduction of cyclic peptides. The TAC-scaffold was equipped with three alkyne moieties with varying chemical reactivity. Two of the alkyne moieties were protected with a silyl-based protecting group: one with a triisopropylsilyl-group and the other with a triethylsilyl-group. This difference in chemical reactivity of the protected alkynes allowed them to be chemically 'addressed' one after the other, making sequential introduction of cyclic peptides possible. The

new scaffold was used for the synthesis of a mimic of a discontinuous epitope of the Pertactin protein of *Bordetella Pertussis*, by sequentially introducing cyclic peptides corresponding to the peptide loops present in this epitope onto the scaffold. The use of a single ligation method and the convergent synthesis route demonstrated the robustness and convenience of this approach. This approach is a new addition to the relatively scarce methods for the introduction of both different and several cyclic peptides onto a scaffold for the synthesis of discontinuous epitope mimics. Our approach is expected to be applicable to a wide range of discontinuous epitope mimics containing three loops.

Chapter 4 described an improved orthogonally protected trialkyne scaffold suitable for the sequential introduction of azide-functionalized cyclic peptides. The complete synthesis of the scaffold from commercially available materials was described. The synthesis route proved to be efficient and afforded the new trialkyne scaffold in good yields. The scaffold was used for the sequential introduction of cyclic peptides corresponding to an epitope of the HIV protein gp120. Furthermore, the procedure for the sequential introduction was optimized. Compared to the procedure described in chapter 3, it was no longer necessary to perform the CuAAC reactions under microwave irradiation. This allowed the first CuAAC reaction to be combined with the first deprotection step, which increased the efficiency of the procedure. The overall yield of the sequential introduction of cyclic peptides onto the scaffold was also increased from 3% to 15% compared to the procedure described in chapter 3.

Chapter 5 described investigations into the biological activity of synthetic mimics of the CD4-binding site of the HIV protein gp120. The CD4-binding site is highly conserved and is therefore an attractive target for an immune response. Three mimics were synthesized using the procedures described in chapter 4. The mimics differed only in the order in which the peptides were introduced onto the scaffold and thus their relative positioning on the scaffold. The three mimics were evaluated for their ability to inhibit the binding of natural gp120 to CD4 in an ELISA assay. The three mimics were equally potent in their inhibition of this interaction, which suggests that the relative positioning of the peptides on the scaffold in the three mimics is similar with respect to CD4.

Furthermore, a comparison was made between protein mimics based on cyclic peptides and mimics based on linear peptides. A protein mimic based on linear peptides was synthesized and evaluated in the ELISA assay. The protein mimic based on linear peptides was able to inhibit the interaction between gp120 and CD4, but to a lesser extent than the mimic based on cyclic peptides. Furthermore, the protein mimic based on cyclic peptides showed a better proteolytic stability than the protein mimic based on linear peptides. These results showed the importance of using cyclic peptides in protein mimics.

To improve the biological evaluation of the synthesized protein mimics, ITC was explored to assess the protein mimic's ability to bind to CD4. Preliminary experiments using ITC suggested that this technique is able to measure the binding to CD4 and this result encourages

further exploration of this method of evaluating gp120 protein mimics.

In **chapter 6**, a first attempt at the synthesis of an epitope mimic suitable for conjugation to a carrier protein was described. Relatively small synthetic compounds are often conjugated to a carrier protein in order to increase the immune response. The scaffold described in chapter 4 and 5 was equipped with a thiol moiety that would allow for the conjugation to the carrier protein. However, the protecting group on the thiol (trityl) was not compatible with the procedure for the sequential introduction of cyclic peptides onto the scaffold. An alternative procedure was used that was compatible with the trityl group. However, this procedure was slow and low-yielding. Nevertheless, the formation of the final construct was demonstrated, but the synthesis was not optimal and will have to be modified and/or optimized to reliably yield protein mimics suited for conjugation to a carrier protein.

Nederlandse Samenvatting

De interacties tussen eiwitten zijn cruciaal in vele biologische processen. Eiwit-eiwit interacties zijn bijvoorbeeld betrokken bij het immuun systeem (o.a. antilichaam-antigen interactie), eiwit productie, celdeling en signaaltransductie. Het verstoren of veranderen van deze interacties kan grote gevolgen hebben. Het gedeelte van een eiwit wat betrokken is bij een interactie met een ander eiwit wordt een epitoop genoemd. Epitopen worden ingedeeld gebaseerd op hun structuur in twee categorieën: continue en discontinue epitopen. Continue epitopen bestaan uit een lengte aminozuren die naast elkaar zitten in de primaire structuur van het eiwit. Discontinue epitopen daarentegen bestaan uit meerdere lengtes aminozuren die niet bij elkaar liggen in de primaire structuur van het eiwit maar door de vouwing van het eiwit bij elkaar worden gebracht in de ruimte.

Ondanks de potentie is het gericht inhiberen of activeren van eiwit-eiwit interacties voor therapeutische doeleinden nog erg lastig. De traditionele "small molecule" medicijnen zijn vaak te klein om voldoende effect te hebben op de grote oppervlakken die vaak gemoeid zijn met eiwit-eiwit interacties. Epitoop mimetica kunnen hier de oplossing verzorgen. Epitoop mimetica zijn synthetische constructen die de essentiële atomen van een epitoop bevatten en bestaan vaak uit peptiden die corresponderen met de aminozuren van het epitoop. Epitoop mimetica zouden niet alleen dienst kunnen doen als eiwit-eiwit interactie inhibitors, maar ook als synthetische vaccins en synthetische antilichamen.

Een veel gebruikte aanpak voor het maken van epitoop mimetica is om peptiden, die corresponderen met de aminozuur sequentie van het na te bootsen epitoop, samen te brengen op een zogeheten steiger molecuul. Het steiger molecuul vervangt in essentie de rest van het eiwit waardoor alleen het epitoop overblijft. Desalniettemin blijft de synthese van epitoop mimetica een uitdaging door de grootte en complexiteit van deze constructen.

Het onderzoek in dit proefschrift beschrijft de ontwikkeling van een nieuwe methode voor de synthese van epitoop mimetica door middel van het sequentieel introduceren van cyclische peptiden op een steiger molecuul.

Hoofstuk 2 beschrijft twee methodes voor de cyclizatie van peptiden die twee cysteine residuen bevatten. In beide methodes zit er tevens een azide functionaliteit in de linker tussen de cysteines. Het azide maakte het mogelijk om de uiteindelijke cyclische peptiden op een steiger molecuul vast te zetten met koper gecatalyseerde azide-alkyn cycloadditie (CuAAC). Voor de eerste methode werd er een benzylisch dibromide ontwikkeld. Dit dibromide was in staat onbeschermde peptiden snel en efficiënt te cyclizeren. Met deze methode werden zes cyclische peptiden gesynthetiseerd, waarvan de sequentie overeen kwam met een deel van een epitoop van HIV gp120 of het Pertussis eiwit Pertactin. In de tweede methode werd een bromomaleimide derivaat gebruikt voor de cyclizatie van peptiden. Door de instabiliteit van de producten van deze reactie bleek deze methode niet in staat cyclische peptiden op een betrouwbare manier te kunnen maken.

Hoofdstuk 3 beschrijft de ontwikkeling van een nieuw steiger molecuul dat geschikt is voor de sequentiële introductie van cyclische peptiden doordat het uitgerust werd met drie alkyn groepen met elke een verschillende chemische reactiviteit. Twee van de drie alkynen waren beschermd met een silyl gebaseerde beschermgroep, de ene met een triisopropylsilyl groep en de ander met een triethylsilyl groep. Door dit verschil in reactiviteit is het mogelijk de alkyn groepen één voor één te gebruiken voor het introduceren van een cyclisch peptide. Dit nieuwe steiger molecuul werd vervolgens gebruikt voor de synthese van een mimeticum van een epitoop uit het Pertactin eiwit van *Bordetella Pertussis* door cyclische peptiden met een overeenkomende sequentie één voor één te introduceren. Methodes voor synthetiseren van eiwit mimetica door het gecontroleerd introduceren van verschillende peptiden op een steiger molecuul zijn schaars en de beschreven methode is een nieuwe toevoeging hieraan. Deze methode wordt verwacht toepasbaar te zijn op vele discontinue epitopen bestaande uit drie loops.

Hoofdstuk 4 beschrijft een verbeterd, orthogonaal beschermd trialkyn steiger molecuul wat geschikt is voor de sequentiële introductie van cyclische peptiden. De complete synthese route wordt beschreven vanaf commercieel verkrijgbare materialen. Met deze efficiënte synthese route is het mogelijk om het nieuwe steiger molecuul te synthetiseren in een goede opbrengst. Het steiger molecuul kon daarna gebruikt worden voor de introductie van peptiden die overeenkomen met het epitoop van het HIV eiwit gp120. De procedure voor de sequentiële introductie van de peptiden beschreven in dit hoofdstuk is verbeterd ten opzichte van degene beschreven in hoofdstuk 3, voornamelijk door het weglaten van de magnetron bestraling tijdens de CuAAC reacties. Hierdoor was het mogelijk de eerste CuAAC reactie te combineren met de eerste ontschermingsstap. De opbrengst voor de gehele procedure verbeterde hierdoor van 3% naar 15%.

Hoofdstuk 5 beschrijft de synthese van mimetica van het CD4-bindings epitoop van het gp120 eiwit en het onderzoek naar de biologische activiteit van deze mimetica. Het CD4-bindings epitoop is sterk geconserveerd over verschillende soorten HIV, wat het een aantrekkelijk doelwit maakt voor een immuun respons. Door middel van de procedure beschreven in hoofdstuk 4 werden drie mimetica van het CD4-bindings epitoop gesynthetiseerd. Het enige verschil tussen deze drie mimetica was de volgorde waarin de cyclische peptiden op het steiger molecuul waren geïntroduceerd en hierdoor dus de relatieve positionering op het steiger molecuul. De drie mimetica werden gebruikt in een ELISA set-up om te bepalen of ze in staat waren de binding van gp120 aan CD4 te inhiberen. De drie mimetica bleken even potent te zijn, wat suggereert dat de relatieve positionering van de peptide op het steiger molecuul nagenoeg gelijk is ten opzichte van CD4.

Verder werd er ook een vergelijking gemaakt tussen eiwit mimetica gebaseerd op cyclische peptiden en mimetica gebaseerd op lineaire peptiden. Een mimeticum gebaseerd op lineaire peptiden werd gesynthetiseerd en in dezelfde ELISA getest op zijn potentie als inhibitor. Het

lineaire mimeticum was in staat de binding tussen CD4 en gp120 te remmen, maar het was niet zo potent als de mimetica gebaseerd op cyclische peptiden. Verder werden de mimetica ook getest op hun stabiliteit in serum. Het mimeticum gebaseerd op cyclische peptiden bleek erg stabiel te zijn in serum, waar het mimeticum gebaseerd op lineaire peptiden dat veel minder waren. Vooral dit laatste resultaat laat zien dat het gebruik van cyclische peptiden een voordeel heeft bij het maken van epitoop mimetica.

Ten slotte werd er gekeken of het mogelijk was om ITC te gebruiken om de potentie van de mimetica te onderzoeken. De eerste test experimenten suggereerde dat deze techniek de binding tussen CD4 en de mimetica kon meten. Dit resultaat moedigt verder onderzoek van gp120 mimetica door middel van ITC aan.

In **hoodstuk 6** wordt een eerste poging beschreven om een epitoop mimeticum te maken dat geschikt is voor het conjugeren aan een drager eiwit. Conjugatie aan een drager eiwit wordt gedaan om de immuun respons te versterken. Het steiger molecuul dat beschreven is in hoofdstukken 4 en 5 werd uitgerust met een thiol groep. De gebruikte beschermgroep op het thiol (trityl) bleek niet stabiel te zijn tijdens de procedure voor de sequentiële introductie van de cyclische peptiden. Hierdoor moest de procedure worden aangepast, wat ten koste ging van de opbrengst. Desalniettemin werd er aangetoond dat het uiteindelijke mimeticum was gevormd. De synthese was nog niet optimaal en zal moeten worden aangepast om het maken van mimetica, die geschikt zijn voor het conjugeren aan een drager eiwit, mogelijk te maken.

Appendices

Curriculum Vitae
List of publications
Acknowledgements/Dankwoord

Curriculum Vitae

Paul Werkhoven was born on December 3rd 1987 in Nijmegen, the Netherlands. In the summer of 2005 he graduated from the Christelijk Gymnasium Utrecht, after which he started his Bachelor's studies chemistry at Utrecht University. In 2008-2009 he served as the treasurer on the board of the Utrecht chemistry student association "U.S.S. Proton". After finishing his Bachelor's in 2009, he started his Master's Drug Innovation. During this period, he did a 9-month internship in the department of Medicinal Chemistry and Chemical Biology at Utrecht University on the synthesis and evaluation of peptide-based proteasome inhibitors. After this, he did a 6-month internship at Philips Research on the topic of a hydrogen peroxice activatable probe as a diagnostic tool for heart failure. After obtaining his Master of Science degree in 2011, he started his PhD research project at the department of Medicinal Chemistry and Chemical Biology at Utrecht University under the supervision of prof. dr. Rob Liskamp and dr. ir. John Kruijtzer. The results of this research project are described in this thesis.

List of publications

P.R. Werkhoven, M. Elwakiel, T.J. Meuleman, H.C. Quarles van Ufford, J.A.W. Kruijtzer and R.M.J. Liskamp *Molecular construction of HIV-gp120 discontinuous epitope mimics by assembly of cyclic peptides on an orthogonal alkyne functionalized TAC-scaffold* Org. Biomol. Chem **2016**, *14*, 701-710

P.R. Werkhoven, H. van de Langemheen, S. Van der Wal, J.A.W. Kruijtzer and R.M.J. Liskamp *Versatile convergent synthesis of a three peptide loop containing protein mimic of whooping cough pertactin by successive Cu(I)-catalyzed azide alkyne cycloaddition on an orthogonal alkyne functionalized TAC-scaffold* J. Pept. Sci. **2014**, *20*, 235-239

P.R. Werkhoven and R.M.J. Liskamp in *Biotherapeutics: Recent Developments using Chemical and Molecular Biology* (Eds: L.H. Jones and A.J. McKnight) RSC books, **2013** pp. 263-284

S. Tschan, A.J. Brouwer, P.R. Werkhoven, A.M. Jonker, L. Wagner, S. Knittel, M.N. Aminake, G. Pradel, F. Joanny, R.M.J. Liskamp, B. Mordmüller *Broad-Spectrum Antimalarial Activity of Peptido Sulfonyl Fluorides, a New Class of Proteasome Inhibitors* Antimicrob. Agents Chemother. **2013**, *57*, 3576-3584

A.J. Brouwer, A. Jonker, P.R. Werkhoven, E. Kuo, N. Li, N. Gallastegui, J. Kemmink, B.I. Florea, M. Groll, H.S. Overkleeft, and R.M.J. Liskamp *Peptido Sulfonyl Fluorides as New Powerful Proteasome Inhibitors* J. Med. Chem., **2012**, *55* (24), 10995–11003

Acknowledgements/Dankwoord

Na vier en een half jaar promoveren lijkt de tijd voorbij gevlogen. Ik heb een geweldige tijd gehad en heb ontzettend veel geleerd, op professioneel en persoonlijk vlak. Ik had niet zo ver kunnen komen zonder de mensen om mij heen en ik wil dan ook graag die mensen bedanken.

Allereerst wil ik graag mijn promotor **Rob Liskamp** bedanken. Jouw enthousiasme en jouw vertrouwen in mijn kunnen hebben mij altijd gemotiveerd. Je hebt me vier jaar lang geïnspireerd door met een heleboel ideeën te komen maar ook door me de ruimte te geven voor mijn eigen ideeën. Ondanks dat er (voor een groot deel van mijn aio-tijd) een zee tussen zat hadden we altijd goed contact en stond je altijd klaar om te helpen als ik dat nodig had.

Ook wil ik graag mijn co-promotor **John Kruijtzer** bedanken. Tijdens mijn vier jaar bij MedChem heb ik ontzettend veel van je geleerd. Je kennis over (peptide)chemie is net zo indrukwekkend als de verzameling papier in je kantoor. Dank voor al je hulp en input, je enthousiasme als ik de nieuwste resultaten kwam vertellen en dat je altijd klaar stond voor een babbeltje bij de koffieautomaat.

Ik wil ook graag een heleboel collega's bedanken die mijn vier jaar bij MedChem tot een fantastische tijd hebben gemaakt. **Arwin**, mijn MedChem carrière ben ik bij jou als masterstudent begonnen en ik heb ontzettend veel van je geleerd, zowel tijdens mijn stage als tijdens mijn promotie. Bedankt voor alle adviezen en praatjes over van alles en nog wat en bedankt voor alles wat je regelde op het lab. **Linda**, ontzettend bedankt voor alle ELISA's die je voor mij hebt gemeten. **Dirk**, je hebt een geweldige kennis van peptidechemie en was altijd bereid te helpen. **Nathaniel**, it was always a great pleasure discussing both chemistry and the latest series or movies with you. **Paula** en **Natatia**, dank voor al jullie advies en hulp met de praktische zaken.

Peter, ons promotietraject liep aardig gelijk op en daardoor zaten we vaak in hetzelfde schuitje. Tijdens de vele koffiemomentjes konden we altijd ideeën en suggesties uitwisselen en klagen over wat er allemaal mis ging/was op het lab. Ook tijdens de tripjes naar de cola-automaat of het boodschappen doen voor de borrel was het altijd gezellig. Bedankt dat je mijn paranimf wil zijn. **Timo**, je stond altijd klaar om je ongezouten mening te geven over van alles en nog wat, om even een bakkie te halen, maar ook om een bureaupils te drinken na een lange dag. Ik hoop dat je je koffie-inname wat kan minderen nu ik er niet meer ben. **Alen**, my across the desk neighbour. I enjoyed talking with you about food and drinks, both dutch and slovenian, good and bad. I hope for you the next person occupying my desk has shorter legs. **Laurens**, het was me een genoegen om met jouw af en toe over de serieuze gebeurtenissen in de wereld te praten, met af en toe een net iets te vieze grap er doorheen. **Matthijs**, dank voor de dagelijkse dosis droge humor en je Brabantse gezelligheid op de borrels. **Marjon**, je stond altijd wel klaar om even een koffie te halen en het over spelletjes te hebben.

Jack, als labgenoot kon ik altijd bij je aankloppen met wat praktische vraagjes of voor een anta-flu, als ik tenminste boven de snoeiharde metal uitkwam. **Steffen**, lange tijd ben je mijn buurman geweest en in die tijd heb ik veel van je geleerd. Dank voor al je suggesties en de

discussies over chemie. **Hilde**, jij stond altijd klaar met een mening, ik vond het allemaal wel best en dat ging heel goed samen. **Loek**, jij kon als geen ander de sfeer altijd lekker luchtig houden. **Gwenn**, ik kwam pas later op het project erbij, maar ik heb me altijd als part of the team gevoeld. Dank voor alle discussies en ideeën over ons project. **Helmus**, het was altijd fijn ons project met jou te bespreken. Dank voor alle discussies, suggesties en project ideetjes. I would also like to thank all other MedChem colleagues, current and former, that contributed in one way or another to make my time there memorable.

Tijdens mijn promotietraject heb ik ook een aantal studenten mogen begeleiden. **Shaïsta**, **Moheb** en **Tom**, ontzettend bedankt voor jullie bijdrage!

Ook buiten MedChem wil ik graag wat collega aio's uit het David de Wied bedanken. **Kristel**, ik kon altijd wel wat stikstof lenen als onze tank weer eens leeg was. Dank voor je brabantse gezelligheid als je onze borrels kwam bezoeken. I was also part of the UIPS PhD comittee. **Anna**, **Atanaska**, **Renske** en **Andhyk**, I have enjoyed organizing the retreat (especially the pubquiz) and the pizza evenings with you. I also want to thank all the people from the Glasgow lab, **Susan**, **Anna**, **Raik**, **Dominik**, **Frederike**, **Natalia**, **Ondra**, **Ariadna**, **Tobias**, for giving me a warm welcome and making my 2 months over there a great time.

Ik heb natuurlijk niet al mijn tijd op het lab doorgebracht en daarom wil ook graag mijn vrienden bedanken die voor de nodige gezelligheid en ontspanning hebben gezorgd. **Tim**, scheikundevriend van het eerste uur. Dank voor al die festivals, feestjes en avonden van voetbal, bier, vet vreten en gamen. Bedankt dat je mijn paranimf wil zijn. **Joost**, omdat we in dezelfde periode zaten tijdens het afronden van de promotie heb ik veel gehad aan onze gesprekken over promoveren en het al het geregel daaromheen. Ook bedankt voor de alle squashochtenden en zelfgebrouwen biertjes. **Els**, bedankt voor de broodnodige schop onder de reet die jij Joost, en daarmee mij, kon geven. En natuurlijk ook bedankt voor alle taarten en toetjes. **Frank**, bedankt voor alle squashochtend en koffiepauzes. **Tiemen**, het was me altijd een genoegen om met je over de betere dingen in het leven (bier, vlees, vuur en whisky) te praten. Dan wil ik ook nog alle andere primus mensen, **Bieneke**, **Janne-Mieke**, **Winnie**, **Nikki**, **Arjan**, **Jeroen**, **Annemarie** en **Lillian**, bedanken voor alle vrijdagavonden vol speciaal bier, vocking worst en kaasstengels en alle andere feestjes en festivals.

Dan natuurlijk ook nog **Harrison**, **Wouter**, **Wouter**, **Dave**, **Sus**, **Steven**, **Jesse**, **Maarten**, **Joost**, **Lykele**, **Gijs** en **Kaz**. Kerels, we kennen elkaar al jaren en ook al zagen we elkaar niet altijd even frequent, het was elke keer als vanouds als we elkaar wel zagen. Ik waardeer jullie vriendschap enorm en hoop dat we nog een hele lange tijd bevriend zullen blijven. Bedankt voor alle weekjes in de schuur, de feesten, de spelletjes en kroegavondjes, de interesse in mijn werk en alle gezelligheid in het algemeen. Nog een speciaal bedankje voor Wouter Mulders voor het doorlezen van mijn hele proefschrift.

Dan wil ik ook nog graag mijn familie bedanken. **Mam**, je was altijd geïnteresseerd in mijn onderzoek en dat heeft me altijd gemotiveerd door te gaan. Dank voor je onvoorwaardelijke

steun, aanmoediging en liefde. **Pap**, ik heb altijd geweten dat wat er ook gebeurt je er altijd voor me zult zijn. Ik vind het geweldig te zien hoe jij nu ook met je promotie bezig bent en geniet van onze gesprekken over de overeenkomsten en verschillen tussen onze promoties. **Loes**, ik vind het knap hoe jij je leven helemaal naar je eigen zin hebt ingericht (zeker nu met de kleine Tessa erbij) en daarin ben je een voorbeeld voor me. **Tom**, onze persoonlijkheden zijn redelijk verschillend, maar ik kan altijd met je lachen. **Ben**, ik vind leuk dat je ook aan je promotie bent begonnen en ik hoop dat ik je gaandeweg nog kan helpen. Ik hoop dat net zo'n leuke tijd zal hebben als ik heb gehad. **Floor**, ik vind het super om te zien hoe jij je volledig in het studentenleven stort en hoe jij je ontwikkeld tot een volwassen vrouw. **Grootje**, ook al lag mijn onderzoek niet echt in jouw straatje was je altijd benieuwd hoe het ging. Ik heb altijd gevoeld dat je trots op me was.

Lieve **Christine**, ik zou je voor zo veel dingen willen bedanken, zoals je onvoorwaardelijke steun en liefde maar ook de soms hard nodige reality checks en pepers in mijn reet. Je bent er altijd voor me, door dik en dun, en ik kijk er naar uit om de rest van mijn leven met jou te delen.